FINAL TECHNICAL REPORT
GT PROJECT A-2550

MARINE AIR TRAFFIC CONTROL AND LANDING SYSTEM (MATCALS) INVESTIGATION

By

E. S. Sjoberg
T. G. Farill
P. A. Cloninger
B. Perry
J. P. Garmon
P. P. Britt

Prepared for

NAVAL ELECTRONIC SYSTEMS COMMAND
WASHINGTON, DC 20360

Under

Contract No. N00039-80-C-0082

May 1983

GEORGIA INSTITUTE OF TECHNOLOGY
A Unit of the University System of Georgia
Engineering Experiment Station
Atlanta, Georgia 30332

GTEES

UNCLASSIFIED

SECURITY CLASSIFICATION OF THIS PAGE *(When Data Entered)*

REPORT DOCUMENTATION PAGE

READ INSTRUCTIONS BEFORE COMPLETING FORM

1. REPORT NUMBER	2. GOVT ACCESSION NO. AD-A130309
3. RECIPIENT'S CATALOG NUMBER	
4. TITLE *(and Subtitle)* Marine Air Traffic Control and Landing System (MATCALS) Investigation	5. TYPE OF REPORT & PERIOD COVERED Final Technical Report April, 1982 - April, 1983
	6. PERFORMING ORG. REPORT NUMBER GIT/EES A-2550 FTR
7. AUTHOR(s) E. S. Sjoberg, T. G. Farrill, P. A. Cloninger, B. Perry, J. P. Garmon, P. P. Britt	8. CONTRACT OR GRANT NUMBER(s) N00039-80-C-0082
9. PERFORMING ORGANIZATION NAME AND ADDRESS Georgia Institute of Technology Engineering Experiment Station Radar and Instrumentation Laboratory Atlanta, Georgia 30332	10. PROGRAM ELEMENT, PROJECT, TASK AREA & WORK UNIT NUMBERS
11. CONTROLLING OFFICE NAME AND ADDRESS Naval Electronic Systems Command Washington, D.C. 20360	12. REPORT DATE May 1983
	13. NUMBER OF PAGES 138 + i thru xiv
14. MONITORING AGENCY NAME & ADDRESS *(if different from Controlling Office)*	15. SECURITY CLASS. *(of this report)* UNCLASSIFIED
	15a. DECLASSIFICATION/DOWNGRADING SCHEDULE

16. DISTRIBUTION STATEMENT *(of this Report)*

This document has been approved for public release and sale; its distribution is unlimited.

17. DISTRIBUTION STATEMENT *(of the abstract entered in Block 20, if different from Report)*

18. SUPPLEMENTARY NOTES

19. KEY WORDS *(Continue on reverse side if necessary and identify by block number)*

Air Traffic Control	Precision Approach Radar	Transmit Frequency Selection
Airport Surveillance Radar	Radar	
Fiber Optic Data Link	Radar Receiver Sensitivity	
MTI Improvement	Radar Tracking Errors	
MATCALS	Statistical Data Analysis	

20. ABSTRACT *(Continue on reverse side if necessary and identify by block number)*

Georgia Tech investigated several areas relating to the development of the Marine Air Traffic Control and Landing System (MATCALS). Several factors relating to the specification and testing of the MATCALS Airport Surveillance Radar (ASR) were studied. These include:

1) MTI improvement factor. Models of the amplitude distributions and spectral characteristics are identified and explained in the light of specifications for an ASR system;

(continued)

DD FORM 1 JAN 73 1473 EDITION OF 1 NOV 65 IS OBSOLETE

UNCLASSIFIED

SECURITY CLASSIFICATION OF THIS PAGE *(When Data Entered)*

20. Abstract (continued)

2) L-band versus S-band transmit frequency considerations are enumerated with emphasis on the phenomenological limitations of the MTI improvement factor.

3) Three methods of measuring a radar's minimum detectable signal level are discussed. These include direct measurement, determination of the tangential sensitivity, and noise figure measurement.

4) Remoting of the MATCALS CCS from the ASR using a fiber optic data link was investigated. The cost of the optical components for such a system is shown to be approximately $33,000 per system.

Data from the AN/TPN-22 test flight program is also presented. The statistical analysis methods are explained and effects of the multipath fence and enhanced F-4J target are explored. A preliminary conclusion from the brief analysis is that the major source of azimuth tracking error in the radar itself.

The MATCALS Air Traffic Control mission was studied in order to define the ASR performance requirements. The overall Marine aviation mission, organization, operational scenarios, aircraft capabilities, and combat environments were included in the analysis.

One conclusion, in addition to the ASR specifications, is that logistics and radar availability are of equal or greater importance to the mission success than are minor changes in radar performance.

EXECUTIVE SUMMARY

This final technical report summarizes the major accomplishments on contract N00039-80-C-0082 during the period April 1982 through April 1983. The current effort comprised three tasks. The first task was support of the TV-tracker system previously delivered to Patuxent Naval Air Station, the second was technical assistance to NAVELEX in the area of Airport Surveillance Radar (ASR) specifications and analysis, and the third was analysis of the air traffic control mission as applied to the MATCALS ASR. Under the direction of the NAVELEX technical monitor, portions of the funds for the first and second tasks were used by Georgia Tech to support a flight test program at Patuxent NAS which had been planned by Georgia Tech under previous MATCALS efforts.[1,2] These flight tests were successfully completed in September of 1982. Preliminary analysis of the data has been completed and is described in Section 4 of this report. Georgia Tech wishes to acknowledge the support and cooperation of Mr. Kenneth Potyen and the staff of Patuxent NAS, without whose help the flight tests could never have been performed.

TV-Tracker System Support

A TV-tracker system was built by Georgia Tech and installed at the MATCALS test facility at Patuxent NAS in December of 1981. The system superimposes a cursor, driven by the AN/TPN-22 tracking solution, on a TV display of the landing scene. During the course of this contract, the quality of the video signal from a government furnished television camera degraded to the point of being unusable. This condition was not remedied and, consequently, no reportable work was performed on this task during the current effort.

Air Traffic Control System Definition

Four areas for investigation were identified under this task. A brief synopsis of each of those areas is included below.

MTI Improvement Factor

The improvement factor required of an MTI filter depends upon the expected target and clutter signal distributions and the required detection performance. At decimeter wavelengths, Rayleigh models of target and clutter statistics are often used, as represented by the Swerling target models. For a given probability of detection and probability of false alarm, the required single pulse, signal-to-interference (S/I) ratio can be computed for each Swerling case, as shown, for example, in Figures 2.7 and 2.23 of Skolnik's Introduction to Radar Systems.[3] Trees and rain will cause the worst clutter which the MATCALS ASR will encounter.

The backscatter coefficient (σ^o) of the tree clutter has been examined at a variety of transmit frequencies and incidence angles. Tables and graphs of backscatter coefficients for the various parameters have been compiled by Skolnik,[3,4] Nathanson,[5] Long,[6] and others. The results vary considerably from source to source and no single number uniquely characterizes tree clutter. Considering the variety of σ^o values reported, the choice is almost arbitrary for a theoretical analysis. Barring the possibility of actually measuring the reflectivity of the area of interest, a value of -20 dB for σ^o represents a conservative estimate. Considerably less information is available concerning the spectral properties of tree clutter. The L-band data are particularly sparse; however, the data which are available indicate that tree clutter will have frequency components of up to only a few Hertz. Considering, the minimum target velocities for the MATCALS scenario, tree clutter is not likely to present a severe problem.

Airport surveillance radars (ASR) characteristically employ cosecant-squared type fan beams to attain the necessary elevation coverage. By their very nature, these radars are extremely susceptible to volume clutter effects and, in most cases, employ some means of reducing the effect either through the use of circular polarization or special rain filters. Measuring the effectiveness of these filters requires some assumption of potential rain clutter characteristics.

The backscatter reflectivity (η^o) of rain clutter is strongly dependent upon rain rate. the most representative equation for rain reflectivity is

$$\eta^o = Cr^m$$

where η^o is the reflectivity in m^2/m^3, r is the rain rate in mm/hr, and C and m are constants dependent upon the transmit frequency. This equation has been demonstrated to be reasonably accurate up to 95 GHz.[9] Empirical data indicate that rain is 25 times more reflective at S-band that at L-band.

The wide variety of phenomenological conditions in which rain can be present, implies a wide range of possible spectral characteristics. Rain rates from 0.25 mm/hr to 100 mm/hr have been observed in wind conditions ranging from 0 mph to over 100 mph. The extent and type of radar coverage also affects the spectra. A short range radar with a narrow beamwidth will see a more limited rain spectrum than a long range airport surveillance radar. In fact, the ASR's under consideration are susceptible to the most severe rain clutter effects due to their wide elevation beamwidths and long detection ranges. Of the several factors which contribute to the spectrum of rain clutter, the most important, by far, for an ASR is wind shear. This phenomenom will typically cause the rain clutter spectrum to run up to 140 Hz at L-band and 280 Hz at S-band.

Transmit Frequency Selection

The transmit frequencies employed in airport surveillance radars extend from 1.2 GHz (L-band) to 3 GHz (S-band). The 3 GHz upper limit is primarily driven by the detection range requirements; at higher transmit frequencies, weather-induced attenuation becomes severe. The 1.2 GHz lower limit is a result of physical limitations on the size of both the antenna and the waveguide. The fact that production ASR systems operate at both L- and S-band frequencies suggests that no clear-cut choice between the two exists.

Physical size of the antenna gives an advantage to S-band systems which require an aperture of only one half of that at L-band for equal beamwidths. Electronic hardware at both frequencies is excellent and essentially equal in performance. It appears, also, that some form of waveguide pressurization or dessication is required because of the transportability and setup time requirements.

The greatest differences between L- and S-bands involve the effects of environmental phenomena and the radar and signal processing techniques used to remove them. The most pronounced interference is induced by meteorological reflectivity, but the effects of attenuation, ground clutter, and multipath interference must also be considered. The effects of atmospheric and meterological attenuation are almost negligible at both L- and S-band frequencies.

Rain clutter presents a larger problem to S-band radars than to L-band radars. The reflectivity of rain varies inversely with the fourth power of the wavelength. So, for identical resolution cells, the S-band radar will receive 16 times (12 dB) more rain clutter than the L-band radar. If the same antenna size is assumed, the S-band resolution cell will be one-half the size of the L-band cell, so the net increase in rain clutter backscatter from L- to S-band is approximately 9 dB. Because of this, all production S-band ASR's employ circular polarization to reduce the rain clutter interference. Most manufacturers assume a circular polarization rain reduction of approximately 20 dB. Circular polarization also reduces the strength of the target return by approximately 7 dB. This results in a net improvement of 13 dB. Since the rain return within the resolution cell at S-band is 9 dB greater than at L-band, the 13 dB improvement due to circular polarization actually results in 4 dB better rain rejection at S-band than a simple L-band system with no rain rejection processing.

The use of circular polarization at L-band is generally not considered necessary because of the lower rain clutter reflectivity. However, the AN/TPS-65 L-band system does employ a filter designed specifically for rain rejection. This implies that rain clutter was of significant concern to one L-band manufacturer.

The theoretical improvement factor attainable in an MTI system at L- and S-bands is limited by the spectral spread of the clutter return. This spread is the result of both antenna scanning and internal clutter motion. These effects have been documented in detail for both simple cancellers and staggered PRF systems. For nominal L- and S-band radar systems in a clear-air-tree clutter environment, the MTI improvement factor for both systems is limited by antenna scanning and PRF staggering. The S-band system is limited to a 50 dB improvement; the L-band system is limited to a 56 dB improvement. In a rain clutter environment, the L-band improvement is limited to 41 dB due to PRF staggering. The S-band improvement in rain is limited to 27 dB for a triple delay canceller or 35 dB for a quadruple delay canceller where the limit on improvement is due to the effect of PRF staggering. This results in a 6 dB advantage at L-band in rain clutter, unless circular polarization is employed at S-band. In that case, the L- and S-band systems should have approximately equal performance. Note that this performance prediction is predicated on obtaining optimal performance from the two systems. In practice, this is not achieved. Oscillator instabilities, MTI processor design, and other factors limit the MTI improvement to about 35 dB for S-band systems and 50 dB for L-band systems.

Radar Receiver Sensitivity

Radar receiver sensitivity can be evaluated by directly measuring the minimum discernible signal (MDS), by measuring tangential sensitivity (St) and calculating MDS, or by measuring noise figure (Fn) and calculating MDS.

MDS is measured as the signal power level at the input of the receiver with the signal minimally discernible in the receiver output above the noise floor. Tangentential sensitivity is indicated when the top of the noise envelope from the receiver is even with the bottom of the envelope of the signal plus noise. Radar receiver noise figure can be measured using a standard noise source and a noise figure meter, using either manual or automatic methods.

Fiber Optic Data Link Feasibility Study

The use of fiber optics (FO) in the communications industry, the medical field, and the military area has grown tremendously over the past five years and shows further growth potential for the future. The usefulness of FO in these areas is due to its well known advantages of wide bandwidth, low cost, weight and size reduction, electrical isolation, almost complete immunity to electromagnetic interference (EMI), and low loss.

A survey of several fiber optic system manufacturers was made to determine the cost of currently available optical fiber cable and electro-optical components for the MATCALS application. This information has been used to determine the cost of remoting a radar transmitter from the operations shelter by employing a fiber optic link. Under the assumed conditions and if multiplexing is not employed, a minimum of five fibers and five transmitter-receiver pairs will be required. The cost for such a system would be as follows:

Five transmitter-receiver pairs	$13,500.00
Three km of fiber cable	$19,500.00
Cost per link	$33,000.00
Cost for 17 links	$561,000.00

AN/TPN-22 Flight Test Program

Previous Georgia Tech reports[1,2] recommended that a flight test program be undertaken utilizing the AN/TPN-22 radar system, the MATCALS precision approach

radar (PAR). These tests were successfully completed in September 1982. This flight test program served two purposes. First, it gathered a statistically significant data set for evaluation of amplitude processing tracking algorithms developed by Auburn University and Georgia Tech. These data provide a baseline for evaluating and comparing the different processing techniques. Second, it gathered data useful for isolating the sources of radar tracking error to either radar instrumentation errors, target induced errors, or environmentally induced errors. The flight tests utilized two pieces of equipment designed by Georgia Tech to isolate these errors: a multipath fence and a circularly polarized corner reflector. The details of the analysis and design of these experimental tools have been described in a previous Georgia Tech report.(1) Theoretically, both environmentally induced errors, such as multipath interference and clutter, and target scintillation and glint are completely eliminated by utilizing the multipath fence and the circularly polarized corner reflector mounted in the radome of the F-4J test aircraft; thus, leaving only the radar instrumentation errors.

The AN/TPN-22 flight data analysis accomplished in the current phase of the contract consisted of developing and adapting software to read the data tape, generate the desired statistics of the data, and plot the statistics. The following preliminary conclusions were drawn from the flight test data.

(1) Multipath interference appears to be present in the elevation track error data. The multipath fence did not have any measurable effect on the elevation or azimuth errors. There seems to be contradictory data which require further analysis for a suitable explanation.

(2) The corner reflector reduced the RMS azimuth errors at short range by about 15% and had no effect at long ranges. Thus, the target induced errors of scintillation and glint appear to contribute only about 15% of the total azimuth error even at short range. Environmental errors should not be a major factor to the azimuth tracking performance. Hence, the radar instrumentation errors are the primary source of azimuth tracking inaccuracies at all ranges.

(3) Within the experimental accuracy, the elevation RMS error displayed no sensitivity to the corner reflector being mounted in the aircraft. This is a very surprising result since it was predicted that frequency induced target scintillation would be the major source of elevation tracking error.(2) Georgia Tech hesitates to draw conclusions from these data without further

analysis because the data are contradictory, contrary to theory, and the multipath fence did not seem to reduce multipath interference effects. Further study of the data should resolve these inconsistencies.

ATC Mission Analysis

The development of MATCALS by the Naval Electronic Systems Command will provide an automated terminal area air traffic control and ground derived landing control for all weather operations. MATCALS comprises several elements which together provide for all the required functions and is organized into three subsystems: air traffic control subsystem, all-weather landing system, and control and central subsystem. The air traffic control subsystem consists of the airport surveillance radar (ASR) which provides range and bearing information, and the radar beacon component which provides range, bearing, and altitude information to transponder equipped aircraft.

Baseline performance specifications for the ATC subsystem were determined by performing a mission analysis that addressed the overall Marine aviation mission, the organizational concept, operational scenarios, aircraft capabilities, and typical combat environments. The analysis was conducted with the intent of generating a revised set of parameters that describe the desired operational capabilities.

The resulting ASR performance requirements derived from this study are listed below:

Maximum Range	60 nm
Target RCS	1 m^2
Target Velocity	50 - 600 kts
Range Resolution	150 m
Range Accuracy	100 m
Azimuth Resolution	2.2^o
Azimuth Accuracy	0.3^o
Half-Power Azimuth Beamwidth	2.2^o
Elevation Beam Shape	csc^2
Maximum Altitude Coverage	40,000 ft
Azimuth Coverage	360^o
Scan Rate	15 rpm

In addition to the performance characteristics of the ASR, the logistics aspects are extremely important in the development of a radar system intended for tactical use, and a balance between these considerations and the performance considerations must be made. Included in these considerations are: maintenance and test equipment, supply support, transportation and handling, and operator and maintenance personnel training.

Interviews with operational Marine Air Traffic Control Squadron personnel revealed that these considerations are perceived to be significantly more important than minor variations in the performance characteristics. Their rational is that the present radar system's operational performance (detection range, etc.) is adequate. The ability to deploy in a timely manner, repair a failure in a timely and efficient manner, obtain a replacement component, and train maintenance personnel in the allotted school program time will, in the final analysis, determine the operational readiness of the radar unit.

The following specific comments concerning maintainability were made by Marine Air Traffic Control Squadron personnel:

1. Provide a dual channel system.
2. Provide simple switching so that maintenance personnel can safely work on one channel while the other is operational.
3. Provide non-pressurized waveguides.
4. Provide other than water cooled system.
5. Provide a rugged, adjustable antenna that is easily erectable and not easily damaged.
6. Provide easily repairable components (cards) or ensure that an adequate supply of replacement parts is available at the unit.

PREFACE

The university associated participants in this investigation included the Engineering Experiment Station at the Georgia Institute of Technology in Atlanta, Georgia; the Engineering Experiment Station at Auburn University in Auburn, Alabama; and Flight Transportation Associates, Inc., in Boston, Massachusetts. Georgia Tech acted as prime contractor to the Naval Electronic systems Command in Washington, D. C. under Contract No. N00039-80-C-0082. Auburn University and Flight Transportation Associates were subcontractors to Georgia Tech under Contract Nos. 1-A-2550 and 2-A-2550, respectively.

Dr. Robert N. Trebits served as Project Director for the first four months of this investigation, designated Georgia Tech project A2550. At that time, Mr. Eric S. Sjoberg, who has worked on the Georgia Tech MATCALS program for several years, was appointed Project Director. Dr. Charles L. Phillips coordinated the Auburn University project activities, and Mr. William C. Hoffman coordinated the Flight transportation Associates project activities. The Navy Project Engineer was Mr. Dan Brosnihan, who is also the MATCALS Program Manager.

This final technical report emphasizes the program activities performed by Georgia Tech during the contract period. Separate reports were generated by Auburn University and Flight Transportation Associates to document their research efforts on this MATCALS program. The authors of this report include Mr. Eric S. Sjoberg, Mr. Trent G. Farrill, Ms. Peggy A. Cloninger, Mr. Benjamin Perry, Dr. J. P. Garmon and Mr. P. P. Britt. The technical guidance provided by NAVELEX personnel has been appreciated, with particular acknowledgement to Mr. Charles Gill, Mr. Daniel Brosnihan, and Mr. Lewis Buckler.

TABLE OF CONTENTS

TABLE OF CONTENTS

(continued)

LIST OF ILLUSTRATIONS

LIST OF ILLUSTRATIONS

(continued)

LIST OF TABLES

SECTION 1
INTRODUCTION

The current phase of Georgia Tech's participation in the MATCALS program began in April 1982 and ended one year later. Three tasks comprised the current effort. The first task was support of the TV-tracker system previously delivered to Patuxent Naval Air Station, the second was technical assistance to NAVELEX in the area of Airport Surveillance Radar (ASR) specifications and analysis, and the third was an analysis of the air traffic control mission as applied to the MATCALS airport surveillance radar.

The first task area (support of the TV-tracker system) received only cursory attention during the current contract because of malfunctions in a government furnished camera and lens system which were not resolved during the contract period. Consequently portions of funds from the first and second tasks were redirected under the direction of the NAVELEX technical monitor to support a previously planned flight test program at Patuxent Naval Air Station. The flight tests were successfully completed and data were obtained for future analyses. Portions of these analyses were performed under the current contract and are reported in the following sections. Georgia Tech wishes to acknowledge the support and cooperation of Mr. Kenneth Potyen and the staff of Patuxent Naval Air Station without whose help the flight tests could never have been performed.

SECTION 2
TV-TRACKER SYSTEM SUPPORT

Under previous contracts[1,2], Georgia Tech was tasked by NAVELEX to define and implement a system which displays target aircraft position on a television display of the landing scene as measured by the AN/TPN-22. This TV-tracker was installed at the MATCALS Test Facility at the Patuxent Naval Air Station, Maryland in December of 1981. The tracker's purposes include (1) providing an instantaneous visual presentation of the track quality of the AN/TPN-22 radar, (2) contributing to range safety by making possible visual observation of the test site runway from an indoor operations center, and (3) providing an integrated record of test parameters, conditions, and results on video tape.

The TV-tracker performs these functions by superimposing a cursor upon a television format display of an aircraft on landing approach and moving the cursor in response to real time changes in the tracking solution of the AN/TPN-22 precision approach radar (PAR). Included on this same display is an alphanumeric presentation of test parameters. The TV-tracker system is operated from a terminal keyboard and CRT display. The tracker has an accuracy of better than plus or minus one milliradian in azimuth and elevation. The minimum update rate of the cursor position and alphanumeric test data is five times per second. The system is designed to maintain target visibility from a range of four nautical miles to touchdown and to maintain stable calibration.

During the course of this contract, the quality of the video signal from the government furnished television camera with the telephoto lens degraded to the point that it was unusable. This condition was not remedied and, consequently, no reportable work was performed on this task during the current effort.

SECTION 3
AIR TRAFFIC CONTROL SYSTEM DEFINITION

Georgia Tech was tasked to investigate four areas concerning the MATCALS Airport Surveillance Radar (ASR). These areas were defined during a visit by Mr. Lewis Buckler of NAVELEX to Georgia Tech in January 1983. During that visit, all of Tech's previous work in the area of ASRs and radar beacon systems pertaining to the MATCALS system was presented. Three of the four task areas address concerns of specification and testing for an ASR system. The fourth task was identified during a meeting at NAVELEX, also in January 1983. The four task areas include:

1. Specification of an MTI improvement factor,
2. Generic L-band versus S-band tradeoff considerations for the ASR,
3. Specification of radar receiver sensitivity,
4. Remoting the ASR from the Control and Central Sybsystem (CCS) via a fiber optic data link.

The following subsections present the results of these studies.

3.1 MTI IMPROVEMENT FACTOR

The improvement factor required of an MTI filter depends upon the expected target and clutter signal distributions and the required detection performance. At decimeter wavelengths, Rayleigh models of target and clutter statistics are often used, as represented by the Swerling target models. For a given probability of detection (P_D) and probability of false alarm (PFA), the required single pulse, signal-to-interference (S/I) ratio can be computed for each Swerling case, as shown for example in Figures 2.7 and 2.23 of Skolnik's Introduction to Radar Systems.[3]

The surface clutter cross section is given by

$$\sigma_c = \sigma^o A$$

where σ^o is the clutter backscatter coefficient and A is the surface area illuminated by the beam. For the MATCALS ASR scenario, the area is approximately

$$A = \left(\frac{c\tau}{2}\right) (R\phi)$$

where $\frac{c\tau}{2}$ is the range resolution, R is the range to the clutter area and ϕ is the 3 dB azimuth beamwidth. The signal-to-clutter ratio at the input to the receiver is

$$\frac{S}{C} = \frac{\sigma_t}{\sigma_c}$$

where σ_t is the target cross section. If the S/C ratio is less than the required S/I ratio, then MTI filtering is necessary, and the required improvement factor, I, is given by

$$I = (S/I)/(S/C)$$

For large clutter areas the total surface clutter backscatter power can exceed the total target backscatter power by several orders of magnitude. However, the clutter power is spread over a much wider Doppler frequency range than that of the target and has its maximum value at zero frequency. The target's Doppler spectrum, on the other hand, is very narrow and is centered at a frequency given by

$$F_d = \frac{2v}{\lambda}$$

where v is the target's velocity radial to the radar line of sight and λ is the radar wavelength. The MTI filter is designed to take advantage of this fact by filtering out the clutter spectral components below its cutoff frequency. The filtered clutter spectrum can be determined by multiplying the original clutter spectrum by the MTI response function.

The MTI improvement factor is the ratio of the area under the original spectrum to the area under the filtered one. For sufficient clutter rejection, this factor should be greater than or equal to the required improvement factor computed previcusly.

3.1.1 RADAR CLUTTER MODELS

The characteristics of radar clutter returns have been extensively examined. However, because of the wide variety of clutter types and target-clutter scenarios, no comprehensive organized systematic approach to clutter modelling exists. The present analysis concerns the clutter backscatter coefficients and spectral characteristics of ground and rain clutter at L- and S-bands. Examples of typical clutter distributions are given, and a list of references is provided for further information.

3.1.2 GROUND CLUTTER

Ground clutter characteristics cannot be easily defined, as they vary greatly with the type of terrain and the incidence angle of the radar beam. Buildings will provide large specular returns with minimal Doppler spread. Trees, on the other hand, are considerably less reflective, but their backscatter contains significant Doppler components. In an MTI radar system, the large building return will be filtered out, while higher frequency components of the tree backscatter might be passed through. For this reason, the present analysis focuses on the characteristics of tree clutter at L- and S-bands.

3.1.2.1 Backscatter Coefficients

The backscatter coefficient (σ^o) of the tree clutter has been examined at a variety of transmit frequencies and incidence angles. Tables and graphs of backscatter coefficients for the various parameters have been compiled by Skolnik,[3,4] Nathanson,[5] Long.[6] and others. The results vary considerably from source to source and no single number can be distilled that uniquely characterizes tree clutter. Skolnik[3] cites curves for median values of σ^o as a function of transmit frequency for various types of terrain. These numbers indicated that the return is relatively insensitive to transmit frequency in the region of interest and that the median σ^o for trees is approximately -20 to -25 dB. Nathanson[5] gives tables of σ^o as a function of transmit frequency and incidence angle. His numbers indicate a σ^o of -25 to -30 dB at low ($\leq 1^o$) grazing angles for both frequencies. At higher incidence angles ($\geq 10^o$) the reflectivity increases to approximately -20 dB for both L- and S-bands. Considering the variety of σ^o values reported, the choice is almost arbitrary for a theoretical analysis. Barring the possibility of actually measuring the reflectivity of the area of interest, a value of -20 dB for σ^o represents a conservative estimate.

3.1.2.2 Spectral Characteristics

Considerably less information is available concerning the spectral properties of tree clutter. L-band data are particularly sparse. Barlow[7] cites power spectra for various types of terrain at 1 GHz. These data indicate a half power Doppler width of approximately 2 Hz for wooded hills in a 20 mph wind. Similarly, Hayes[8] presents a tree clutter spectral model at S-band drawn from 15 mph wind blown trees. This spectral model is presented in Figure 3.1. From the rolloff frequencies shown, it is clear that the

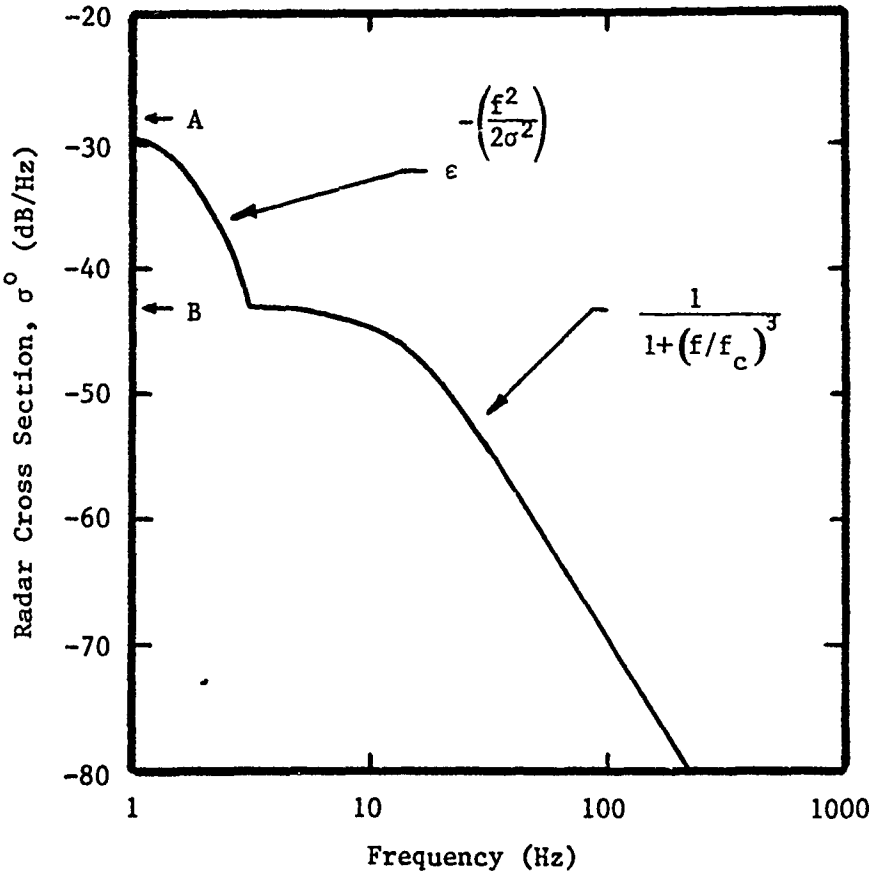

Band	f_c (Hz)	σ (Hz)	A (dB m^2/m^2/Hz)	B (dB m^2/m^2/Hz)
L	-	0.8	-	-
S	1.2	0.1	-22	-37
C	4.2	0.36	-25	-40
X	13.3	1.14	-28	-43
Ku	22.0	1.9	-28	-43
Ka	53.0	3.4	-29	-44
M	140.0	5.7	-29	-44

Decorrelation Time
(for correlation coefficient = 0.15)

Band	Decorrelation Time (ms)
S	56
C	23
X	14
Ku	7.6
Ka	2.3
M	0.56

Figure 3.1. Spectral Distribution of Wind Blown Trees at 15 mph

spectral width of the tree clutter at S-band is also on the order of a few Hertz, which corresponds to tree component velocities on the order of 0.2 mph. Considering the minimum target velocities for the MATCALS scenario, tree clutter is not likely to present a severe problem.

3.1.3 RAIN CLUTTER

Airport surveillance radars (ASR) characteristically employ cosecant-squared type fan beams to attain the necessary elevation coverage. By their very nature, these radars are extremely susceptible to volume clutter effects and, in most cases, employ some means of reducing the effect either through the use of circular polarization or special MTI filters. Measuring the effectiveness of these filters requires some assumption of potential rain clutter characteristics.

3.1.3.1 Backscatter Coefficient

The backscatter coefficient, or reflectivity (η^o), of rain clutter is strongly dependent upon rain rate. The most representative equation for rain reflectivity is

$$\eta^o = Cr^m$$

where η^o is the reflectivity in m^2/m^3, r is the rain rate in mm/hr, and C and m are constants dependent upon the transmit frequency. This equation has been demonstrated to be reasonably accurate up to 95 GHz.[9]

Nathanson[5] presents measured reflectivity data at L- and S-bands for rain rates of 0.25, 1, 4, and 16 mm/hr. At L-band, the reflectivity equation is approximately

$$\eta^o = 2 \times 10^{-11} \, r^{1.67};$$

this gives a value of -97 dBm^{-1} at 4 mm/hr. At S-band the equation is

$$\eta^o = 6.3 \times 10^{-10} \, r^{1.58},$$

which results in a reflectivity of -83 dBm^{-1} at 4 mm/hr. These empirical equations are based on measured reflectivity values derived from Nathanson.[5] The 14 dB difference between the two values indicates that rain is 25 times more reflective at S-band than at L-band.

3.1.3.2 Spectral Characteristics

The wide variety of phenomenological conditions in which rain can be present implies a wide range of possible spectral characteristics. Rain rates of from 0.25 mm/hr to 100 mm/hr have been observed in wind conditions ranging from 0 mph to over 100 mph. The extent and type of radar coverage also affects the spectra. A short range radar with a narrow beamwidth will see a more limited rain spectrum than a long range airport surveillance radar. In fact, the ASR's under consideration are susceptible to the most severe rain clutter effects due to their wide elevation beamwidths and long detection ranges.

In Radar Design Principles,[5] Nathanson presents a discussion of rain phenomenology and the resulting effect upon the Doppler spectrum. He cites four basic mechanisms responsible for rain clutter velocity components: wind shear, beam broadening, turbulance, and fall velocity distribution. Wind shear is the everpresent gradient in wind velocity with altitude which results in a spread of detected radial rain velocities. This effect is particularly severe for radars with a large elevation beamwidth. Beam broadening is the spread in radial velocities detected due to the finite width of the beam in azimuth when the radar is looking crosswind. Turbulance is the fluctuation of wind currents which also results in velocity spreading. Finally, fall velocity distribution is the spread in fall velocities due to varying particle sizes.

Nathanson examines the four mechanisms in great detail in terms of their effect upon radar systems. The basic spectral form is modelled as a Gaussian distribution with the standard deviation being a composite of the four effects. The total standard deviation is given by

$$\sigma_v = (\sigma_s^2 + \sigma_b^2 + \sigma_t^2 + \sigma_f^2)^{1/2} (m/s).$$

where the subscripts denote the four components as cited. The latter three components are on the order of 1 m/s or less, whereas for a broad elevation beamwidth, σ_s can be as large as 5 or 6 m/s. Clearly, wind shear is the predominant effect in the ASR environment.

Figure 3.2 depicts the wind shear spectrum drawn from Nathanson. If the velocity gradient of interest is measured at the half power points on the Gaussian spectrum, it is related to σ_s by

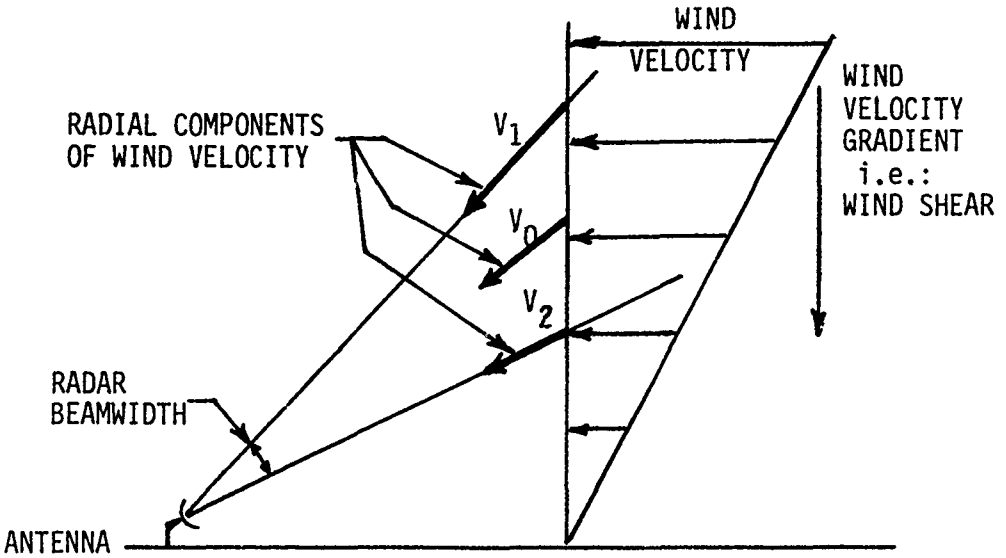

Figure 3.2a. Wind Shear Geometry

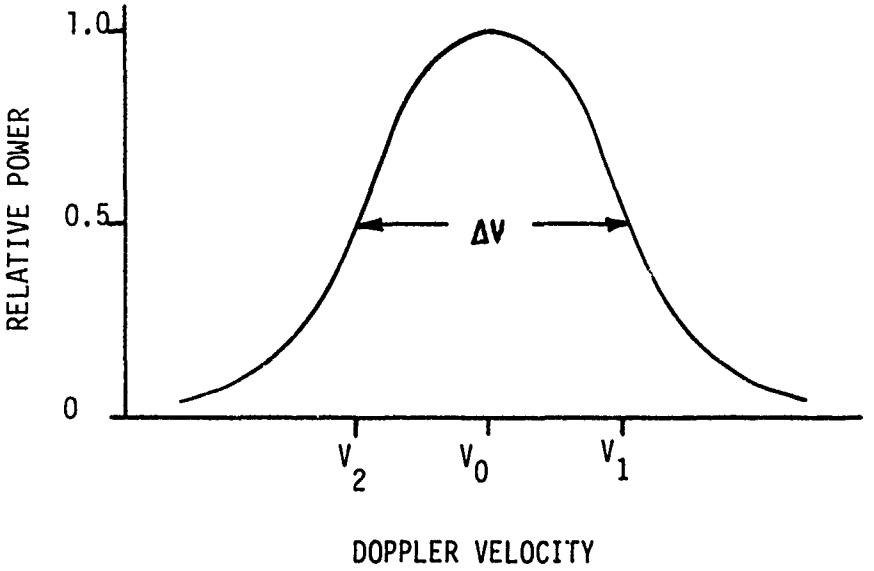

Figure 3.2b. Doppler Spectrum Due to Wind Shear
(from Nathanson, p. 207)

$$\sigma_s = 0.42\ (\Delta V).$$

If $\sigma_s = 5$ m/s, then $\Delta V = 12$ m/s, and the spectrum will run from approximately 0 m/s to approximately 12 m/s, which is 140 Hz at L-band and 280 Hz at S-band. These results compare favorably with measured distributions. Typical distributions may be found in Figure 8.2 of Louis Battan's Radar Observation of the Atmosphere[10] for rain and snow.

3.2 TRANSMIT FREQUENCY SELECTION

3.2.1 INTRODUCTION

The transmit frequencies employed in airport surveillance radars extend from 1.2 GHz (L-band) to 3 GHz (S-band). The 3 GHz upper limit is primarily driven by the detection range requirements; at higher transmit frequencies, weather-induced attenuation becomes severe. The 1.2 GHz lower limit is a result of physical limitations on the size of both the antenna and the waveguide. The fact that production ASR systems operate at both L- and S-band frequencies suggests that no clear-cut choice exists between the two. This discussion will examine some of the parameters involved in a frequency trade-off, the relative importance of the parameters, and the preferred frequency for each.

3.2.2 PHYSICAL LIMITATIONS

The MATCALS scenario requires a compact, transportable ASR system that can be quickly deployed. This clearly places a restriction on the size of both the antenna and the radar system itself. For a fixed aperture size, the L-band 3 dB beamwidth will be twice that at S-band. At S-band, a 1.5° azimuth beamwidth, for example, corresponds to an antenna width of 4 meters. At L-band, the width would have to be 8 meters. The increase in antenna size adversely affects both the durability and the transportability of the ASR system. If the angular accuracy requirements do not demand a 1.5° beamwidth, the transportability of the system could be retained at L-band by using the same 4 meter antenna and accepting a 3° beamwidth. An examination of existing ASR systems compiled in previous Georgia Tech[1,2] reports confirms this latter conclusion. The S-band beamwidths of the ASR-7, ASR-8, GPN-20, and TPN-24 range from 1.2° to 1.5°. The two major L-band systems, the TPS-44 and the TPS-65, have beamwidths of 2.8° to 3°. Clearly, production ASR system all employ antennas of approximately 4 meter aperture.

The size of the rest of the radar system is also of concern. Unlike the antenna size, however, the total system size is a function of numerous independent factors, such as the transmitter size, the amount of waveguide employed, and the complexity of ancillary support equipment. Cooling systems, waveguide pressurization systems, sophisticated signal processing equipment, and other refinements all occupy space and increase the complexity of the ASR These complexities are not strictly wavelength dependent, but are also functions of the sophistication of the system.

3.2.3 HARDWARE CONSIDERATIONS

Theoretical considerations are used to determine radar system parameters such as peak transmit power and antenna aperture size. These requirements must be modified by the capabilities of the existing hardware. This involves consideration of available transmitter sources, reference oscillator stabilities, receiver noise characteristics, waveguide losses and power limitations, antenna tolerances, and antenna servo motor capabilities.

Fortunately, at the wavelengths and ranges under consideration, many of these factors introduce no limitation on the system performance. The required transmitter power and stability are available at both frequencies. Advances in electronic circuitry have enabled production of extremely sensitive receivers at L- and S-band. Digital processing techniques allow efficient and economical multiple delay line cancellers to be employed, and MTI improvement factors greater than 50 dB should be possible. The main limitation on the attainable MTI improvement is not due to hardware restrictions, but rather to phenomenological effects. These factors will be considered in the following section.

The power loss in waveguide is small at decimeter wavelengths, but the problem of arcing is of considerable concern due to the megawatt peak powers transmitted by some of the systems studied. Theoretical power ratings for standard L- and S-band waveguides are presented in Skolnik's Radar Handbook.[4] The power rating of L-band waveguide is three times that of S-band waveguide. Because of this, much more power can be transmitted at L-band without introducing the problem of waveguide arcing. In fact, all production S-band ASR systems employ pressurized waveguide, presumably to circumvent arcing problems. This implementation introduces additional bulk and complexity to the ASR system, making it less useful in the MATCALS scenario. The majority of the L-band systems do not employ waveguide pressurization. The exception

is the TPS-65 which does not actually use waveguide. The TPS-65 uses dielectric coaxial cable which occupies considerably less space than L-band waveguide. Dessicated air is used as the dielectric, so while actual pressurization is not employed, a pumping system is required to transport the dry air in the cable.

The desirability of a simple, easily transportable ASR system must be tempered by the performance requirements of the MATCALS scenario. The MATCALS ASR system will be transported in a jet aircraft at ambient temperatures of below -30°C. It must be quickly deployed and operated in numerous environments including high temperature and humidity conditions. Under these conditions, condensation inside the waveguide is almost inevitable, and some form of pressurization or dessication would be necessary to make the system operational. For this reason, the added complexity and weight of a waveguide pressurization unit is probably a necessary evil because of the wide variety of MATCALS environments.

The required ASR antenna size was considered in the previous subsection. It was determined that antennas of equivalent size could be employed at both frequencies if the increase in azimuth beamwidth at L-band was acceptable. In this case, the L-band system would be somewhat simpler to build since antenna tolerances are less severe at longer wavelengths. On the other hand, if a larger antenna were required, this would put a much greater strain on the antenna gimbals and motor. These parts would be more expensive and more inclined to fail than those for a smaller antenna.

3.2.4 ENVIRONMENTAL FACTORS

The greatest differences between L- and S-bands involve the effects of environmental phenomena and the radar and signal processing techniques used to remove them. The most pronounced interference is induced by meteorological reflectivity, but the effects of attenuation, ground clutter, and multipath interference must also be considered.

3.2.4.1 Attenuations

The effects of atmospheric and meteorological attenuation are almost negligible at both L- and S-band frequencies. From Nathanson's Radar Design Principles,[5] two-way atmospheric attenuation at 0° elevation is 1.3 dB at L-band and 1.6 dB at S-band for target ranges of 60 nmi. These values compare closely to those presented in Skolniks' Radar Handbook.[4]

The effect of meteorological attenuation is also virtually negligible at these long wavelengths. Skolnik presents S-band values for a variety of rain rates. For a 60 nmi maximum range, a 4 mm/hr rain rate would result in 0.3 dB of attenuation; 23 mm/hr results in 1.6 dB of attenuation. At L-band, the attenuation would be even less noticable.

3.2.4.2 Rain Clutter

The influence of rain clutter is of concern in virtually all radar applications, but it is particularly severe for ASR applications. Because of the large elevation coverage required (0.5^{o} to 30^{o}), the entire vertical extent of a rain storm will be illuminated by an ASR. This means that both the reflectivity and the spectral content of the rain clutter will be maximized.

The reflectivity of rain is reported in Nathanson to be -97 dBm^2/m^3 and -83 dB m^2/m^3 for 4 mm/hr rain at L- and S-bands, respectively. A rain rate of 4 mm/hr is considered moderate, but typical, and rain rates of 25 and 50 mm/hr have often been observed. At 50 mm/hr, the rain reflectivity increases to -77 dB m^2/m^3 at L-band and -65 dB m^2/m^3 at S-band.

The reflectivity of rain varies inversely with the fourth power of the wavelength. So, for identical resolution cells, the S-band radar will receive 16 times (12 dB) more rain clutter than the L-band system. If the same antenna width is assumed, the S-band resolution cell will be one-half the size of the L-band cell, so the net increase in rain clutter backscatter from L- to S-band is approximately 9 dB. Because of this, all production S-band ASR's employ circular polarization to reduce the rain clutter interference. Most manufacturers assume a circular polarization rain reduction of approximately 20 dB. Circular polarization also reduces the strength of the target return by approximately 7 dB. In the worst case, this results in a net signal-to-noise ratio improvement of 13 dB. Since the rain return within the resolution cell at S-band is 9 dB greater than at L-band, the 13 dB improvement due to circular polarization actually results in 4 dB better rain rejection at S-band than a simple L-band system with no rain rejection processing.

The use of circular polarization at L-band is generally not considered necessary because of the lower rain clutter reflectivity. However, the TPS-65 L-band system does employ a cascaded filter designed specifically for rain rejection. This implies that rain clutter was of significant concern to one L-band manufacturer.

3.2.5 MTI IMPROVEMENT FACTOR LIMITATIONS

The theoretical improvement factor attainable in an MTI system is limited by the spectral spread of the clutter return. This spread is the result of both antenna scanning motion and internal clutter motion. These effects have been documented in detail by Barton[11] and Skolnik[4], for both simple cancellers and staggered PRF systems.

3.2.5.1 Antenna Scanning Limitations

The motion of the radar beam across the clutter cell induces a spectral component independent of the clutter itself. This spectrum is a function of the beam shape but can be assumed to be Gaussian. From Skolnik's Radar Handbook,[4] Section 17.3, the standard deviation of the clutter spectrum due to antenna scanning is given by

$$\sigma_c = \frac{.265\ f_r}{n} \tag{3.1}$$

where

f_r = the pulse repetition rate,

n = the number of pulses on target, and

σ_c = the spectrum standard deviation due to antenna scanning.

Using Barton's approach for the calculation of MTI improvement factor limitations, Skolnik derives three equations for the improvement factor, I, for single-, dual- and triple-delay cancellors respectively,

$$I_1 = \frac{n^2}{1.39} \tag{3.2}$$

$$I_2 = \frac{n^4}{3.84} \tag{3.3}$$

$$I_3 = \frac{n^6}{16} \tag{3.4}$$

where

n = the number of pulses on target,

I_1 = MTI improvement factor for single-delay, no-feedback, coherent canceller,

I_2 = MTI improvement factor for dual-delay, no-feedback, coherent canceller,

I_3 = MTI improvement factor for triple-dalay, no-feedback, coherent canceller.

The functions are plotted in the Radar Handbook in Figure 17-11.

For a staggered PRF system, there will be an additional, independent limitation on I as a result of the varying pulse repetition frequency. Most clutter returns will vary slowly in amplitude relative to the pulse repetition frequency (f_r). Thus, over a period of a few pulses, any clutter signal can be represented by a linear waveform, $V(t) = C + \alpha t$.[4] If f_r is fixed, a multiple-delay canceller will perfectly cancel the clutter signal since the constant C will be removed by the first stage and the slope, α, will be removed by the second. On the other hand, if pulse-to-pulse staggering is employed, the waveform will be sampled at unequal periods, resulting in a voltage residue. This residue restricts the improvement attainable and is a function of the PRF stagger ratio. According to Skolnik, the improvement limitation is given by

$$I_S = 20 \log \frac{2.5n}{\delta - 1} \tag{3.5}$$

where

n = the number of pulses on target, and

δ = the PRF stagger ratio.

This improvement factor equation is plotted in Figure 17-15 of Skolnik's Radar Handbook.

Equations (3.2) through (3.5) can be applied to the ASR transmit frequency analysis if some nominal values for certain radar parameters are assumed: average f_r = 1,000 Hz, scan rate = 10 rpm, and antenna width = 4 meters. The stagger ratio will be assumed to be 1.2. This value represents a good compromise between improvement factor limitation and staggered response function null depth.

The improvement factor limitations due to antenna scanning for both fixed PRF delay line cancellers and for a staggered PRF system are given in Table 3.1. The main results is that, if dual-delay cancellation or pulse staggering are employed, the MTI improvement achieveable is greater than 50 dB at S-band and 56 dB at L-band.

TABLE 3.1.

MTI IMPROVEMENT FACTOR LIMITATIONS DUE TO ANTENNA SCANNING

FREQUENCY BAND	N	I_1	I_2	I_3	$I_{STAGGER}$
L	50	33	63	70	56
S	25	28	52	70	50

N = The number of pulses on target

I = Maximum MTI improvement factor (dB)

3.2.5.2 Internal Clutter Motion

The improvement factor is also limited by internal clutter motion. The greater the standard deviation of the motion, the broader the clutter spectrum and the more residual clutter power out of the MTI filter. For standard delay line cancellers, Barton[11] derived the improvement factor limitations, assuming Gaussian distributed clutter spectra, to be

$$I_1 = 2\left(\frac{f_r}{2\pi\sigma_c}\right)^2 \tag{3.6}$$

$$I_2 = 2\left(\frac{f_r}{2\pi\sigma_c}\right)^4 \tag{3.7}$$

$$I_3 = \frac{4}{3}\left(\frac{f_r}{2\pi\sigma_c}\right)^6 \tag{3.8}$$

where

I_1 = MTI improvement factor for single-delay, no-feedback, coherent canceller,

I_2 = MTI improvement factor for dual-delay, no-feedback, coherent canceller,

I_3 = MTI improvement factor for triple-delay, no-feedback, coherent canceller,

σ_c = rms frequency spread of clutter power spectrum, Hz,

f_r = radar repetition frequency, Hz.

These equations are plotted in the Radar Handbook in Figures 17-12 to 17-14 as a function of λf_r.

The above equations do not account for PRF staggering. Skolnik derives the improvement factor limitation for a staggered system by substituting Barton's[11] equation for n,

$$n = \frac{1.66\ f_r}{2\pi\sigma_c}, \tag{3.9}$$

into the limitation Equation (3.5). The resulting expression for I is

$$I = 20 \log \left(\frac{0.33}{\delta - 1}\right) \frac{\lambda f_r}{\sigma_\sigma} \tag{3.10}$$

where

σ_σ = rms clutter velocity spread.

This improvement factor is plotted in Figure 17-16 of the Radar Handbook as a function of λf_r.

These four improvement factor limitation equations can be used to analyze the response of the potential ASR systems under consideration. If the general radar parameters presented earlier for pulse repetition frequency (f_r), antenna width, scan rate, and stagger ratio are used, the MTI limitations that result are presented in Table 3.2. Two types of clutter motions were assumed. A standard deviation of clutter motion (σ_σ) of 0.3 m/s was used to determine the MTI response in a typical tree clutter environment. A σ_σ of 3 m/s was also included to predict the performance in a rain clutter environment. The results are interesting. For tree clutter, the improvement factor at both frequencies is essentially limited by the pulse staggering to 55 dB at S-band and 61 dB at L-band. For rain clutter, however, the S-band improvement is limited to 27 dB in a triple delay canceller while the L-band improvement is limited to 41 dB due to staggering. If more sophisticated MTI circuitry were employed at S-band, the improvement in rain clutter could be increased to 35 dB.

To summarize the results, for the nominal ASR systems postulated, in a clear air tree clutter environment, the MTI improvement factor for both systems is limited by antenna scanning and PRF staggering. The S-band system is limited to a 50 dB improvement while that for L-band is limited to 56 dB. In a rain clutter environment, the L-band improvement is limited to 41 dB due to PRF staggering. The S-band improvement in rain is limited to 27 dB for a triple delay cancellor or 35 dB for a quadruple delay cancellor where the limit on improvement is due to the effect of PRF staggering. This results in a 6 dB advantage at L-band in rain clutter, unless circular polarization is employed at S-band. In that case, the L- and S-band systems should have

TABLE 3.2.

MTI IMPROVEMENT FACTOR LIMITATIONS DUE TO INTERNAL CLUTTER MOTION

σ_v (M/S)	FREQUENCY BAND	λf_r (cm Hz)	I_1	I_2	I_3	$I_{STAGGER}$
0.3 (tree clutter)	L	20,000	37	70	70	61
0.3 (tree clutter)	S	10,000	31	58	70	55
3 (rain clutter)	L	20,000	17	38	44	41
3 (rain clutter)	S	10,000	11	19	27	35

approximately equal performance. Note that this performance prediction is predicated on obtaining optimal performance from the two systems. In practice, this is not achieved. Oscillator instabilities, MTI processor design, and other factors limit the MTI performance of S-band systems to about a 35 dB improvement while that for L-band is typically 50 dB.

3.3 RADAR RECEIVER SENSITIVITY

The preferred method of specifing radar receiver sensivity is not to specify it directly, but instead to make it part of the over-all radar performance specification. Thus, the required receiver sensitivity is a function of target model, size and range, atmospheric conditions, clutter model, probability of detection and false alarm rate, radar dwell times, and antenna scan rates. However, there are times when the radar receiver must be purchased as a subassembly. In these cases, it is important to specify the receiver in such a manner that it can be tested against the specification.

Radar receiver sensivity can be evaluated by directly measuring the minimum discernible signal (MDS), or by measuring tangential sensitivity (St) and calculating MDS, or by measuring noise figure (Fn) and calculating MDS.

Minimum discernible signal (MDS) is defined as the minimum input signal level than can be discerned by the operator, i.e., the signal is approximately equal to receiver noise level. Since some operators are much better than others at detecting signals in background noise, measurement errors of 2 or 3 dB can be expected. A typical MDS measurement set-up is shown in Figure 3.3. The input signal is made to replicate the pulses transmitted by the radar as closely as practical. The attenuator is adjusted until the signal just disappears into the background noise as shown in Figure 3.4. Then the signal is varied in time by delaying the signal generator more or less (with respect to the radar trigger pulse) to aid in discerning the signal, and the attenuator is readjusted to make the signal almost disppear into the noise. The process is continued until the signal is judged to be minimally discernible. MDS is read as the signal power level at the input of the receiver (attenuated signal generator output) with the signal minimally discernible in the receiver output above the noise floor.

Tangential sensitivity is measured similarly to MDS. But instead of adjusting the attenuator to make the signal almost disappear into the noise, it is set so that the signal is well above noise. Tangential sensitivity is indicated when the top of the noise envelope is approximately even with the bottom of the envelope of signal plus noise. A typical A-scope display is shown in Figure 3.4. MDS can be estimated by the equation

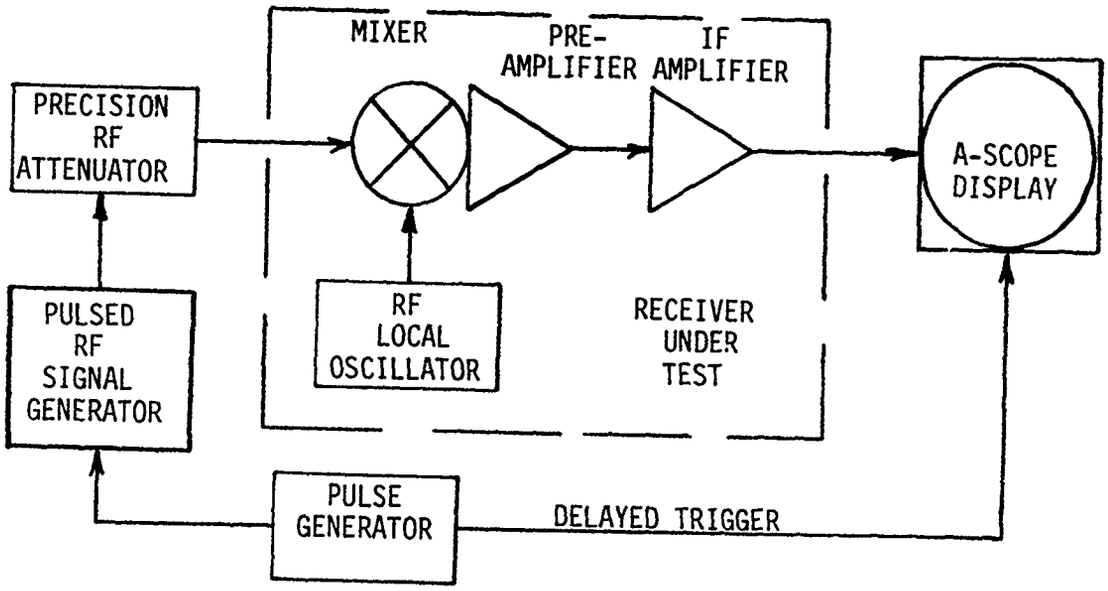

Figure 3.3. Radar Receiver Test Set-up

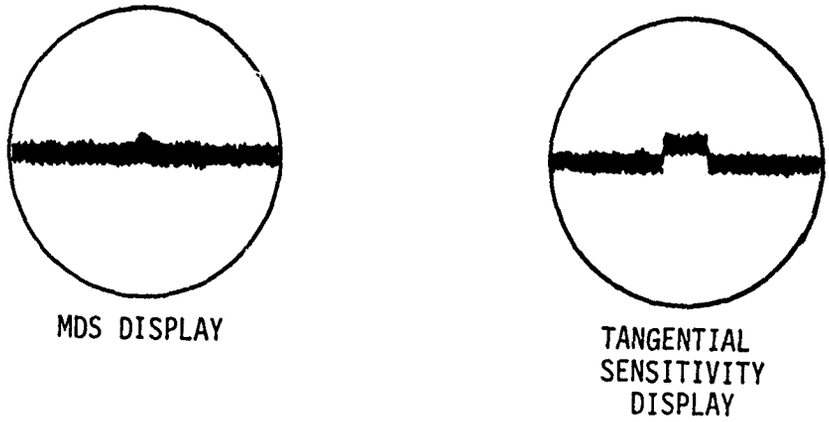

Figure 3.4. Typical MDS Signals

MDS= St-8 dB.

The value of 8 dB, while not universlly accepted, can be justified by examining probability of detection curves for a steady signal in uniform noise. These curves[4,12] indicate that, given a probability of detection of 90% and a probability of false alarm of 10%, the signal-to-noise ratio will be about 8 dB. Other arguments have been used to justify values ranging from 6 to 10 dB.

MDS can be calculated from measured noise figure if the receiver bandwidth, losses, and processing gains are known. Radar receiver noise figure can be measured using a standard noise source and a noise figure meter, using either a manual or automatic methods. The manual procedure is more accurate but the automatic method is much more convenient for repetitive measurements. Measurement accuracy is about 0.7 dB for manual methods and about 1 dB for automatic methods. Under special circumstances, measurements within about 0.1 dB of the National Bureau of Standards can be obtained. But the NBS standard itself has an error potential of 0.5 dB. The theory and test procedure of noise figure measurement is explained in section 5 of Reference 13, the instruction manual for the "AILTECH 75 Precision Noise Figure Indicator." Similar instruments are available from Hewlett Packard, Sanders Associates, and others. Further explanation of noise figure, noise factor, and noise temperature can be found in the literature.[14.15,16] MDS can be calculated from noise figure using the following equation:

$$MDS = kTBFnLs/Gp$$

where k is Boltzmann's constant (-204 dB W/Hz), T is absolute temperature (290 Kelvin), and B, Ls, and Gp are the system constants of noise bandwidth, receiver losses, and processing gain, and Fn is the measured noise figure.

3.4 FIBER OPTIC DATA LINK FEASIBILITY STUDY

3.4.1 BACKGROUND

The use of fiber optics (FO) in the communications industry, the medical field, and the military area has grown tremendously over the past five years and shows further growth potential for the future. The usefulness of FO in these areas is due to its well known advantages of wide bandwidth, low cost, weight and size reduction, electrical isolation, almost complete immunity to electromagnetic interference (EMI), and low loss.[17] Table 3.3 is a comparison of the three major cable types: twisted pair, coaxial, and FO. Among the applications of FO to radar systems and signal processing are FO delay lines for signal processing[18], the phasing of antenna array elements using FO[19], FO slip rings[20], and the use of FO for remoting the radar transmitters from the operations shelter[21]. The Radar and Instrumentation Laboratory of the Georgia Institute of Technology Engineering Experiment Station has evaluated the application of FO technology to radar systems. Refer to the Appendix for a description of a recent Georgia Tech research project which studied remoting of several radars using fiber optics.

The use of FO for remoting the radar transmitter from the operations shelter (OPS) is the subject of consideration for this study. Remoting the transmitter from the OPS allows (1) better radar coverage through geographic dispersion, (2) command and control center protection from homing anti-radiation missiles (HARMS), and (3) improved operations in a jamming environment. An additional advantage to remoting the radar transmitter is that the tactical site selection will be less constrained[22].

Remoting the transmitter from the OPS can be acomplished in three ways: (1) landlines, (2) radio microwave link (RML), or (3) fiber optics. Table 3.4 compares these three remoting techniques in terms of their various pertinent characteristics. The remoting of the AN/FPN-62 radar (by ITT Electro-Optical Products Division[23]) and the AN/TPS-43E radar (by MITRE,[21,24]) have both demonstrated the FO method of remoting radar transmitters. These radars exhibited significant advantages by using FO instead of landlines or an RML. The MITRE radar FO link was half the weight of landlines, while allowing a 45 times greater remoting distance. The RML also cost significantly more. These considerations and physical parameters are indicative of FO and exemplify the propulsive efforts to employ FO in remoting radars.

TABLE 3.3. COMPARISON OF MAJOR COMMUNICATIONS CABLE TYPES

CHARACTERISTIC	TWISTED PAIR	COAXIAL CABLE	FIBER OPTICS CABLE
Length-bandwidth product (MHz km)	1	20	800
Spacing between repeaters (km)	1-2	1-2	2-10*
System cost	Low, slow increase in future	Medium now, slow increase in future	Medium to high, decrease in future
System lifetime (years)	20-40	20-40	10-40
Crosstalk	High	Low	Negligible
Noise immunity	Low	Medium	High
Electrical Input-Output Isolation	No	No	Complete
Vibration tolerance	Good	Good	Good
Short-circuit loading	Yes	Yes	No
Weight, size	High	High	Low
Cable connections	Soldering, standard connectors	Soldering, standard connectors	Splicing, well-aligned connectors
Fabrication control requirements	Loose	Medium	Precise

*Values are for multimode fiber optic systems at 800-900 nm wavelengths. At longer wavelengths, lower loss results in longer repeater spacing.

TABLE 3.4. COMPARISON OF RADAR REMOTING METHODS

CHARACTERISTIC	LANDLINES	RADIO MICROWAVE LINK	FIBER OPTIC
Bandwidth capacity	Low	High	High
Cable Weight	High	None	Low
Terminal equipment weight	Moderate	Heavy	Moderate
Cost	Moderate	High	Moderate
Deployment speed	Slow	Fast	Fast
Line of sight required	No	Yes	No
Maxiumum remoting distance	12,000 ft (4 km)	10 nmi (18.5 km)	10 km** (@ 850 nm) 20 Km** (@ 1300 nm)
Blockage a problem	No	Yes	No
Susceptible to HARMS*	No	Yes	No
Electromagnetic Interference a problem	Yes	No	No
Lightning a problem	Yes	No	No
Expandability	Low	High	High
Status of development	Developed	Developed	Technology demonstrated, more development needed

*Homing anti-radiation missiles

**This assumes a total fiber cable loss of 45 dB (including 5 dB of connector and miscellaneous losses) resulting from losses of 4 dB/km at 850 and 2 dB/km at 1300 nm.

3.4.2 COST ANALYSIS

A survey of several fiber optic system manufacturers was made recently to determine the cost of currently available optical fiber cable and electro-optical components for the MATCALS application. This information has been used to determine the cost of remoting a radar transmitter from the operations shelter by employing a fiber optic link. The following conditions were assumed.

1. Remoting length of 3 km.
2. Transmission requirements:
   a. Two one-way video paths
   b. One one-way audio paths
   c. One two-way control signal path
3. A spare optical fiber will be included in the cable.
4. Transmitter and receiver electronics must operate over a $-20^{o}C$ to $50^{o}C$ range.
5. Optical fiber cable must operate over a $-54^{o}C$ to $+71^{o}C$ range.
6. No repeaters will be employed in the 3 km link, but one cable splice will be allowed.

The companies contacted were ARTEL Communications, ITT-EPOD, and Siecor Optical Cable. The information obtained from these sources was used to estimate the cost of a fiber optic link. If multiplexing is not employed, a minimum of five fibers and five transmitter-receiver pairs will be required. The cost for such a system would be as follows:

Five transmitter-receiver pairs	$13,500
Three km of six-fiber cable	$19,500
Cost per link	$33,000
Cost for 17 links	$561,000

The cost of optical fiber cable and electro-optical transmitter-receiver pairs can be reduced by employing multiplexing. For example, if the two-way communication required for this remoting link can be accomplished by employing two transmitter-receiver pairs and a four-fiber cable, the cost for one 3 km link would then be approximately $17,500 and the cost for 17 systems would be approximately $200,000. Of course, multiplexing hardware will absorb some of the difference, but an overall savings will be incurred if multiplexing techniques are employed.

SECTION 4
AN/TPN-22 FLIGHT TEST PROGRAM

Previous Georgia Tech reports[1,2] recommended that a flight test program be undertaken utilizing the AN/TPN-22 radar system, the MATCALS precision approach radar (PAR). These tests were successfully completed in September of 1982. This flight test program served two purposes. First, it gathered a statistically significant data set for evaluation of amplitude processing tracking algorithms developed by Auburn University and Georgia Tech. These data provide a baseline for evaluating and comparing the different processing techniques. Second, it gathered data useful for isolating the sources of radar tracking error to either radar instrumentation errors, target induced errors, or environmentally induced errors. The flight tests utilized two pieces of equipment designed by Georgia Tech to isolate these errors: a multipath fence and a circularly polarized corner reflector. The details of the analysis and design of these experimental tools are described in a previous Georgia Tech report.[1] Theoretically, both environmentally induced errors, such as multipath interference and clutter, and target scintillation and glint are completely eliminated by utilizing the multipath fence and the circularly polarized corner reflector mounted in the radome of the F-4J test aircraft, thus leaving only the radar instrumentation errors.

Multipath interference can be a significant problem to the AN/TPN-22 radar whenever the main antenna beam intersects the ground. To eliminate these errors, a multipath fence was designed by Georgia Tech and built by NESEA. For the flight test program, the fence was positioned at 310 feet from the radar for those flights with the touchdown offset of 760 feet and at 430 from the radar for those flights with 1500 foot touchdown offset. The expected improvement was previously reported in Reference 1.

The corner reflector, also designed at Georgia Tech and built at the Patuxent Naval Air Station, utilizes a circular polarization grid in front of a trihedral reflector to reflect the correct sense circular polarization. This corner reflector's radar cross section was measured after the flight test by Georgia Tech and was determined to be a nearly perfect even bounce reflector with a radar cross section of approximately 650 square meters (as desired). The radar cross section for the F-4J is only about 10 square meters; therefore, for the test passes with the reflector in place, the numerous scatterers generating the aircraft's return should have been completely dominated by the

echo from the corner reflector, and target induced errors such as scintillation and glint should have been eliminated.

4.1 TEST FLIGHTS

Table 4.1 lists the test flights accomplished in September 1982 and the conditions of each.

TABLE 4.1. TEST FLIGHT CONFIGURATIONS

CONFIGURATION NUMBER	NO. OF PASSES COMPLETED	FENCE	A/C CORNER REFLECTOR	TD RANGE FROM RADAR	COMMENTS
1	2	310'	IN	760'	50' Elevated touchdown
2	3	DOWN	IN	760'	50' Elevated touchdown
3	3	310'	IN	760'	Touchdown on deck
4	6	DOWN	IN	760'	Touchdown on deck
5	3	310'	OUT	762'	50' Elevated touchdown
6	5	DOWN	OUT	762'	50' Elevated touchdown
7	2	310'	OUT	762'	Touchdown on deck
8	3	DOWN	OUT	762'	Touchdown on deck
9	3	430'	IN	1500'	50' Elevated touchdown
10	3	430'	IN	1500'	Touchdown on deck
11	6	DOWN	IN	1500'	Touchdown on deck
12	2	DOWN	OUT	1500	Touchdown on deck

For each flight, tracking data were obtained from the AN/TPN-22 radar and the Automatic Laser Tracking System (ALTS) which serves as the reference for this analysis. Three data tapes were created during each flight test period: (1) the TPN-22 Data Save tape which is a complete record of the actions of the PAR system; (2) the ALTS data which contains the laser tracking data, tagged by the IRIG clock; and (3) a MATCALS data tape, which contains the AN/TPN-22 tracking data tagged by the IRIG clock. Together, these tapes represent a complete record of the flight tests.

During the flight tests, it was observed that the target's return signal with the corner reflector installed was much more stable (i.e., did not fluctuate nearly as much) than it was without the corner reflector. Saturation of the radar receiver was not observed with the reflector installed.

4.2 ANALYSIS PROCEDURE

Figure 4.1 presents the complete analysis procedure for the flight test data.

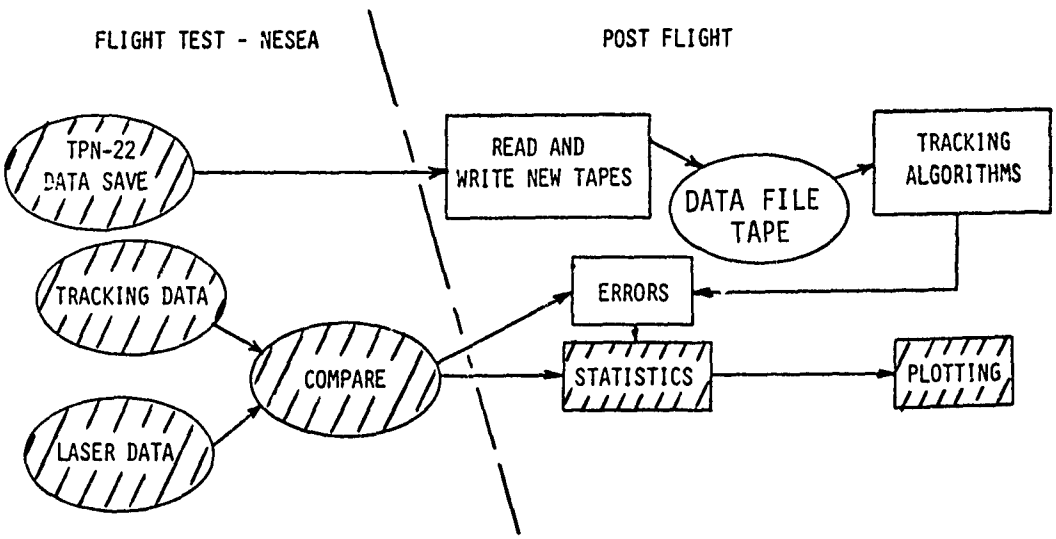

Figure 4.1 Test Flight Data Analysis Procedure

The test flight data were received by Georgia Tech in two forms, the first being the AN/TPN-22 Data Save tape which lists all the radar parameters, including the raw radar return data, for each pass. These data will be used primarly to evaluate new tracking algorithms. Second, a compare data tape which contains the ALTS data, a list of the errors between the ALTS data and the MATCALS tracking data, and the real time clock was written by NESEA. This tape, therefore, contains the tracking error data to be used

to evaluate the tracking performance of the AN/TPN-22 and also the reference position data for comparison when evaluating the new tracking algorithms.

Because of the limited funds available for the analysis of the flight test data, only those areas shown cross-hatched in Figure 4.1 were accomplished during this phase of the contract. The analysis accomplished to date includes generating statistics of the tracking errors contained on the compare tape and plotting those data. During the next phase of the MATCALS program, Georgia Tech will write software to utilize the raw amplitude data contained on the AN/TPN-22 Data Save tape, calculate the errors using the ALTS data as the reference, and compute and plot error statistics. The tracking errors resulting from the new tracking algorithm will then be compared to the current tracking performance and an evaluation made.

The AN/TPN-22 flight test data analysis accomplished in the current phase of the contract consisted of developing and adapting software to read the compare data tape to generate the desired statistics of data and plot the data. Software originally developed by Ken Ross of NESEA was adapted to read the compare data tape and write the data to disk storage for statistical processing. The statistics program, developed by Georgia Tech, generates two types of data: statistics within each pass and statistics across equivalent sets of passes (i.e., those passes with equivalent conditions). For each type of data, the mean and RMS errors within each set of data were computed. The first step in the data analysis procedure was to average errors within each pass. Errors within each pass were averaged over an interval of range to smooth out noiselike effects in the data (while retaining true aircraft motion) and reduce the large quantity of data to a manageable amount to be used in later analysis. The optimum interval over which to perform the smoothing was determined by plotting the mean and standard deviation versus range within the pass obtained by smoothing over 100, 200, and 300 foot intervals for the expected best and worse case configurations. In addition, averaging intervals of 500 feet and 50 feet were utilized for selected plots. These cases were considered extremes of smoothing and were used only as references for the other cases. After systematic comparison of the plots, the 200 foot averaging interval was determined to be optimum for reducing noiselike effects without obscuring meaningful data. The average mean errors thus obtained became the the "new data" to be used in generating the statistics across passes for any particular configuration.

During the process of averaging within a pass, the standard deviation (or RMS error) of the data was also computed. This statistic is a measure of the amount of the

smoothing performed in the averaging process. As such, it is a measure of the RMS deviation, or the noiselike fluctuation within each pass of the reported aircraft position. These data were useful in determining the appropriate smoothing interval and could also indicate the potential value of low pass filtering the reported aircraft position. This data plot also serves as a check of the data because a single wild point could cause a single 200 foot averaging interval to have an unusually large RMS error.

The next step in the analysis procedure is to compute statistics across equivalent passes. Matched 200 foot smoothing intervals are used for each set of passes. Only those intervals containing data for all passes were used in these new computations. The flight tests attempted to gather a statistically significant set of data for each flight configuration. Hence, these data may be viewed as a true measure of the tracking performance of the AN/TPN-22 radar system.

The tracking error averaged across passes indicates whether at a given range the radar will most likely indicate that the aircraft is above or below, to the right or to the left of the correct position. The RMS error, then, indicates the variability about this probable position versus range for both azimuth and elevation. The RMS error term is the best measure of the performance of the radar and can be compared directly to previously predicted performance. Comparison of the plots of these data for the different flight test configurations will make possible the identification of the effects of the three different sources of tracking errors. Flight passes in which the multipath fence and the corner reflector are used should essentially eliminate environmental and target induced errors, leaving only the radar instrumentation errors. Passes with the corner reflector, but without the multipath fence, should add to the previously defined errors, the environmentally induced errors. With the corner reflector removed from the aircraft and the multipath fence erected, then the target scintillation and glint should be evident in addition to the radar instrumental errors. With the multipath fence removed and the corner reflector removed, then all error sources are present. This configuration serves as a baseline performance standard for the AN/TPN-22 radar.

4.3 FLIGHT TEST DATA ANALYSIS

The following subsections present those analyses of the flight test data which were completed in the current effort. The ordinate unit for all the figures in this section is degrees.

4.3.1 AZIMUTH RMS ERRORS WITHIN EACH PASS

Figures 4.2 through 4.13 present the azimuth RMS tracking errors determined within each pass. Some general observations from these data include:

(1) The multipath fence had no measurable effect.

(2) The corner reflector reduced the average RMS error by about 33%, from 0.015^{o} to 0.010^{o}. The average RMS error increases at short range because the azimuth angle is changing rapidly in this region. Therefore there is a larger difference between the data and the mean position within the 200 foot averaging interval. This is verified by the fact that the error data both with and without the corner reflector increase by equal amounts.

(3) The corner reflector also reduced, by about a factor of two, the fluctuation in the RMS error. This indicates that the error data are smoother with the corner reflector than without. This also implies smoother tracking with the enhanced target.

(4) The data from the runs with a 1500 foot touchdown offset with touchdown on the deck (Figures 4.11 through 4.13) stop at a range of 2500 feet because the AN/TPN-22 radar started tracking a centerline reflector at the end of the runway. These runs are thus of limited use to the analysis. Note also on Figure 4.4 there is a bad data point, as shown by the single point being out of line.

4.3.2 ELEVATION RMS ERRORS WITHIN EACH PASS

Figures 4.14 through 4.25 present the elevation RMS errors within each pass. Observations from these plots include:

(1) The multipath fence had no measurable effect.

(2) The corner reflector decreased the average RMS error at long range and had no effect at short range. The decreased error at long range may be due to increased signal-to-noise ratio from the target when enhanced by the corner reflector. At medium-to-close range, the signal-to-noise ratio is sufficient for good tracking without the corner reflector. There is an increase in average elevation RMS errors at short range, as there was for the azimuth errors, but the increase is not as great because of the geometry of the landing scenario: the elevation angle does not change as rapidly near touchdown as does the azimuth angle.

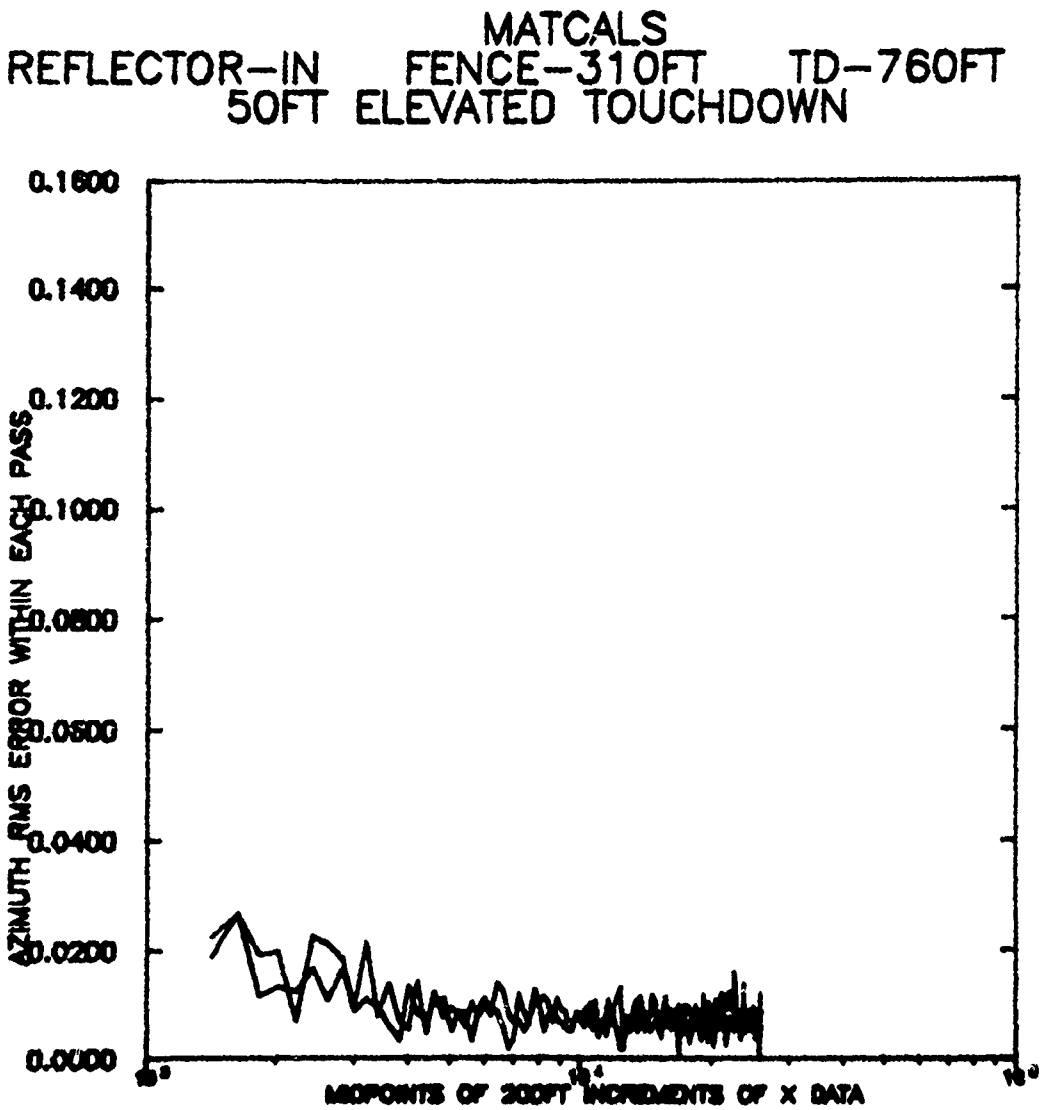

Figure 4.2. Azimuth RMS Error Within Each Pass, Configuration J

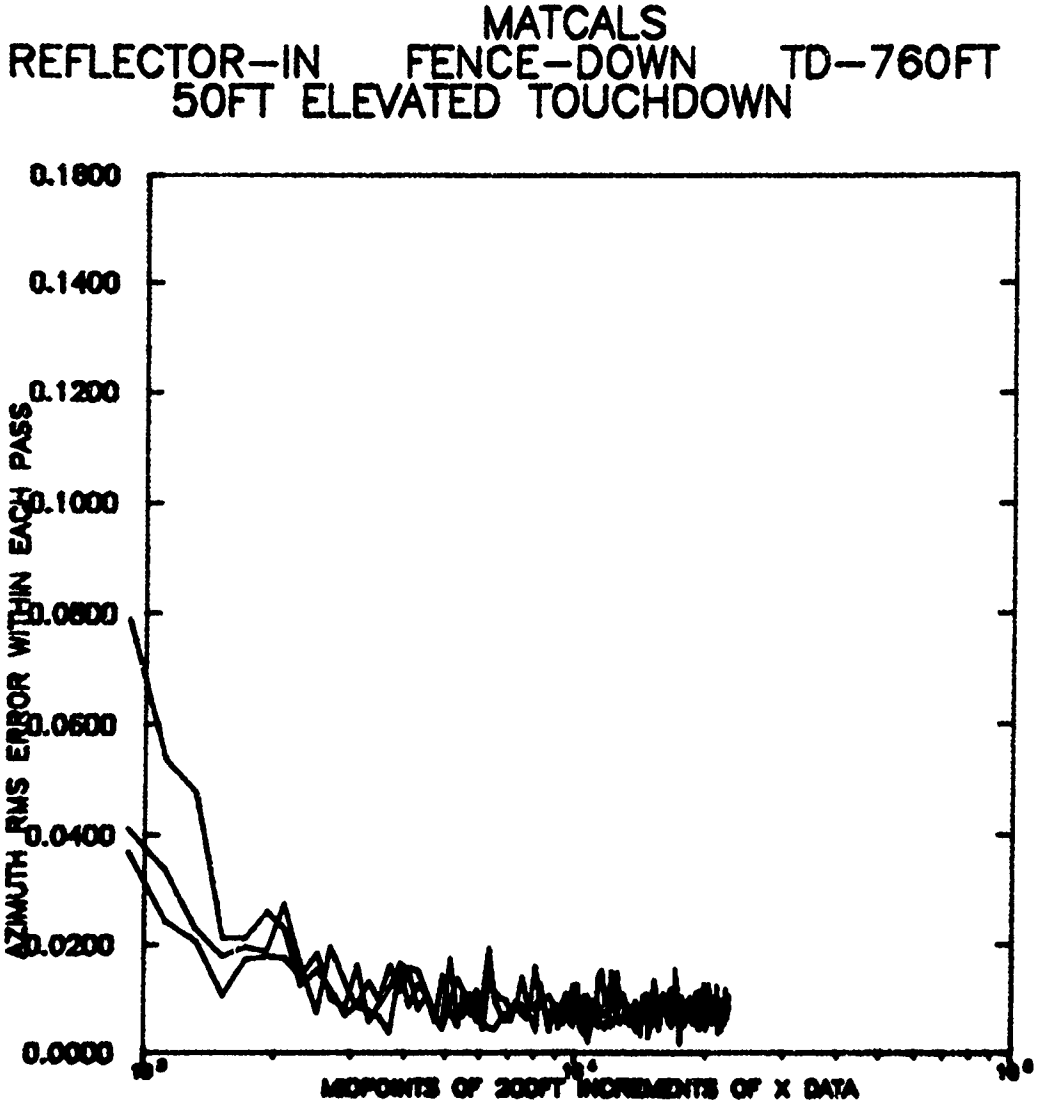

Figure 4.3. Azimuth RMS Error Within Each Pass, Configuration 2

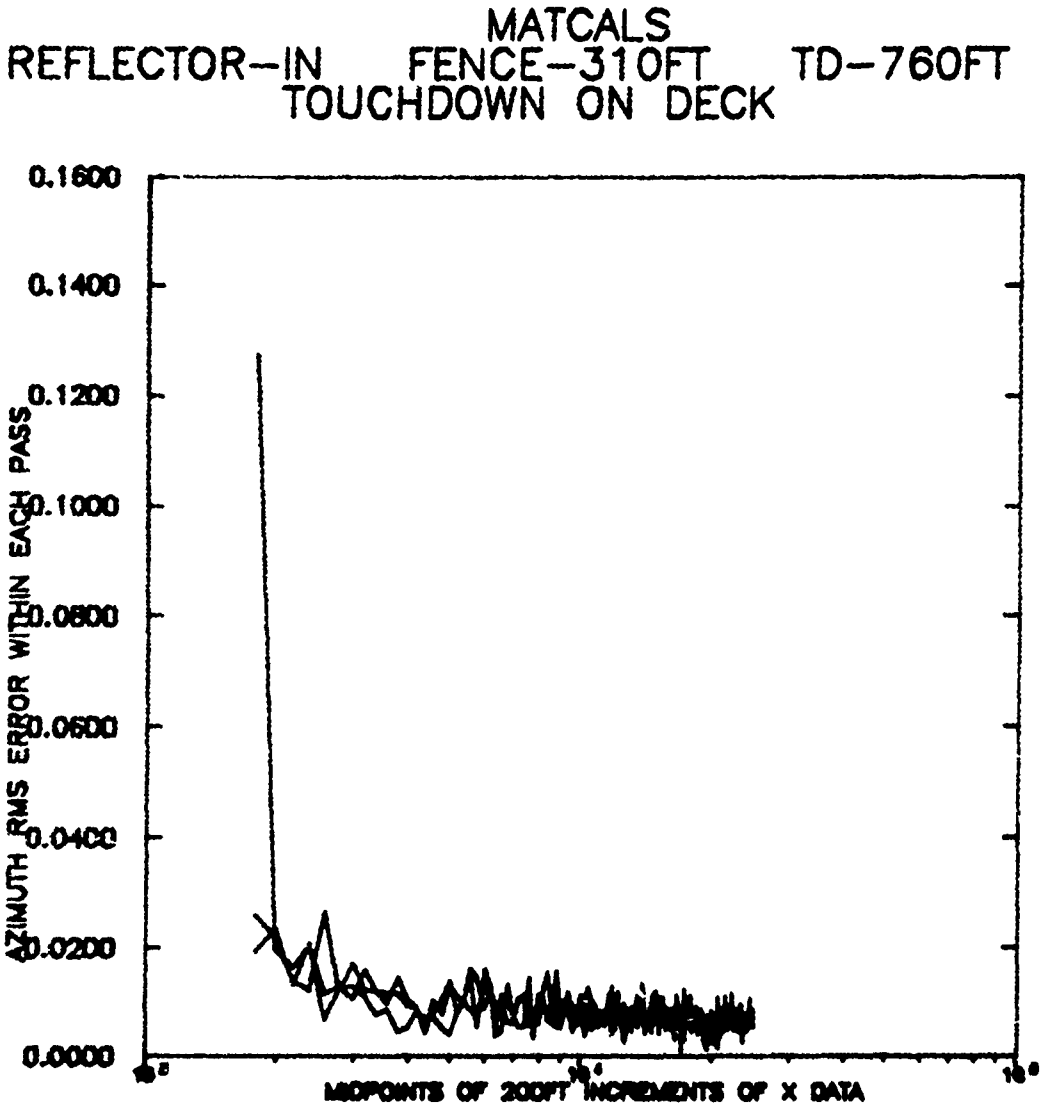

Figure 4.4. Azimuth RMS Error Within Each Pass, Configuration 3

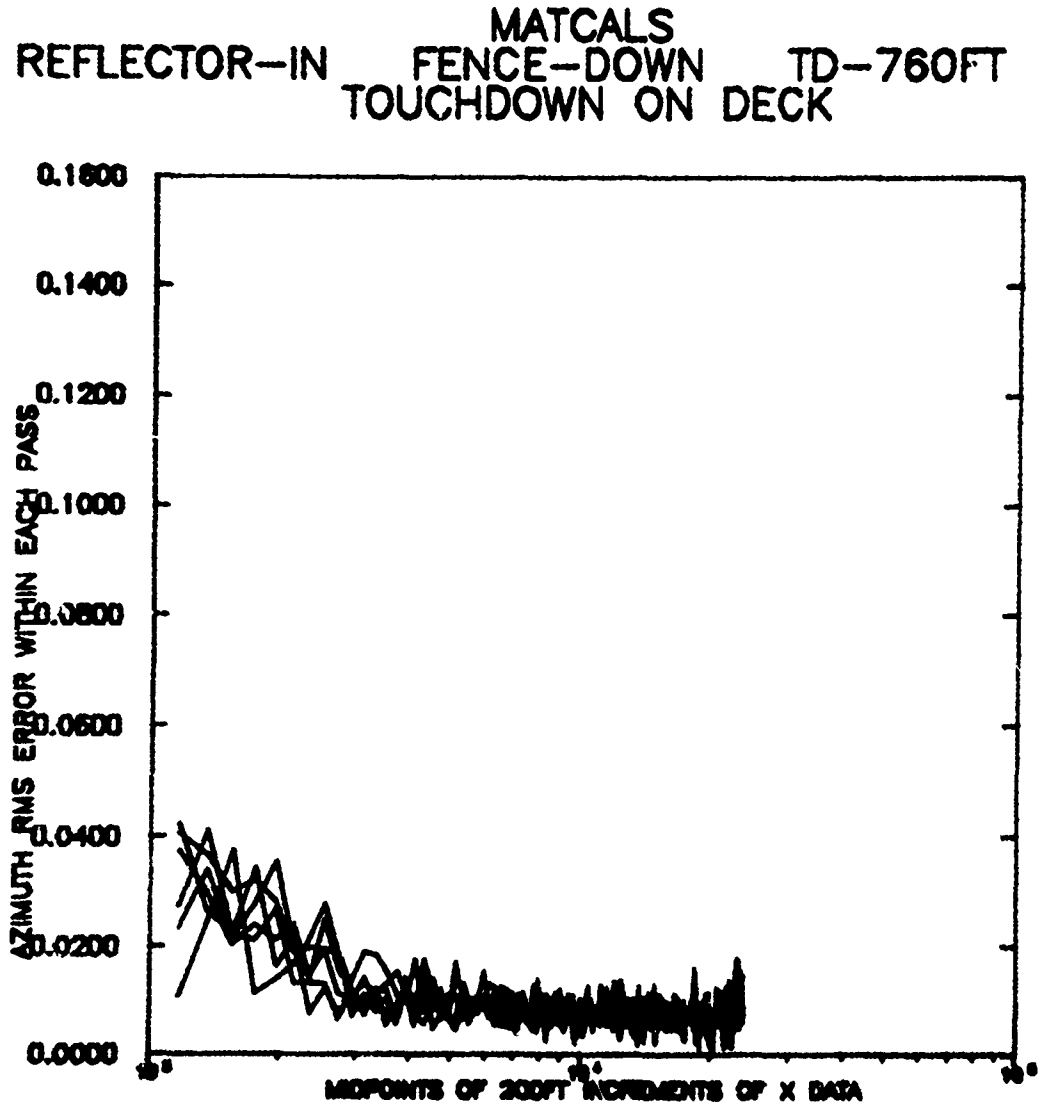

Figure 4.5. Azimuth RMS Error Within Each Pass, Configuration 4

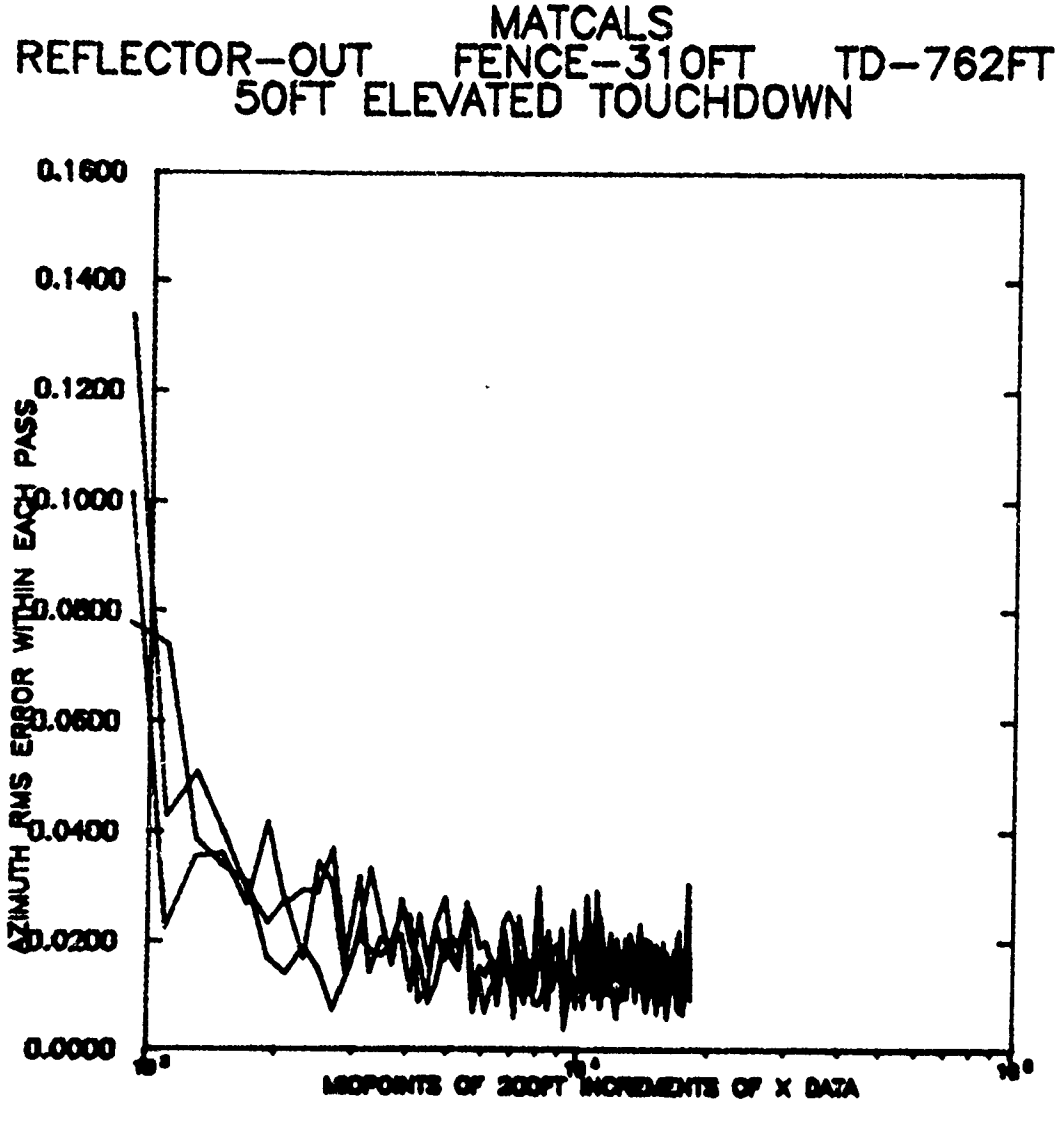

Figure 4.6. Azimuth RMS Error Within Each Pass, Configuration 5

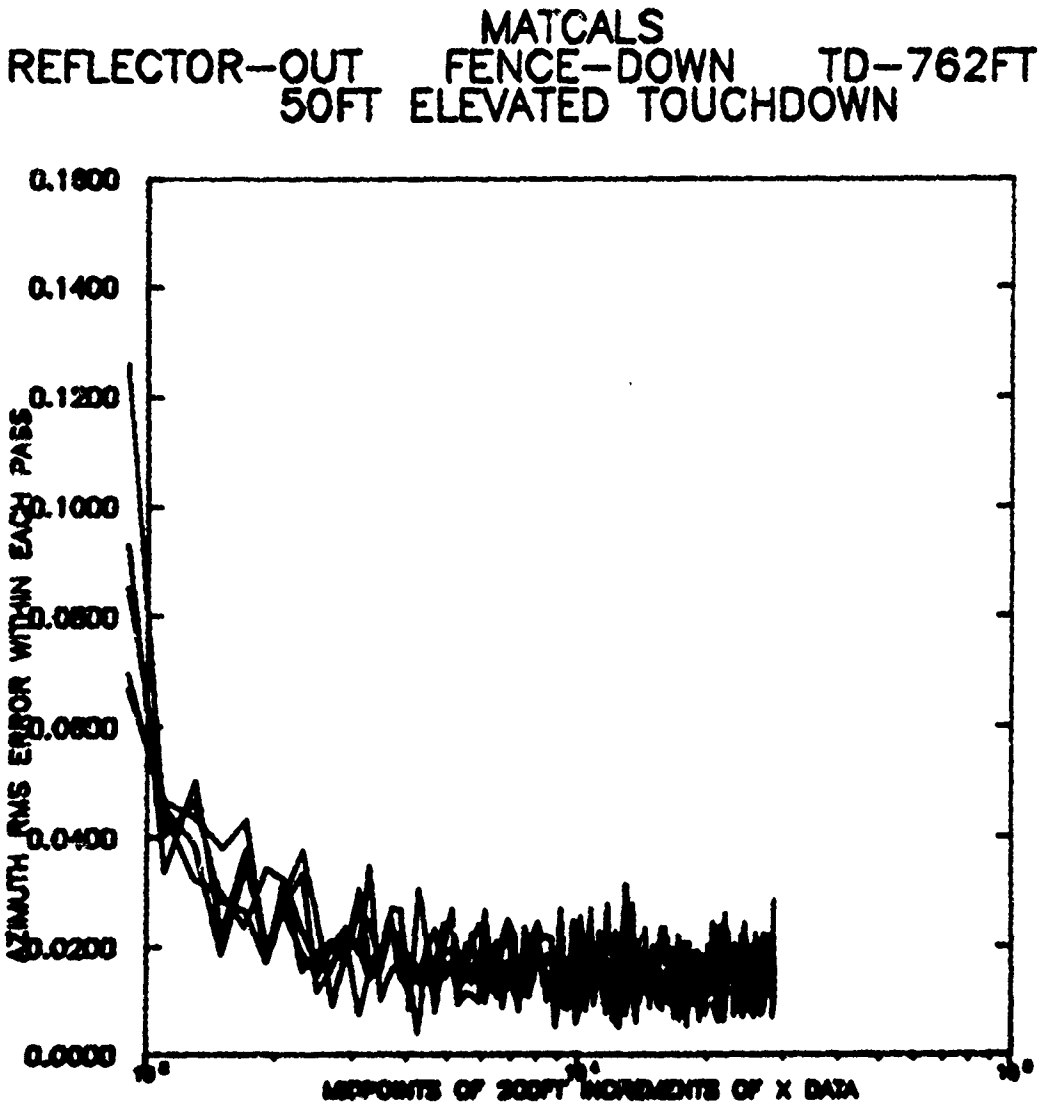

Figure 4.7. Azimuth RMS Error Within Each Pass, Configuration 6

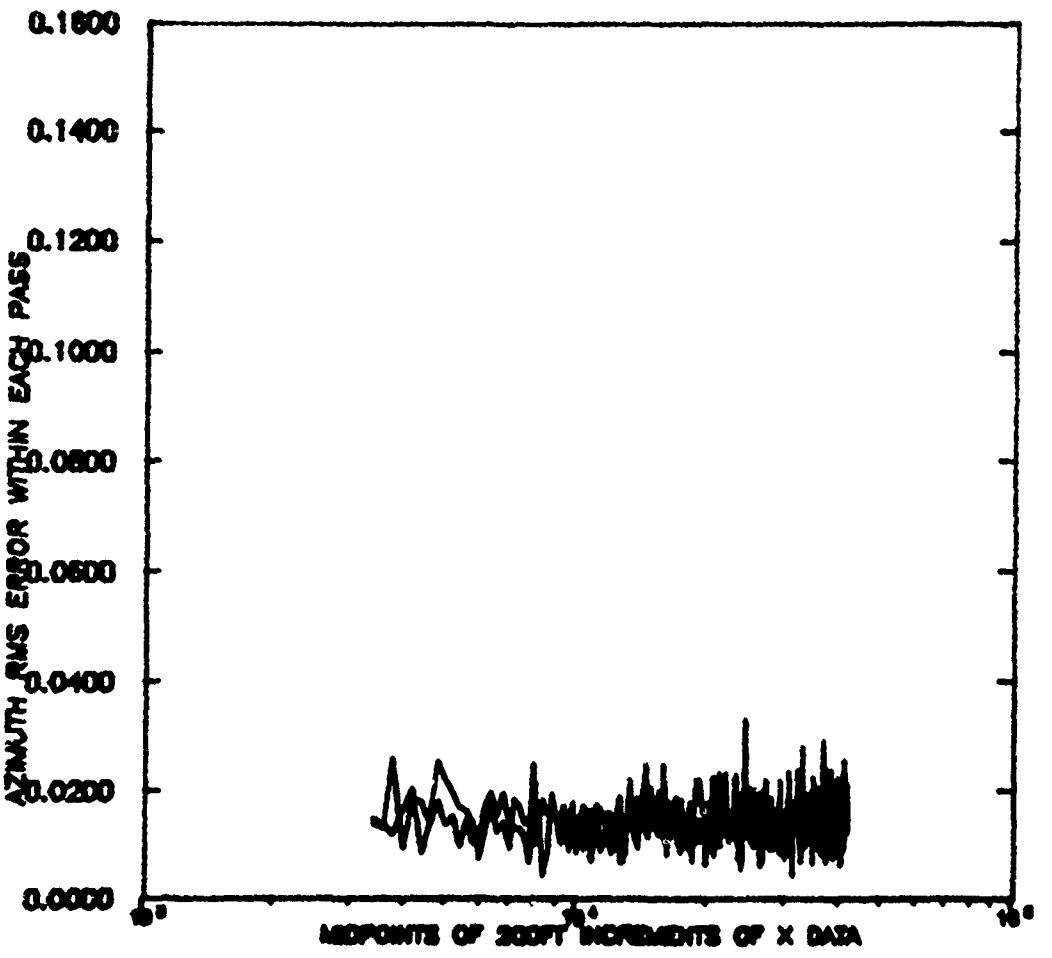

Figure 4.8. Azimuth RMS Error Within Each Pass, Configuration 7

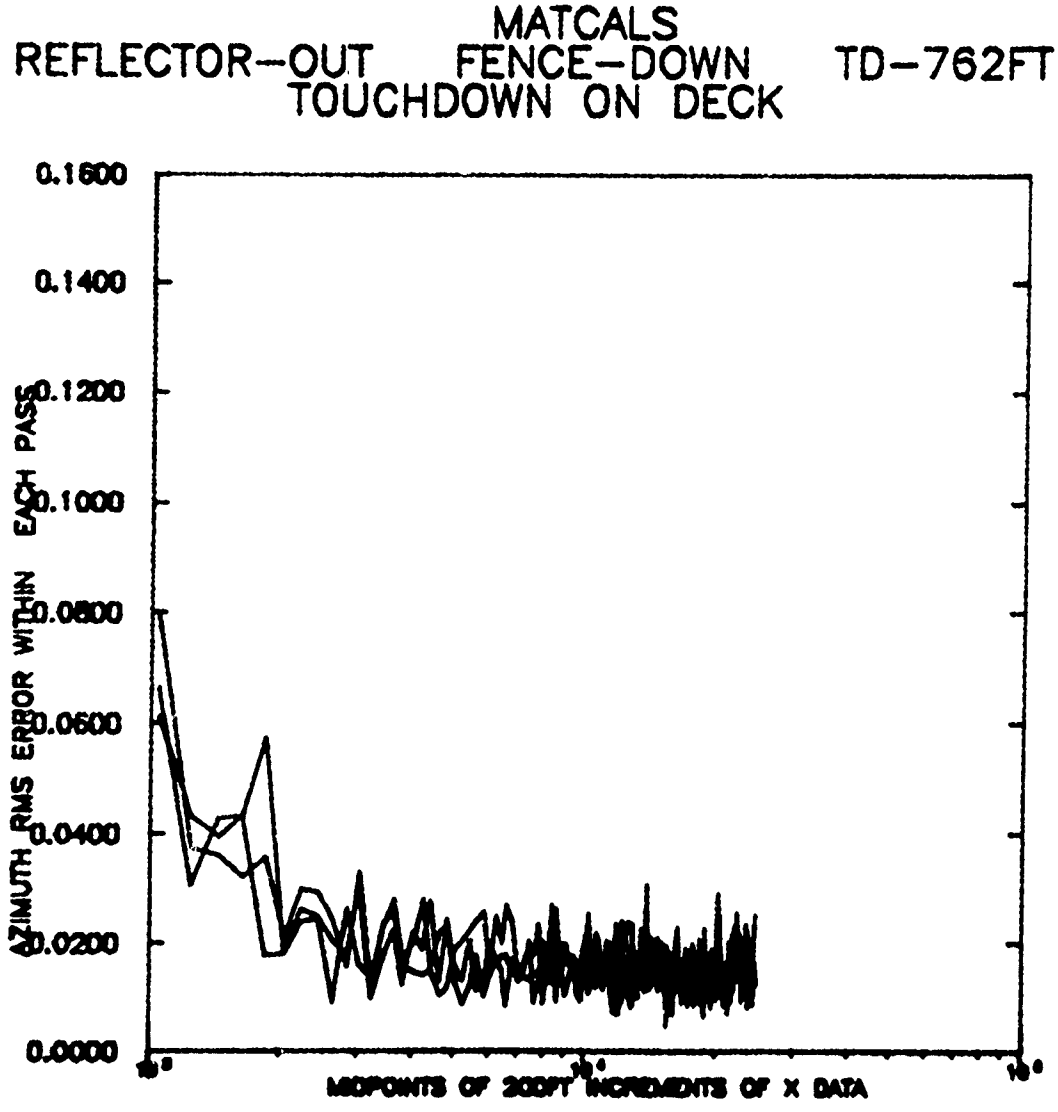

Figure 4.9. Azimuth RMS Error Within Each Pass, Configuration 8

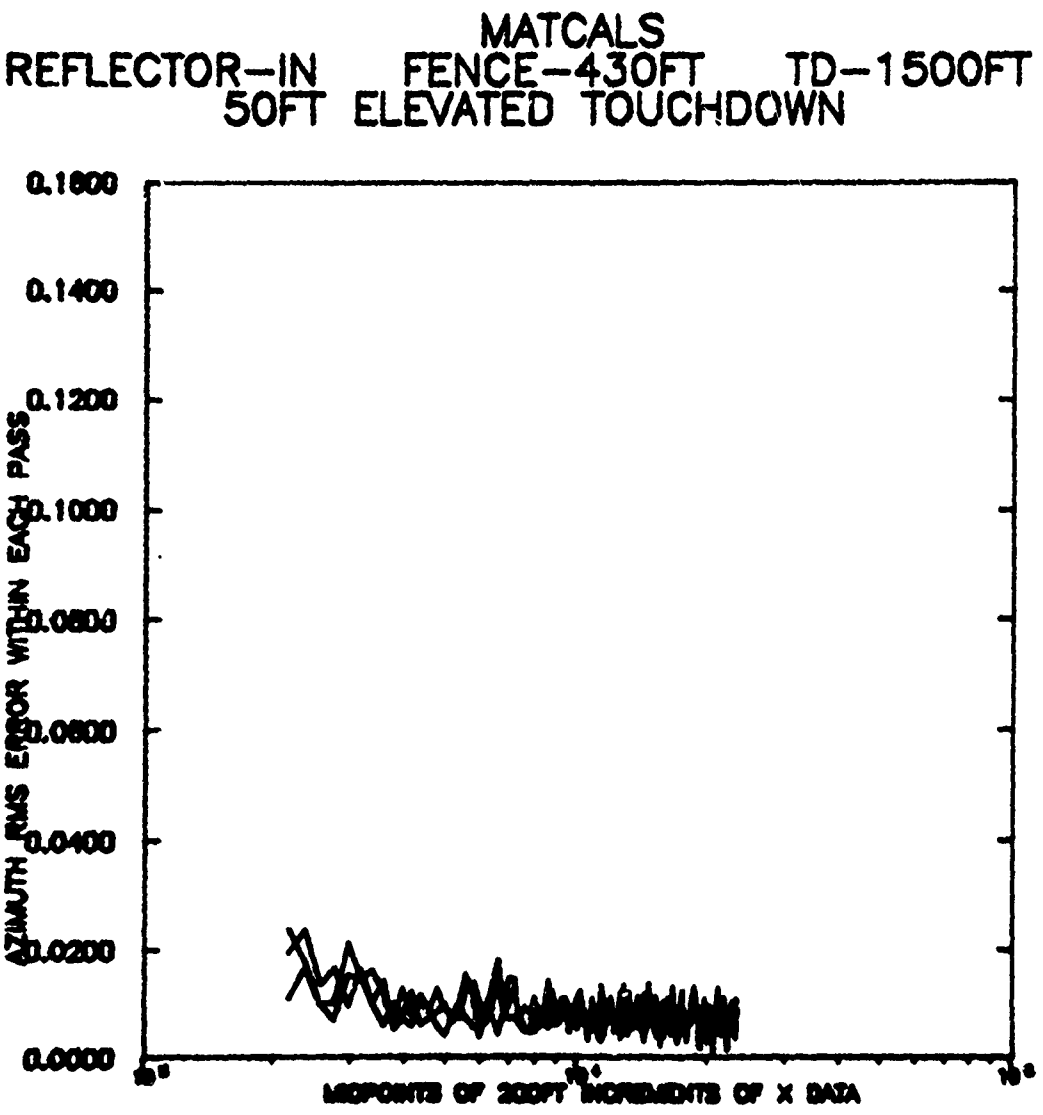

Figure 4.10. Azimuth RMS Error Within Each Pass, Configuration 9

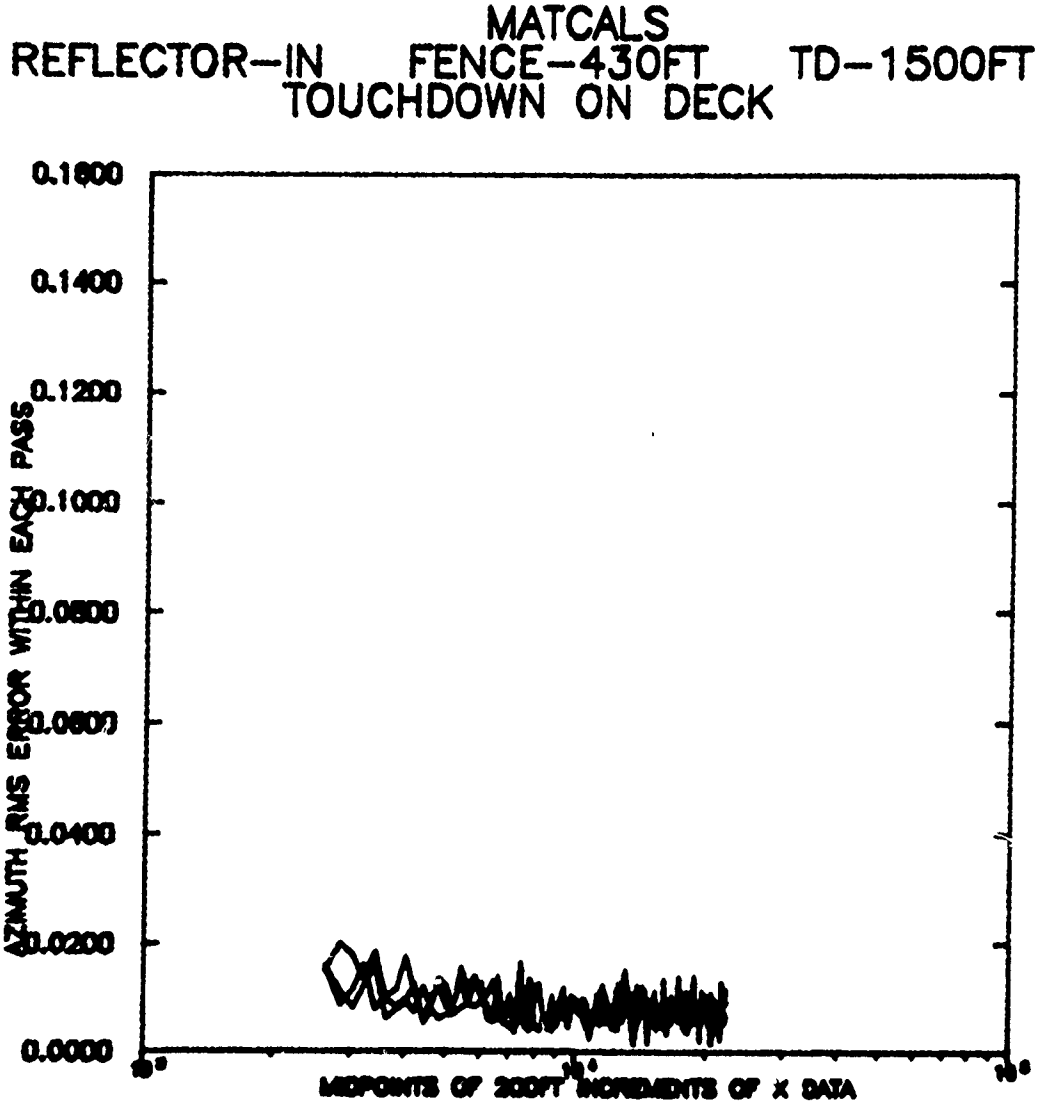

Figure 4.11. Azimuth RMS Error Within Each Pass, Configuration 10

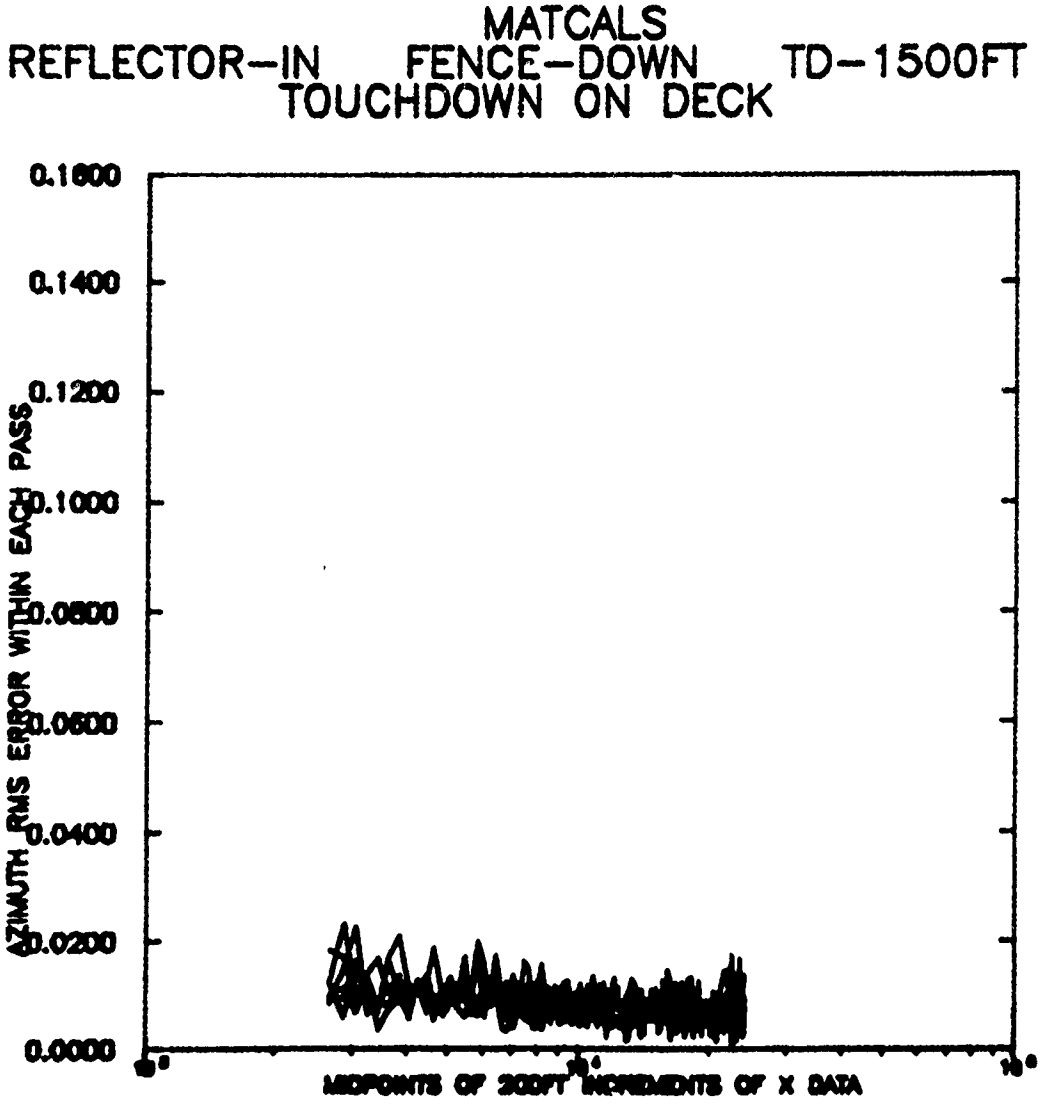

Figure 4.12. Azimuth RMS Error Within Each Pass, Configuration 11

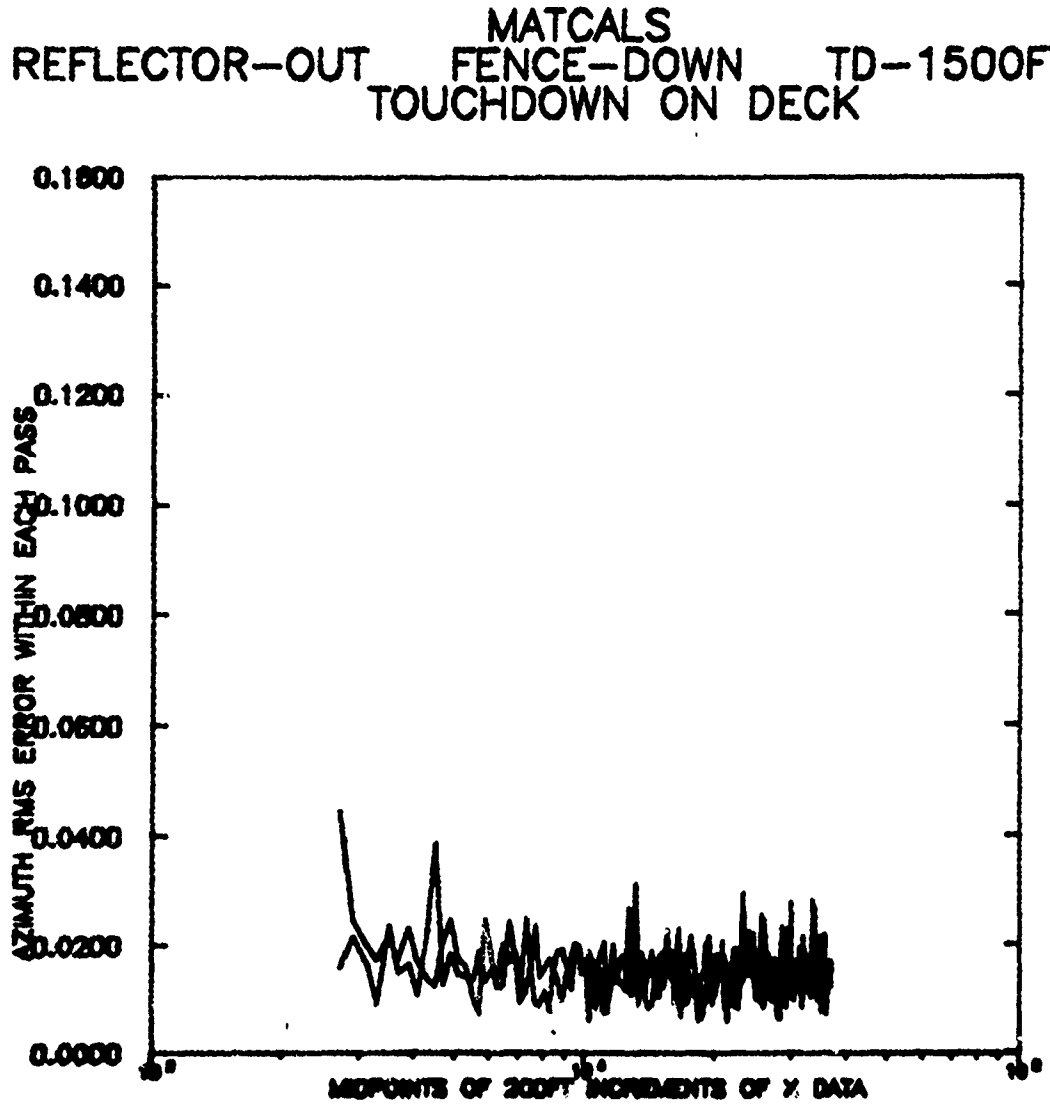

Figure 4.13. Azimuth RMS Error Within Each Pass, Configuration 12

Figure 4.14. Elevation RMS Error Within Each Pass, Configuration 1

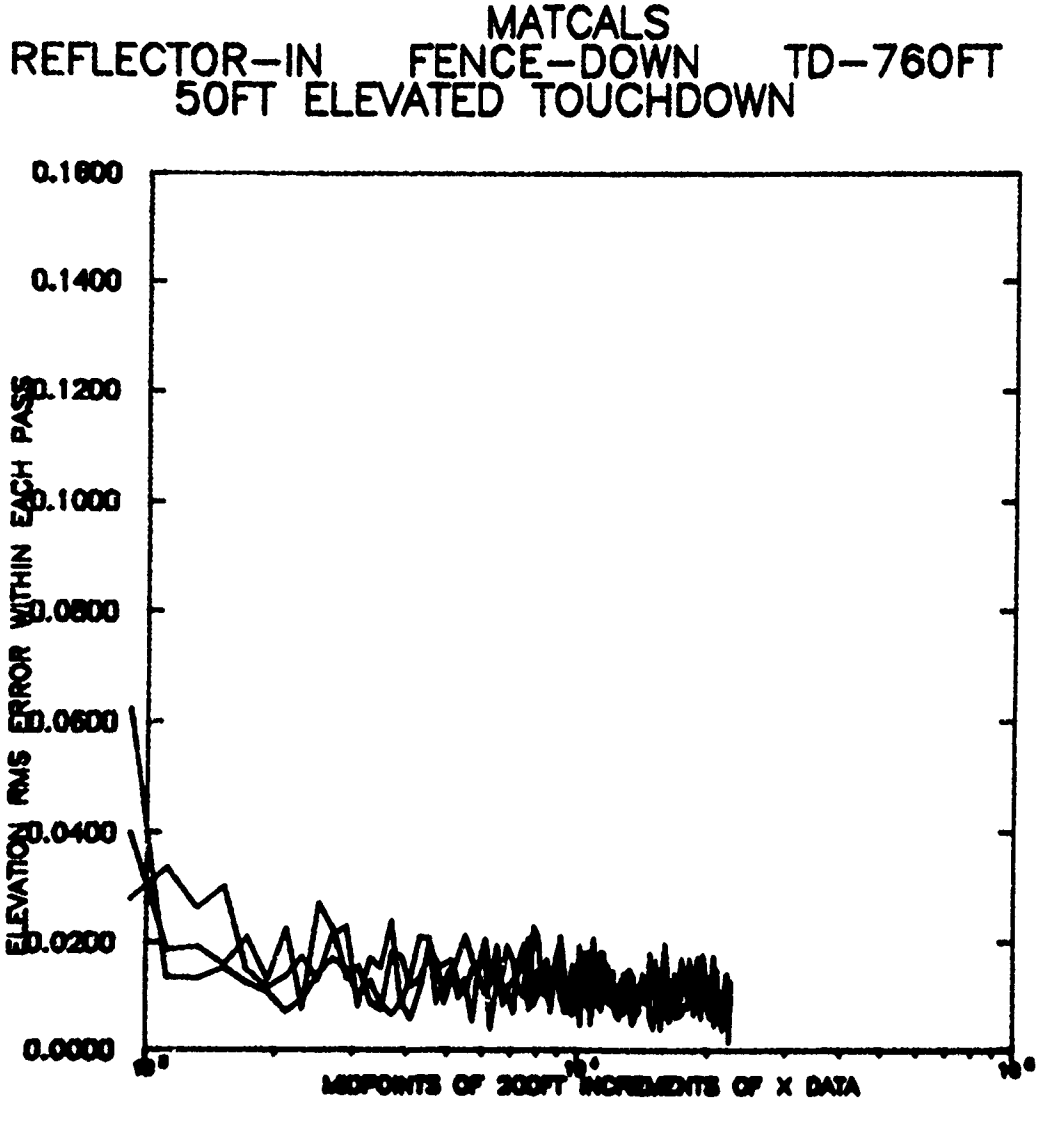

Figure 4.15. Elevation RMS Error Within Each Pass, Configuration 2

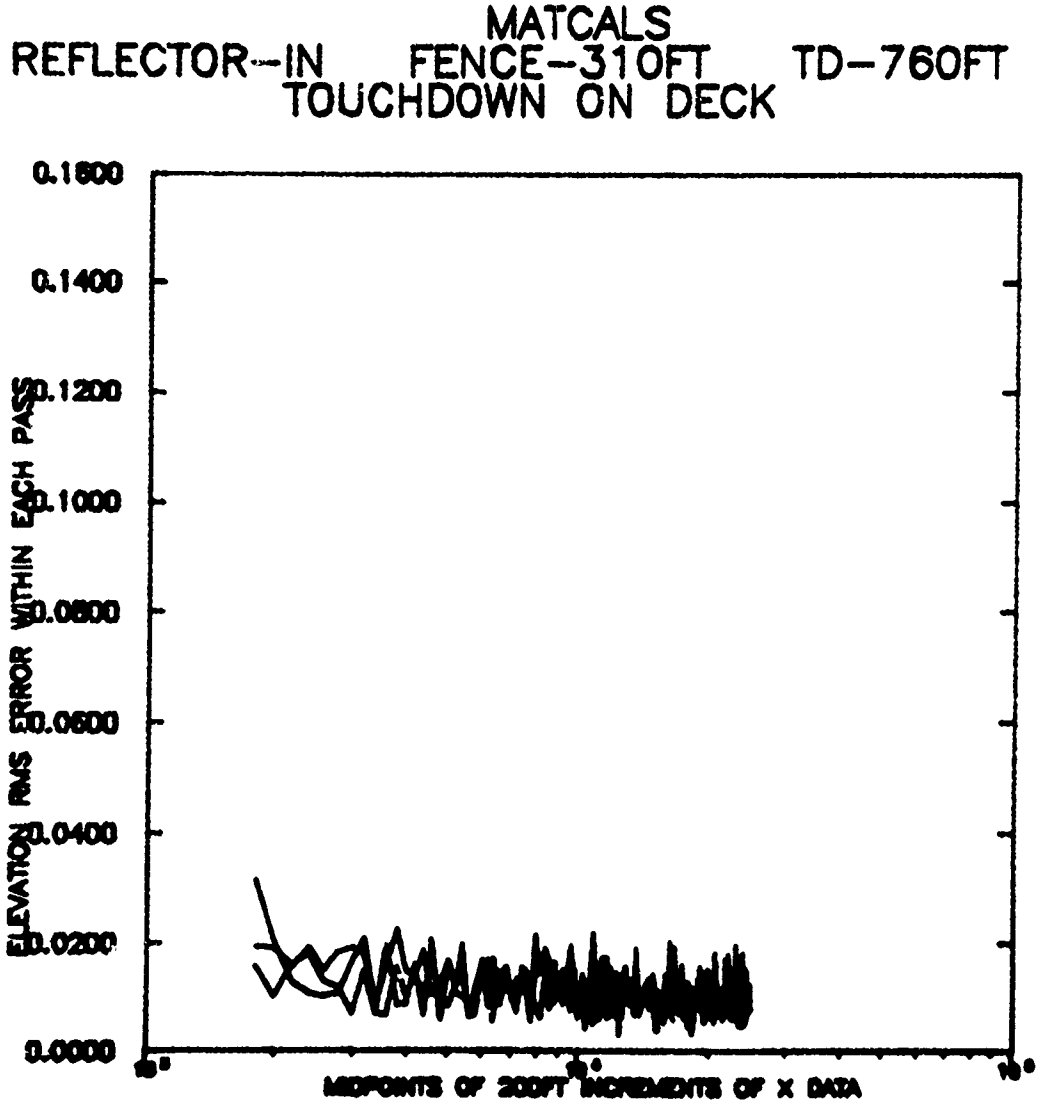

Figure 4.16. Elevation RMS Error Within Each Pass, Configuration 3

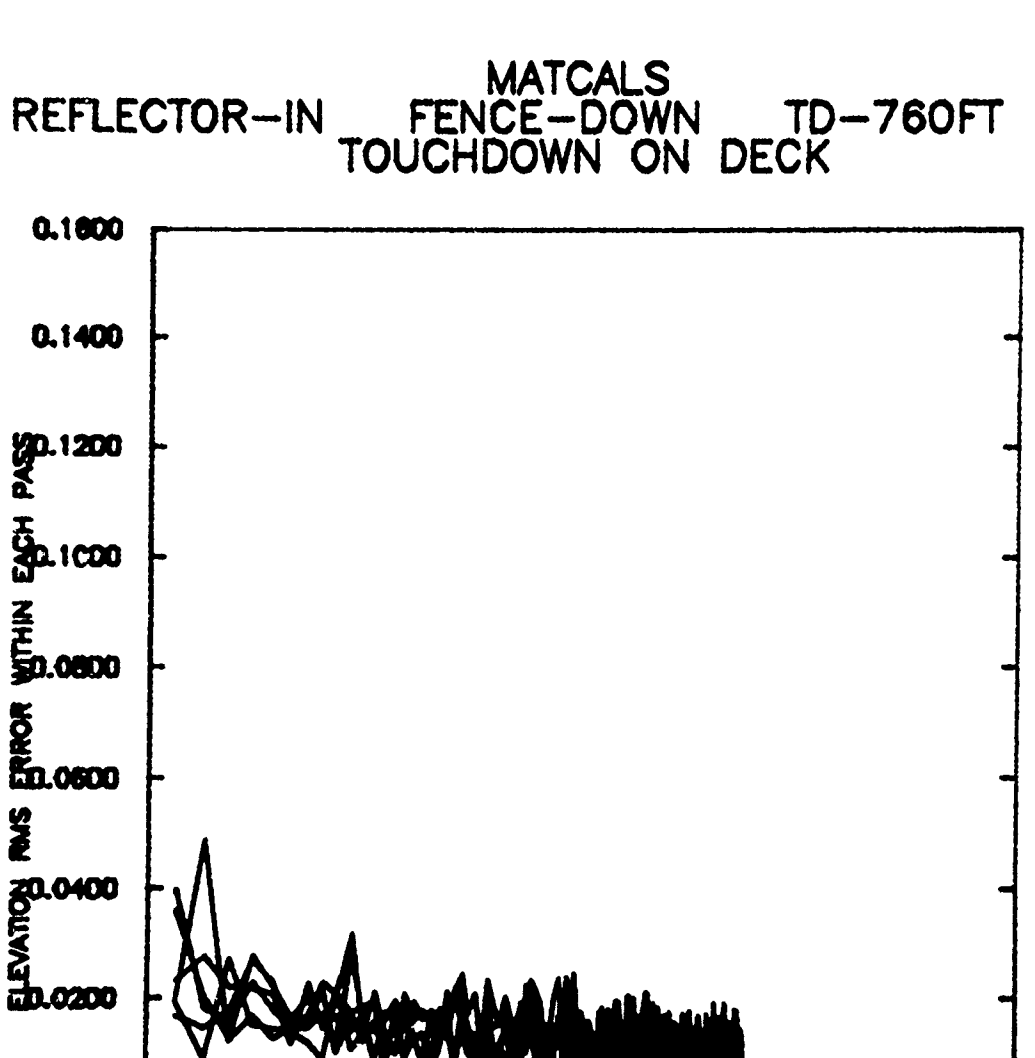

Figure 4.17. Elevation RMS Error Within Each Pass, Configuration 4

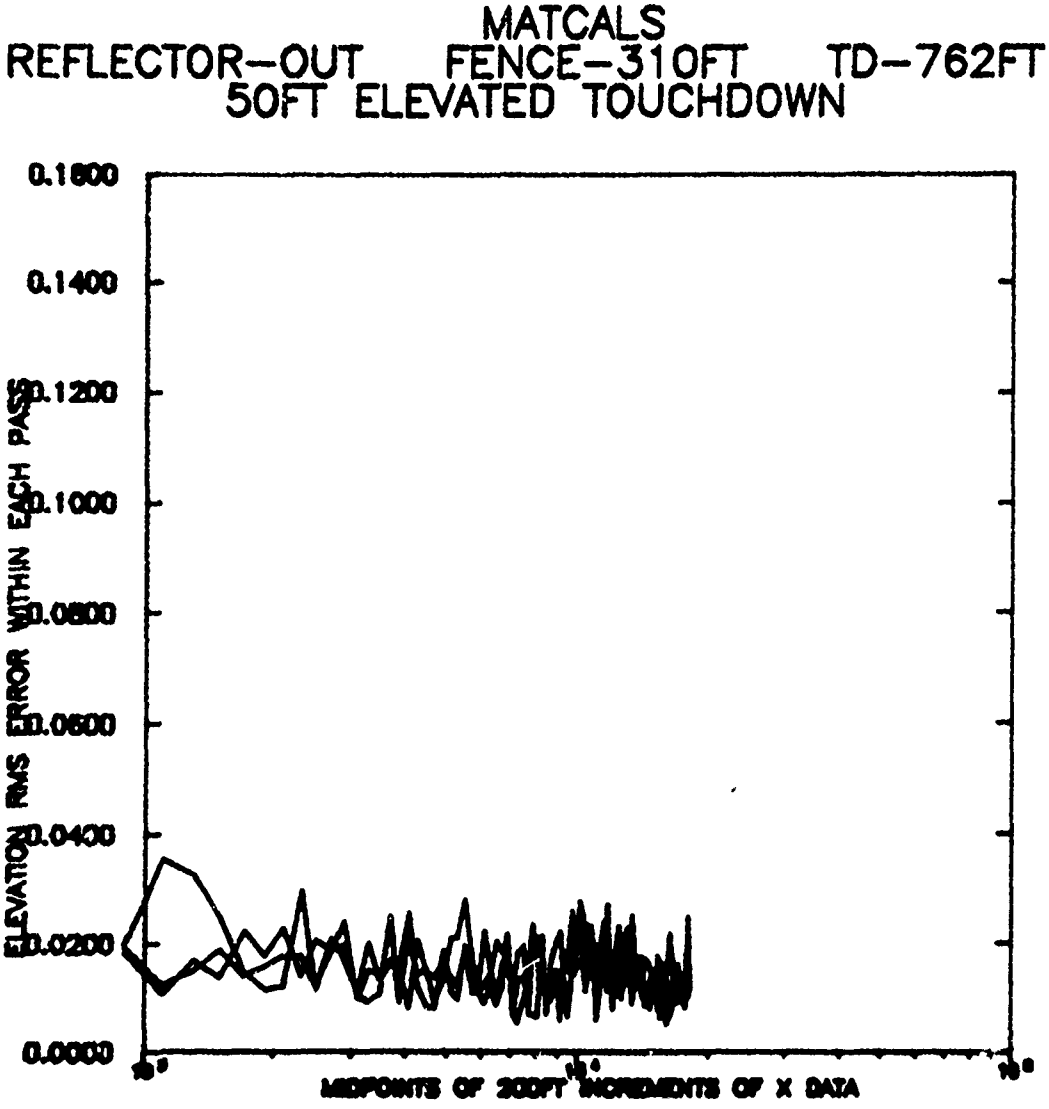

Figure 4.18. Elevation RMS Error Within Each Pass, Configuration 5

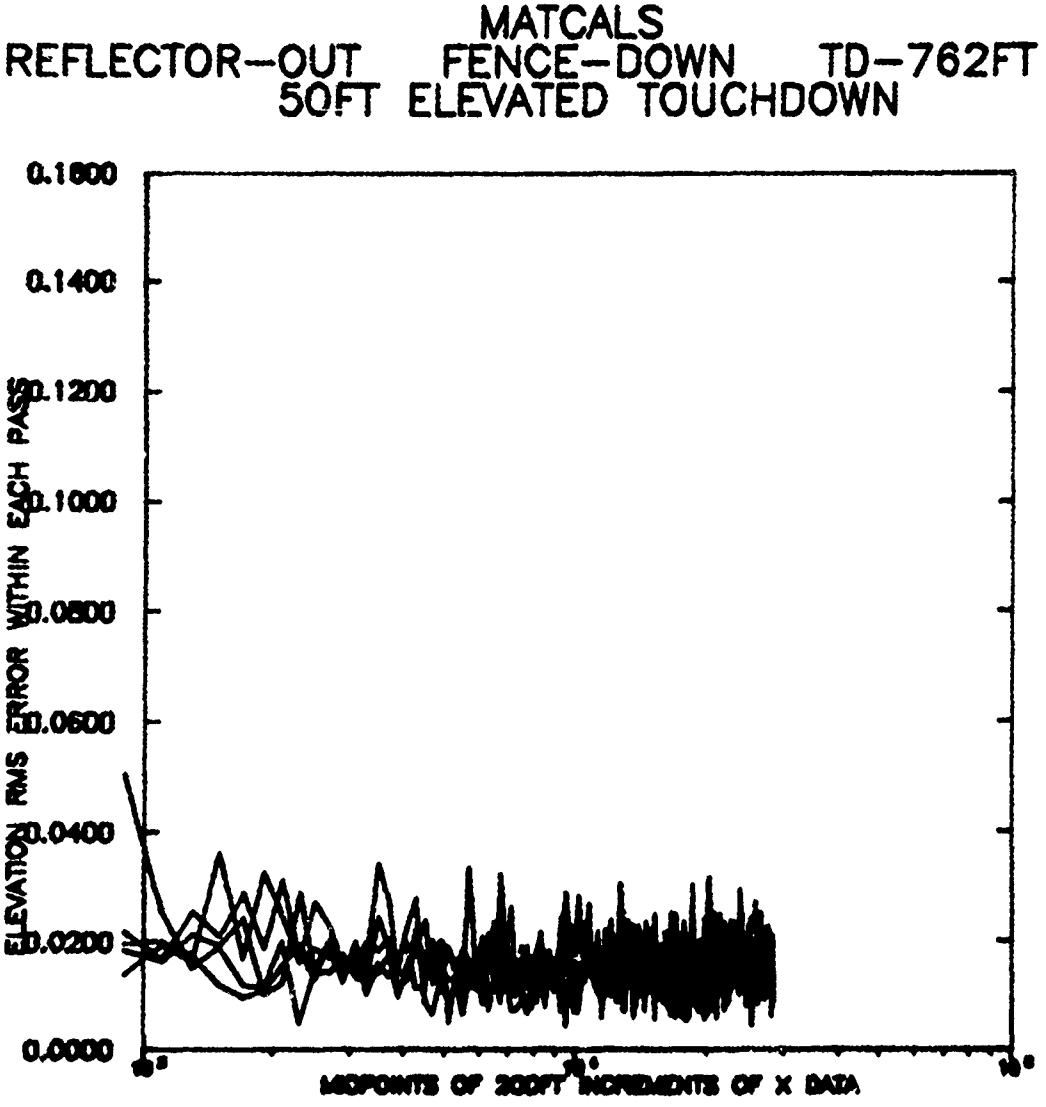

Figure 4.19. Elevation RMS Error Within Each Pass, Configuration 6

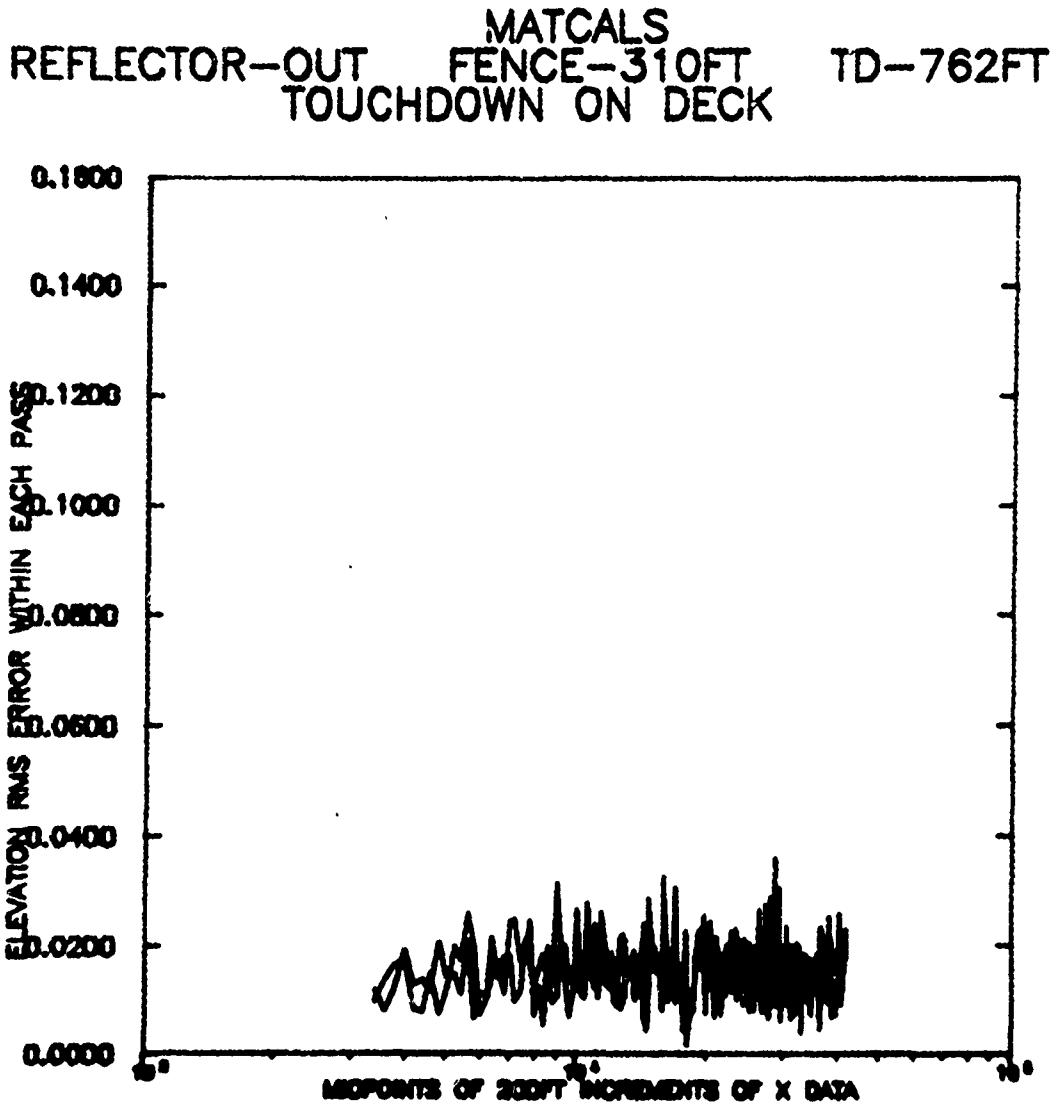

Figure 4.20. Elevation RMS Error Within Each Pass, Configuration 7

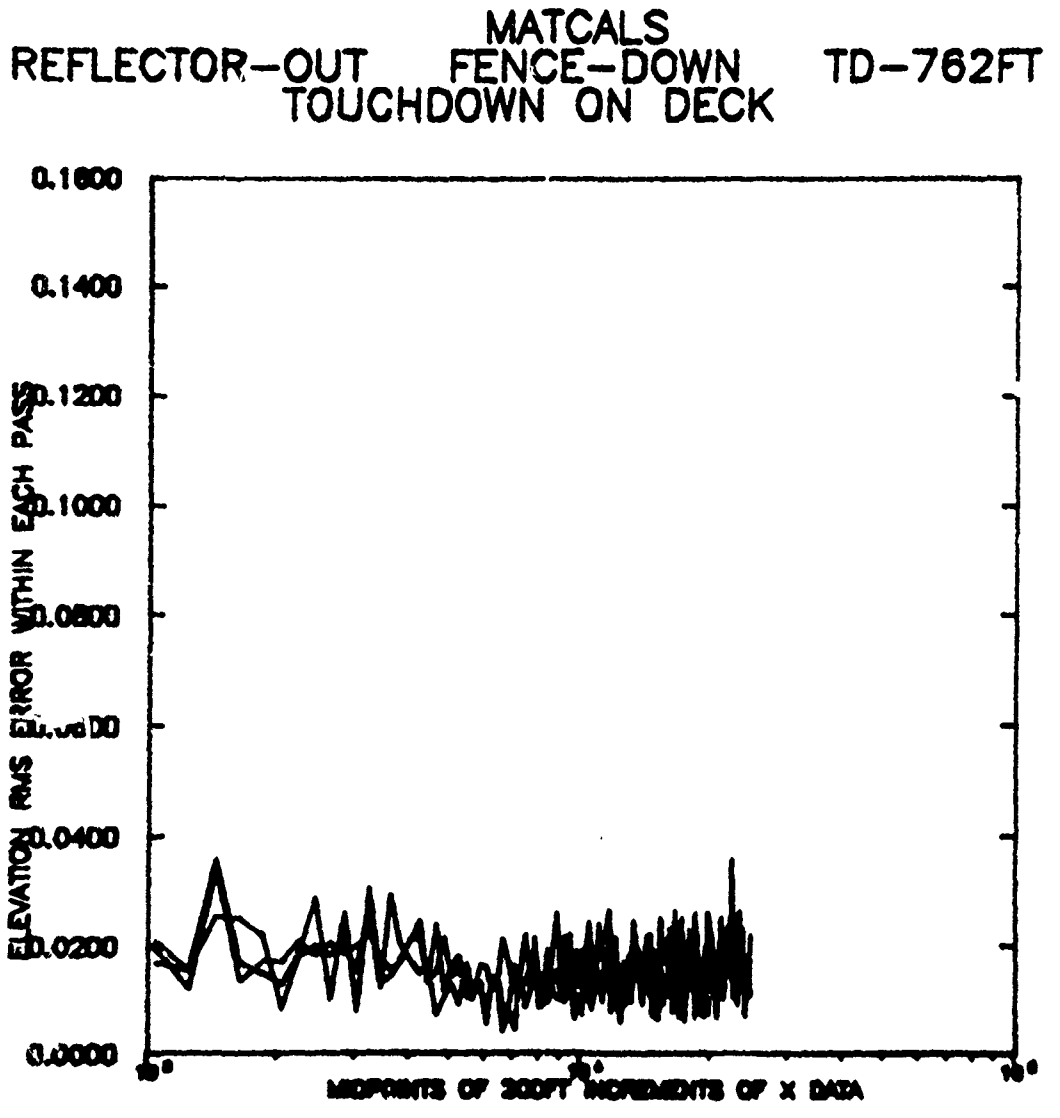

Figure 4.21. Elevation RMS Error Within Each Pass, Configuration 8

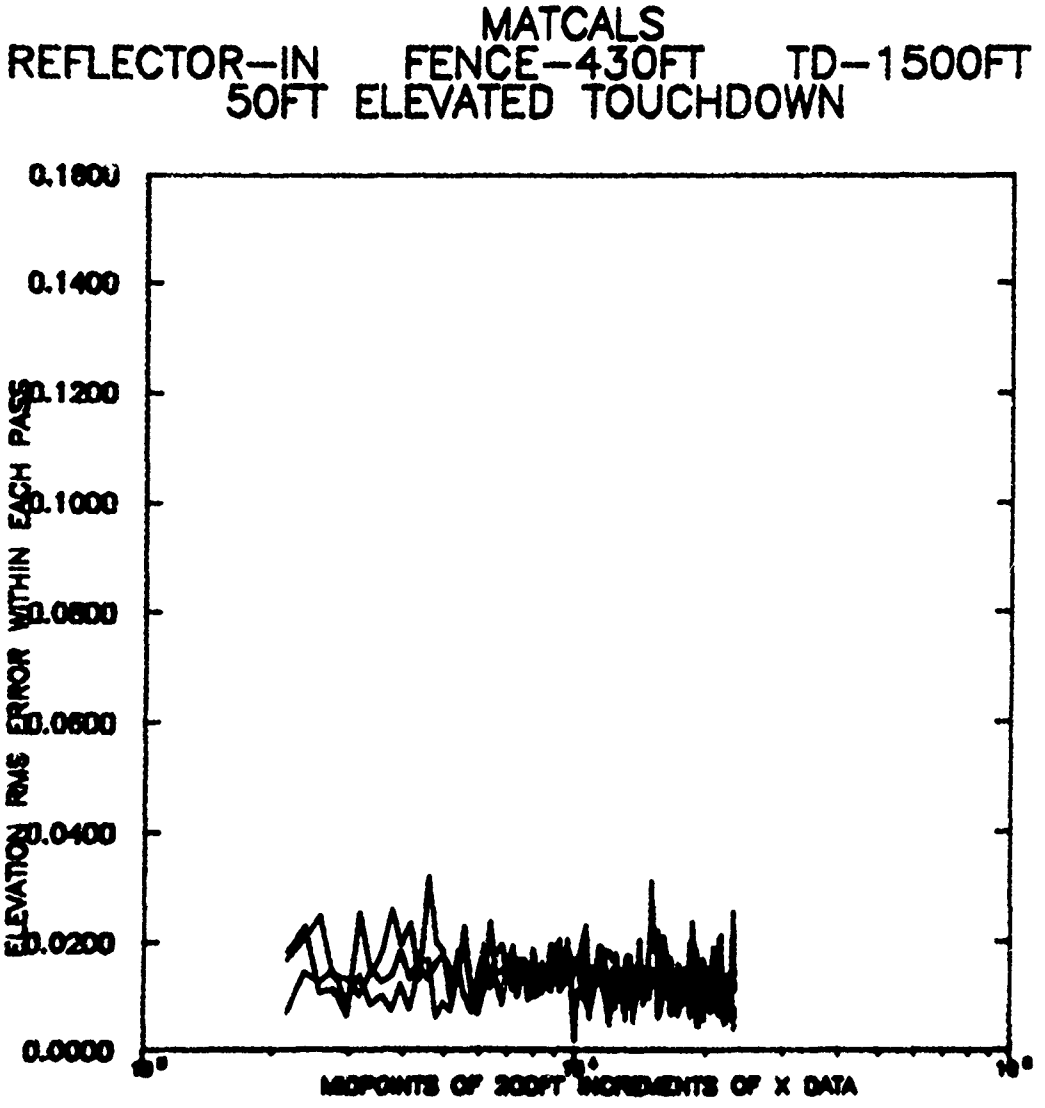

Figure 4.22. Elevation RMS Error Within Each Pass, Configuration 9

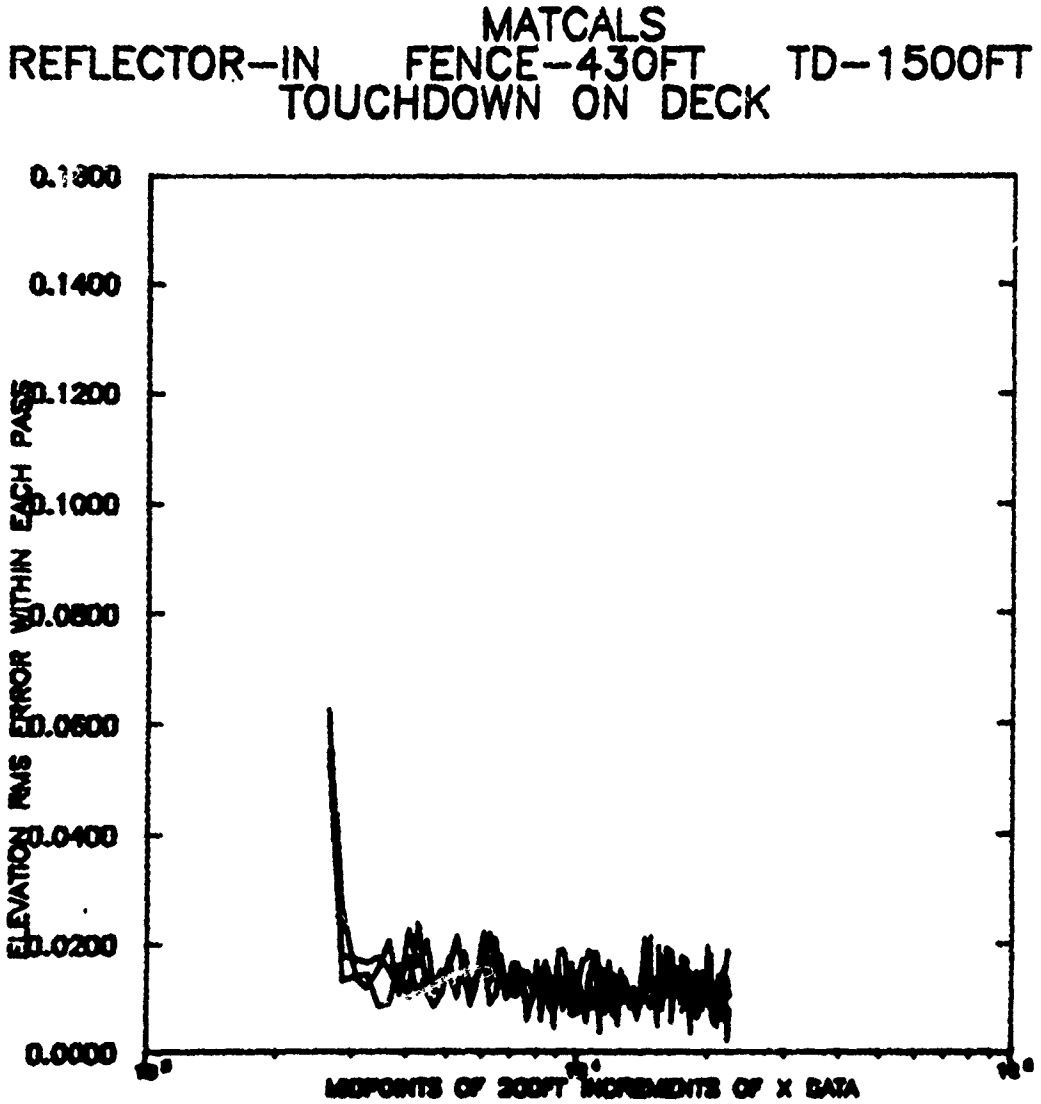

Figure 4.23. Elevation RMS Error Within Each Pass, Configuration 10

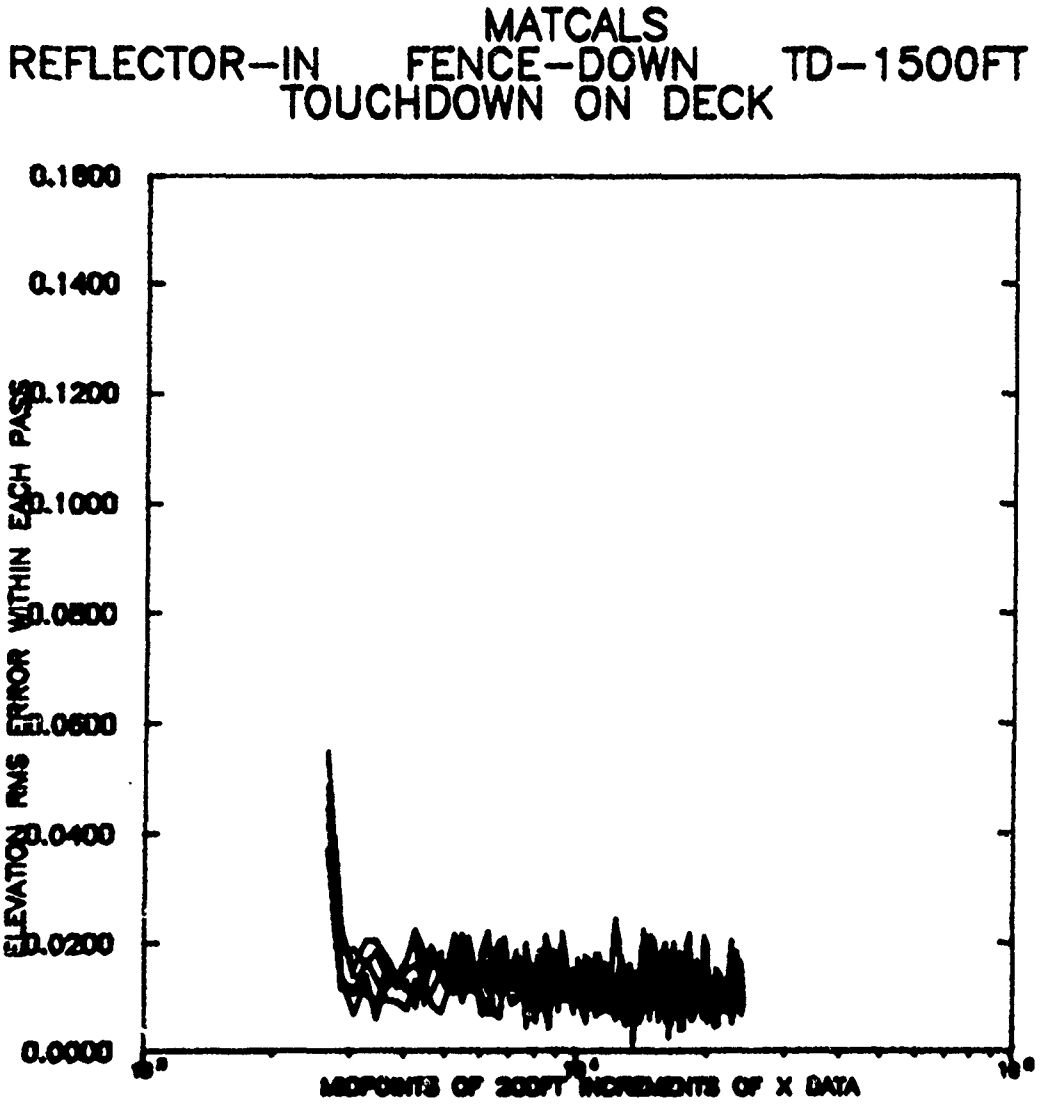

Figure 4.24. Elevation RMS Error Within Each Pass, Configuration 11

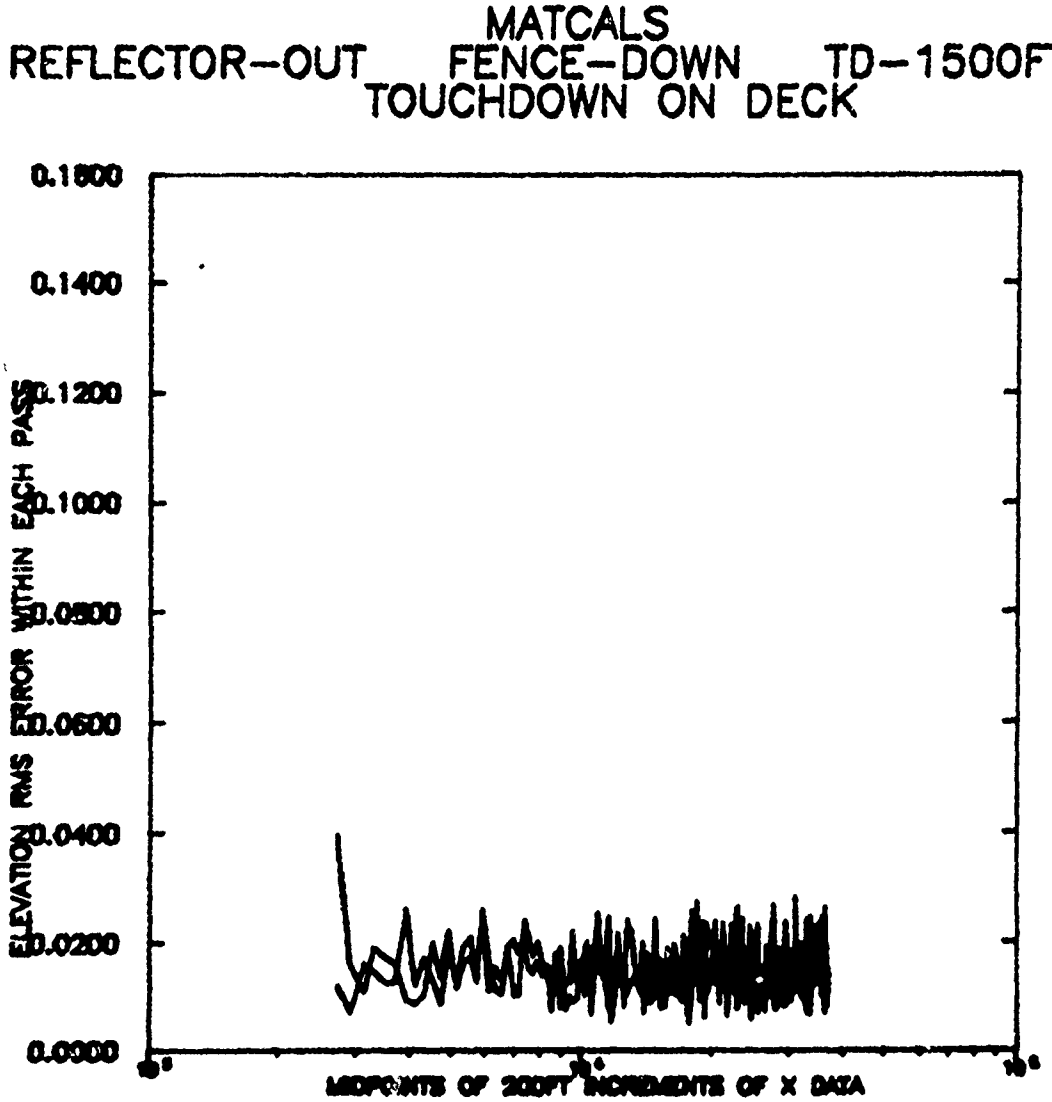

Figure 4.25. Elevation RMS Error Within Each Pass, Configuration 12

(3) The fluctuation in the RMS error with range is again reduced by a factor of 1.5 to 2 when the corner reflector is installed. This again indicates smoother tracking.

Surprisingly, the corner reflector seemed to smooth the azimuth tracking more than the elevation tracking. This is shown by the decreased average and decreased fluctuation of the RMS error with the corner reflector installed.

4.3.3 AZIMUTH ERRORS AVERAGED ACROSS EQUIVALENT PASSES

Plots of these data are shown in Figures 4.26 through 4.37. The most striking and essentially only difference between the figures is the change in the error with and without the corner reflector installed as illustrated in Figure 4.38. At long ranges, there appears to be a constant 0.03^{0} offset in the average errors; at ranges less than about 5000 feet, there is a 2.7 to 3.7 foot horizontal offset in the tracking position of the ALTS versus the AN/TPN-22. A constant distance offset can be attributed to the AN/TPN-22 tracking a different part of the aircraft. For example, when the corner reflector is installed, the AN/TPN-22 should track the nose of the aircraft. When it is removed, the radar tracking centroid may be the point where the engine nacelles join the fuselage, a point of high reflection. This explanation is supported by the fact that the direction of change (i.e., more negative error without the corner reflector) is correct for the reference system used. (Positive azimuth angles with respect to the radar are counter-clockwise when viewed from the top). The result of adding a constant 3.2 foot horizontal offset to the AN/TPN-22 azimuth tracking position is shown as the dashed line in Figure 4.38.

The constant angular offset between runs with the corner reflector installed versus removed has not been explained. Indeed, any explanation is difficult to imagine because something would have had to change between the two flight periods (a span of one day) to account for this difference.

The general shape of the curves may be geometrically explained if the ALTS centroid was offset from the AN/TPN-22 centroid. This effect will be studied further in the next phase of the analysis by plotting the Cartesian coordinate errors, which are contained on the compare data tape, as well as the angular errors.

The multipath fence again had no measurable effect.

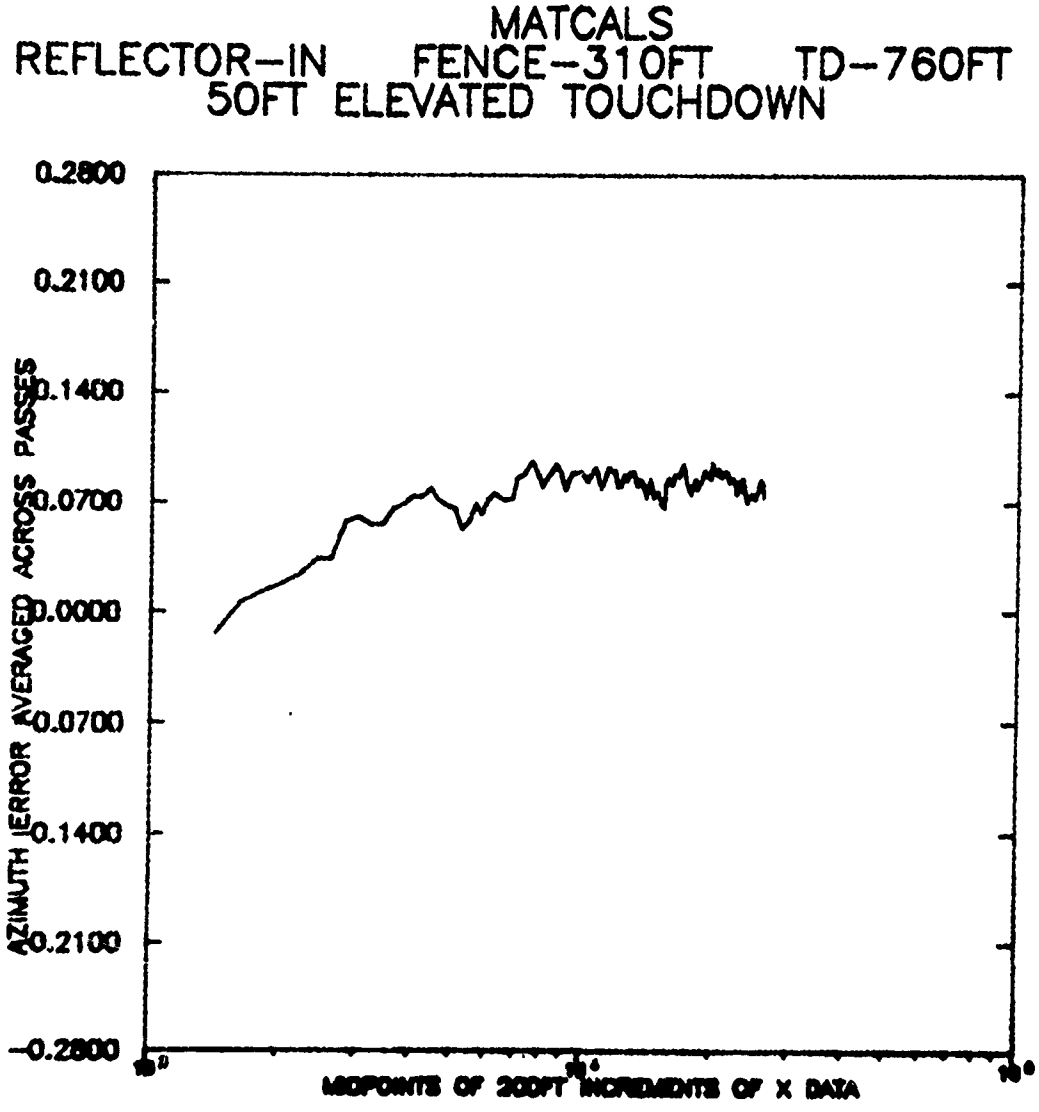

Figure 4.26. Azimuth Error Averaged Across Passes, Configuration 1

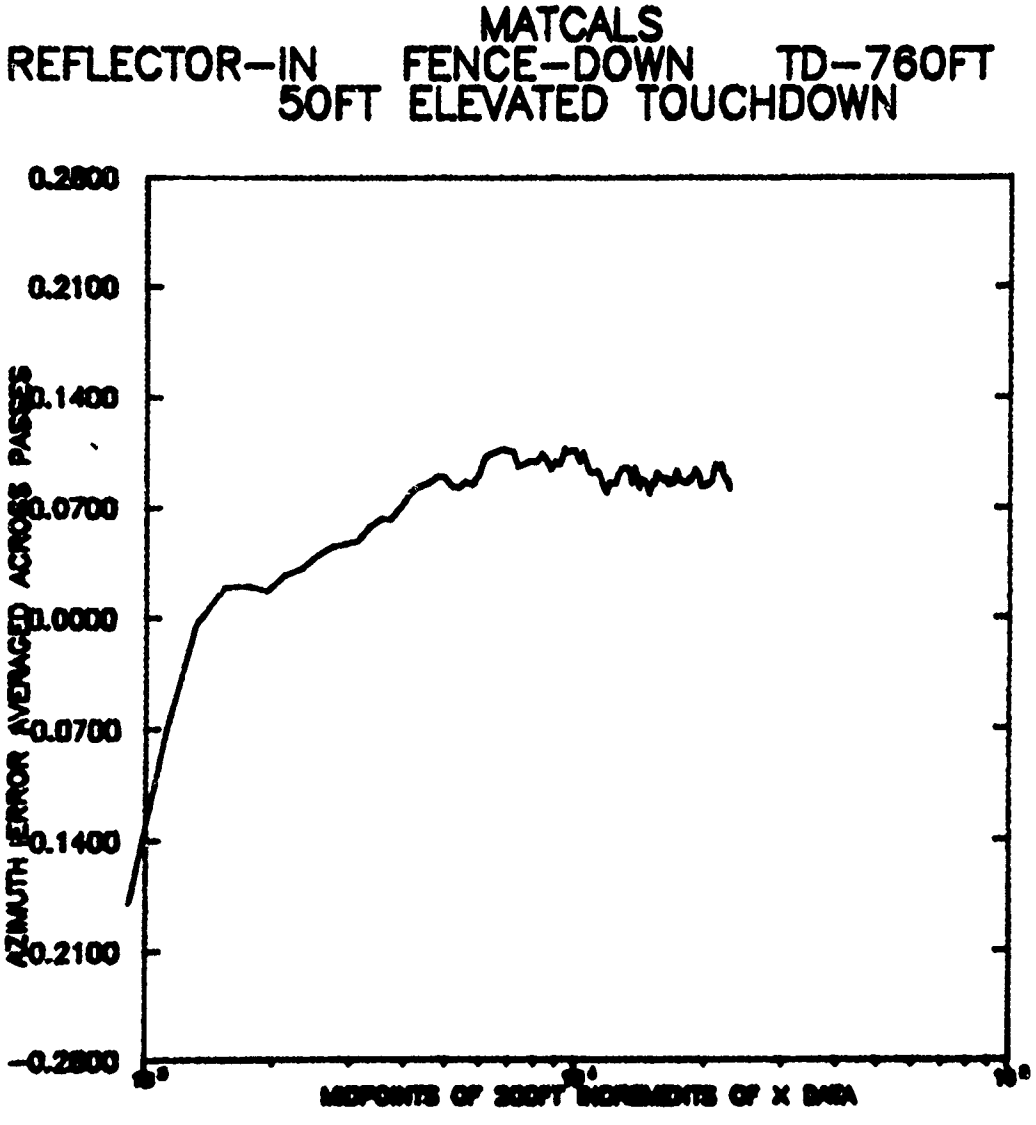

Figure 4.27. Azimuth Error Averaged Across Passes, Configuration 2

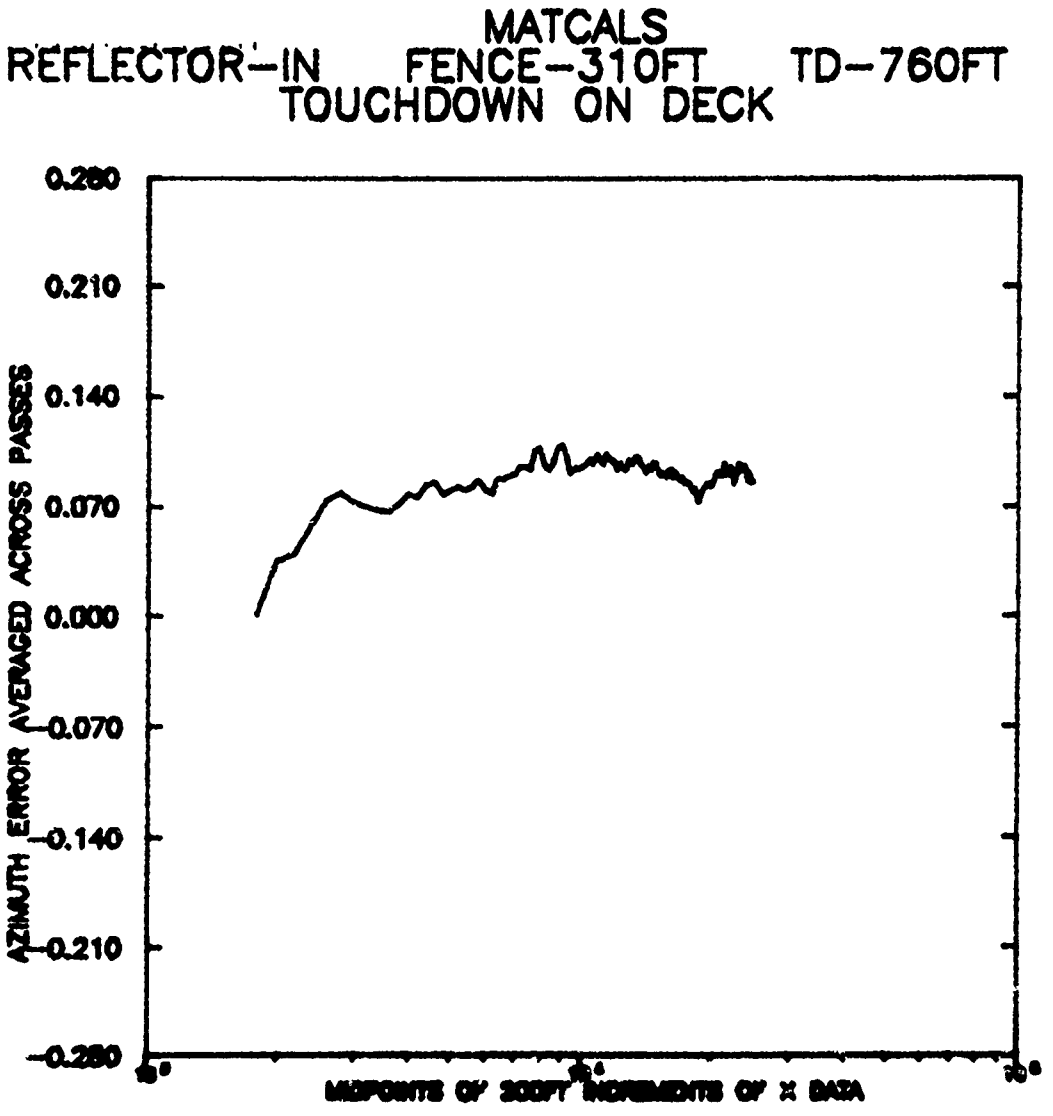

Figure 4.28. Azimuth Error Averaged Across Passes, Configuration 3

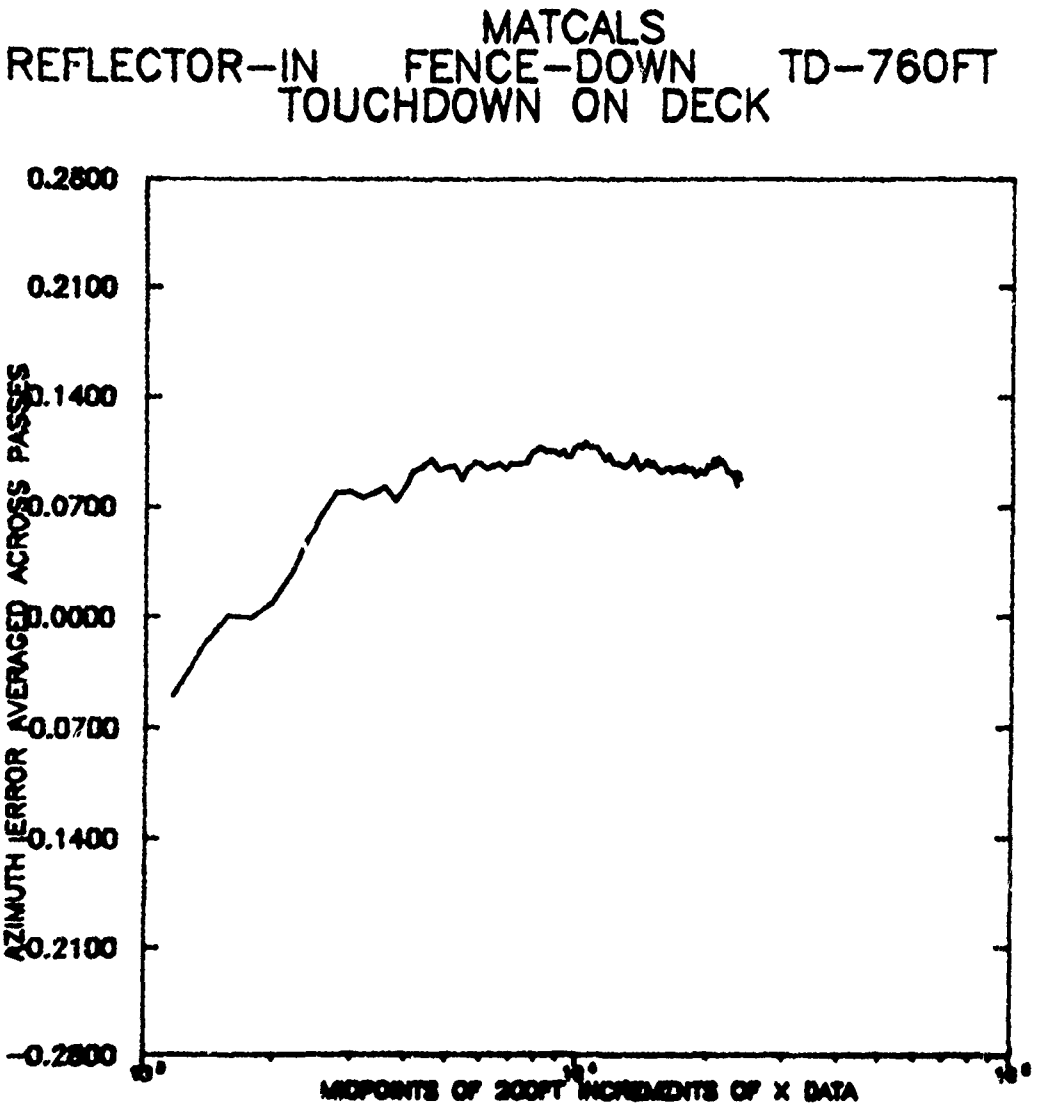

Figure 4.29. Azimuth Error Averaged Across Passes, Configuration 4

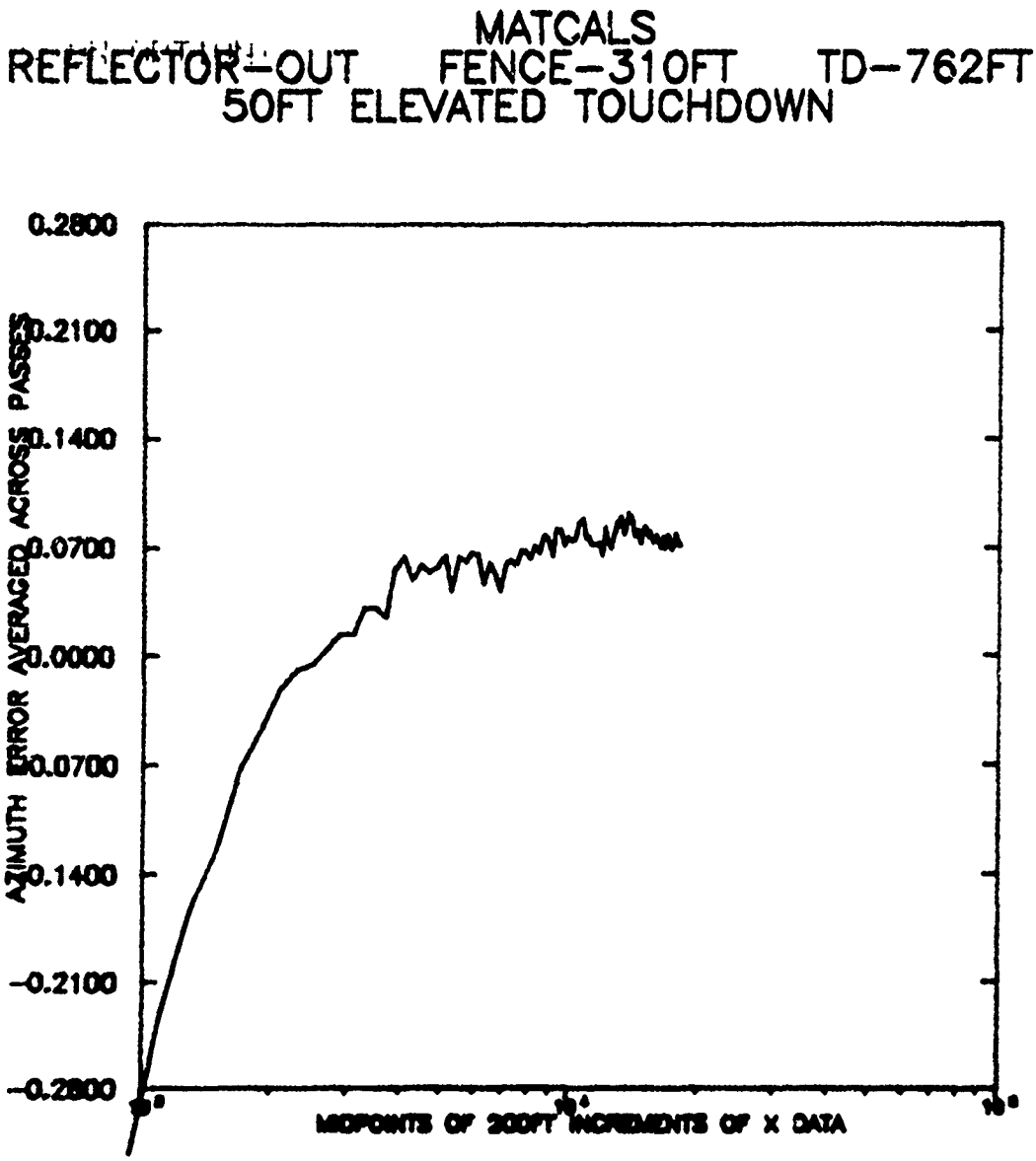

Figure 4.30. Azimuth Error Averaged Across Passes, Configuration 5

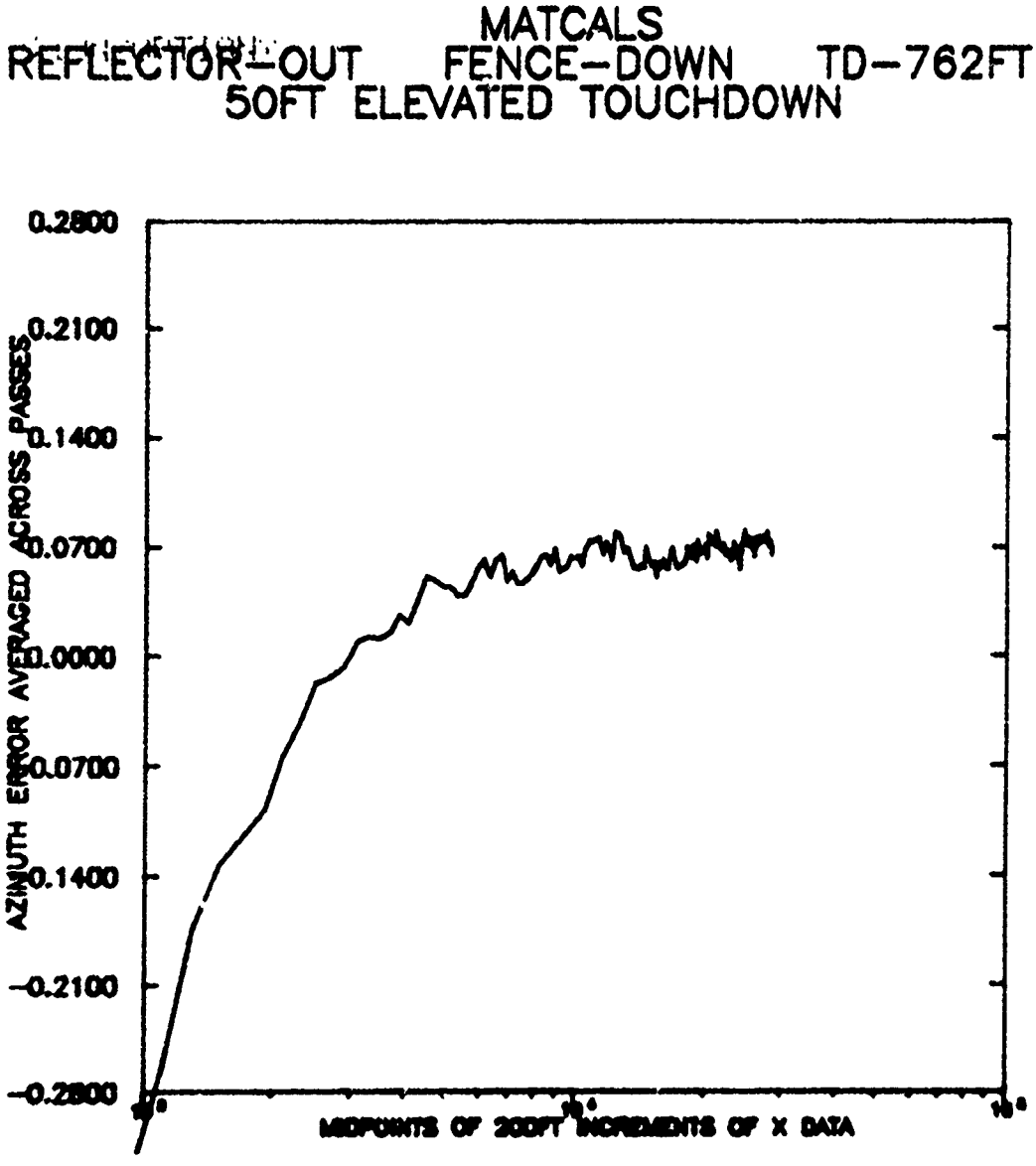

Figure 4.31. Azimuth Error Averaged Across Passes, Configuration 6

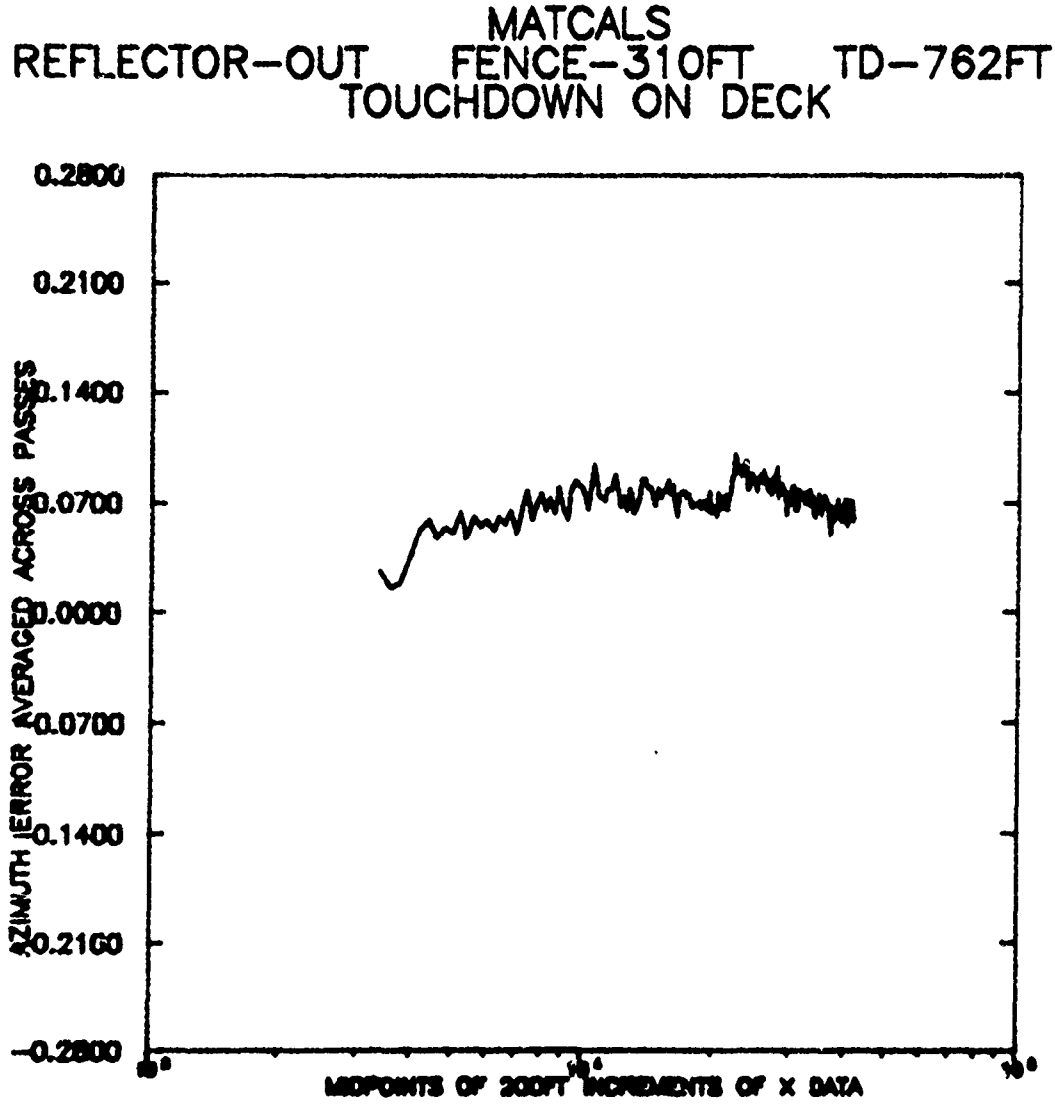

Figure 4.32. Azimuth Error Averaged Across Passes, Configuration 7

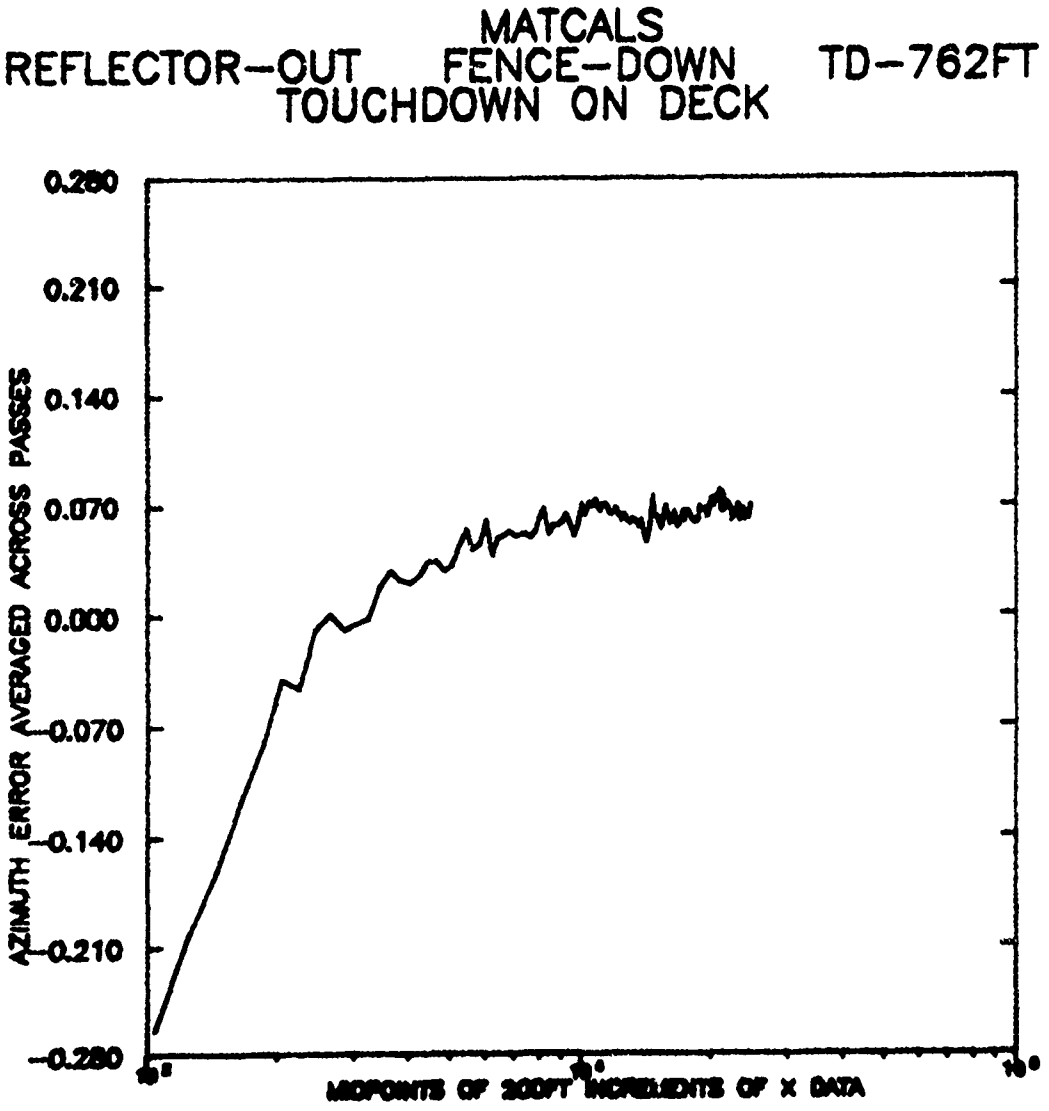

Figure 4.33. Azimuth Error Averaged Across Passes, Configuration 8

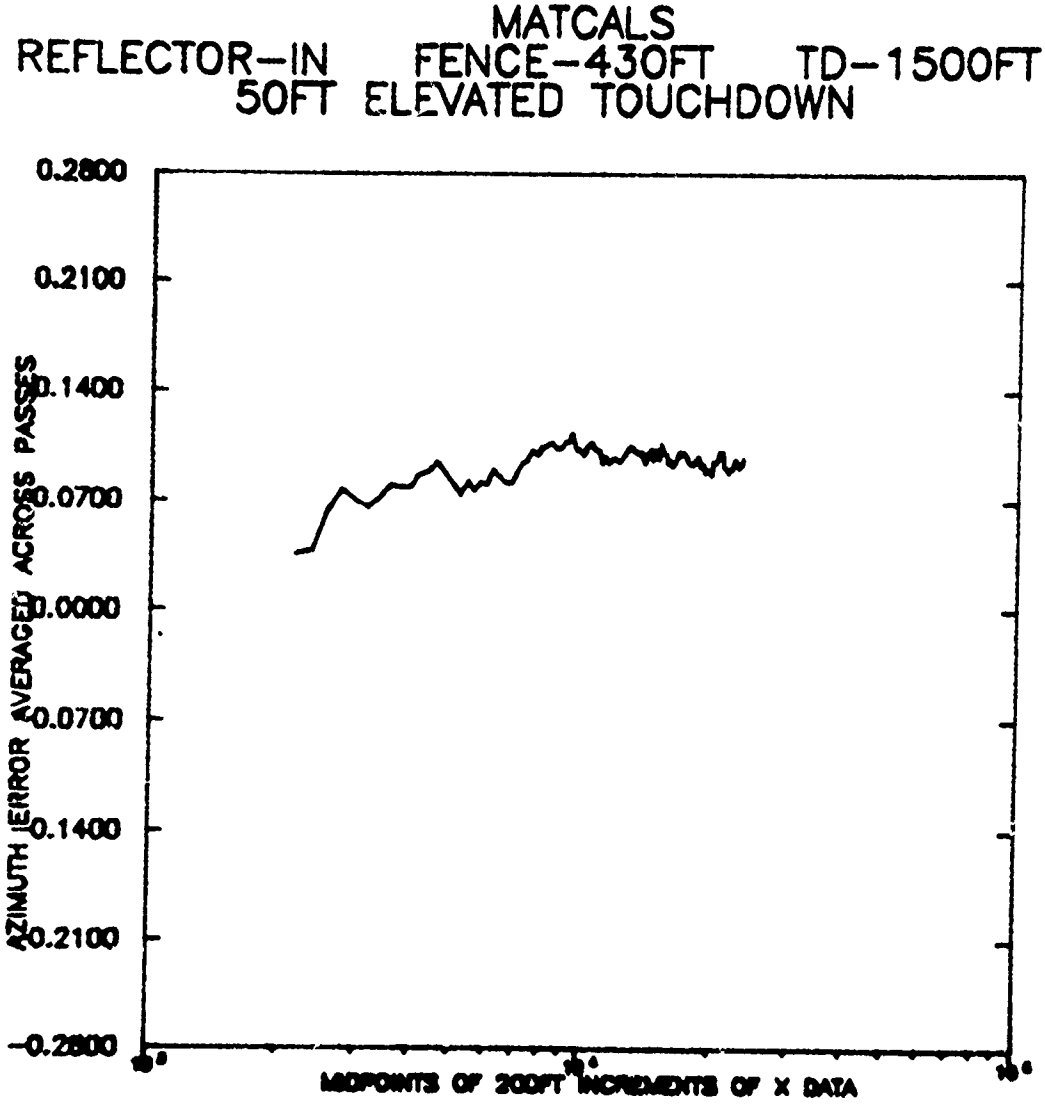

Figure 4.34. Azimuth Error Averaged Across Passes, Configuration 9

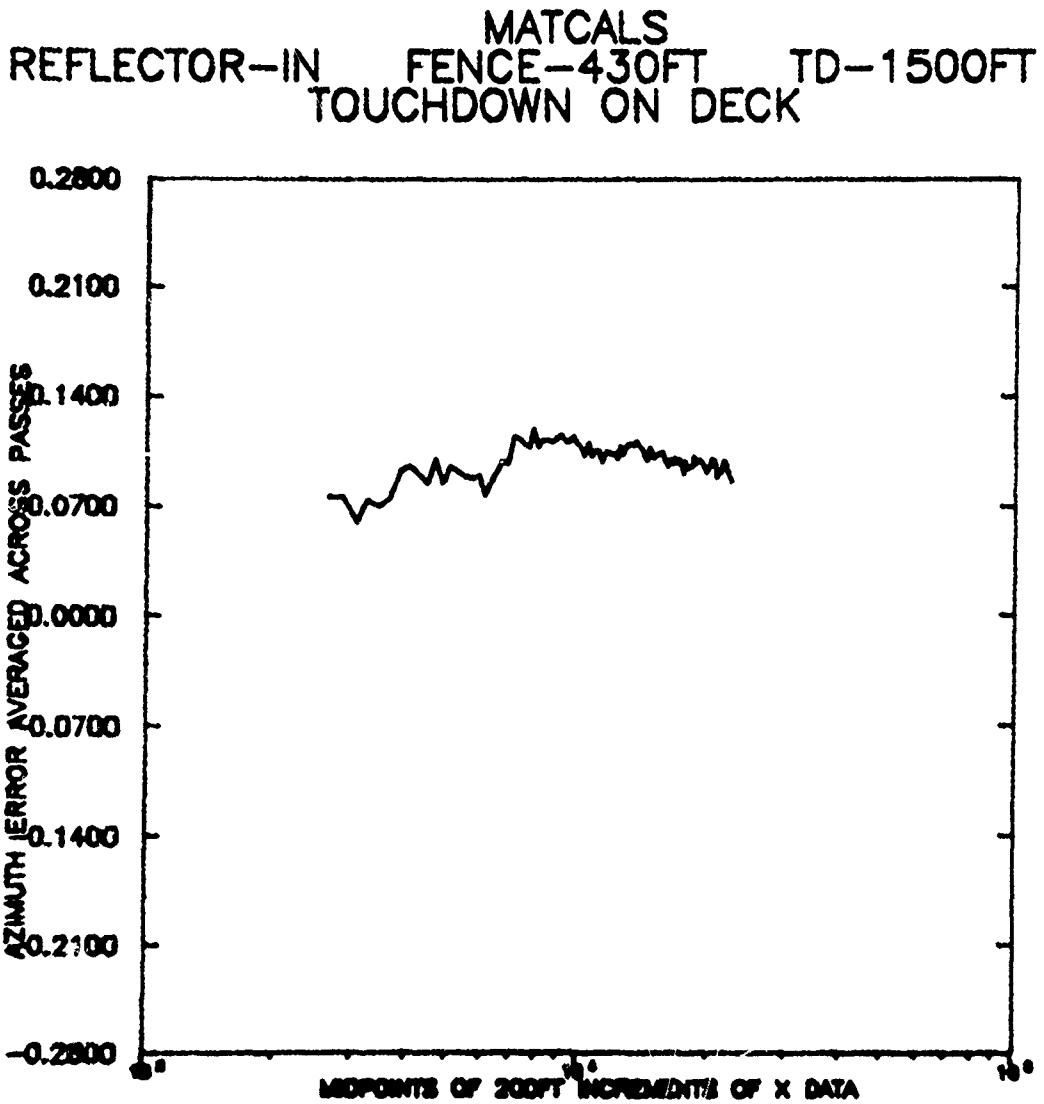

Figure 4.35. Azimuth Error Averaged Across Passes, Configuration 10

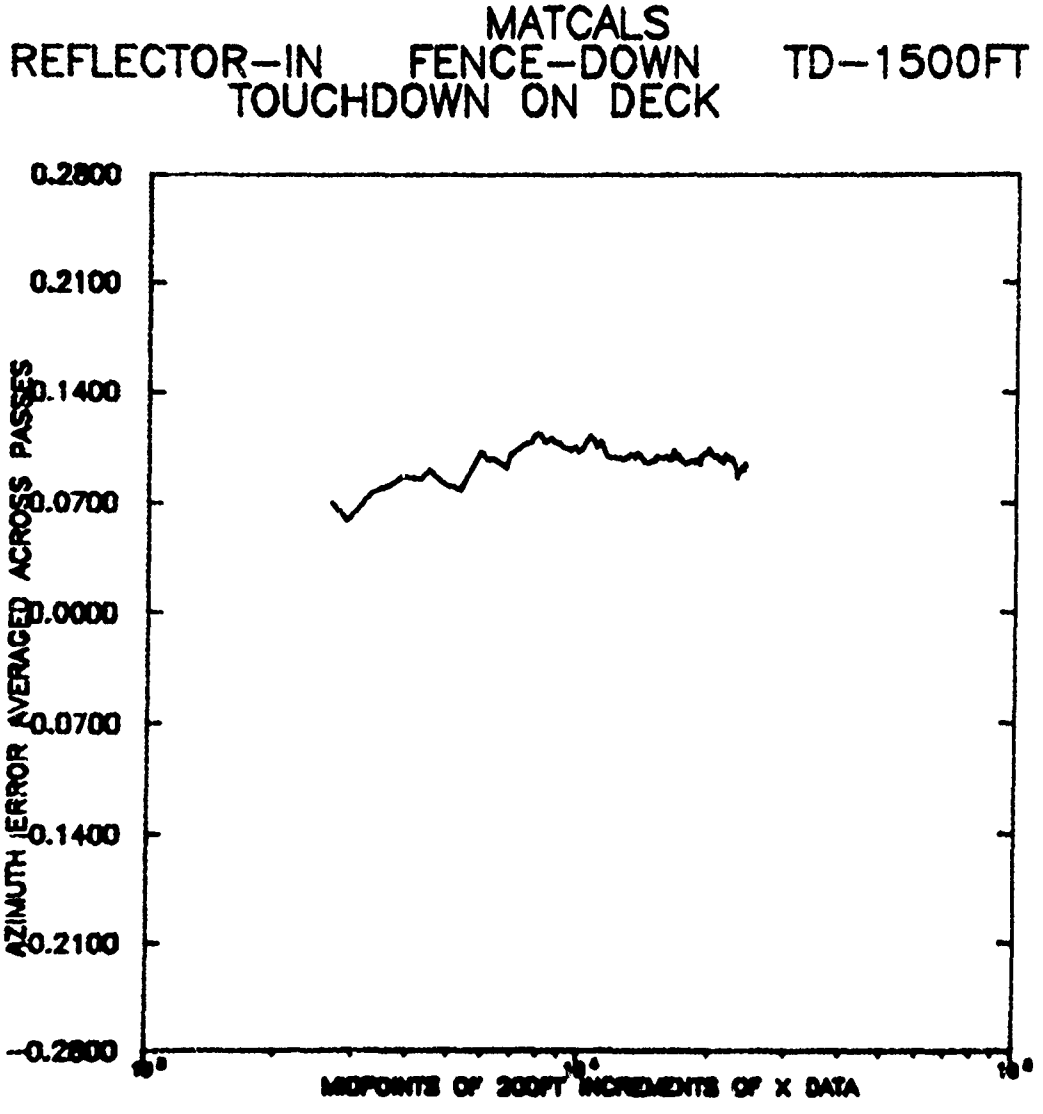

Figure 4.36. Azimuth Error Averaged Across Passes, Configuration 11

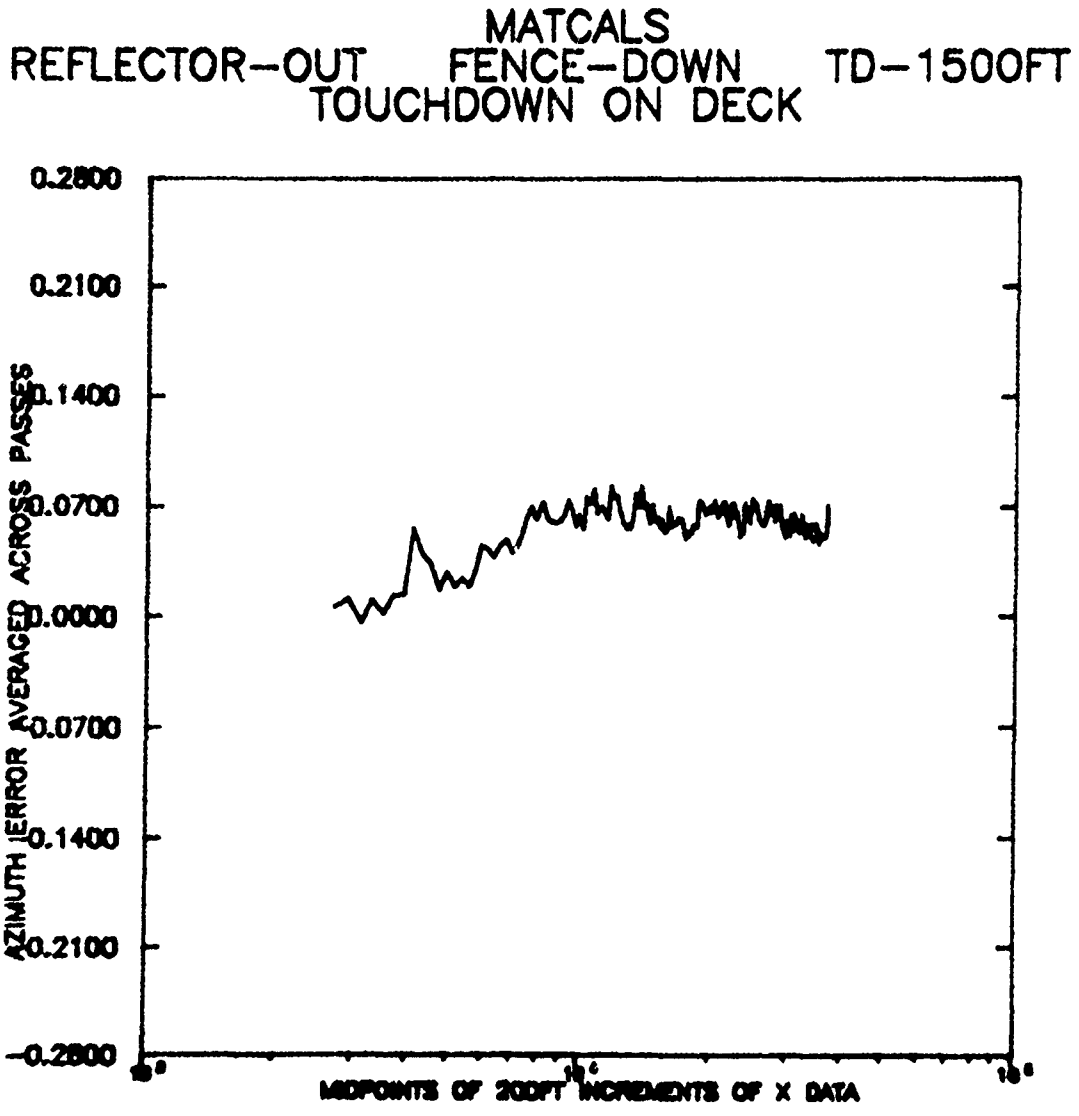

Figure 4.37. Azimuth Error Averaged Across Passes, Configuration 12

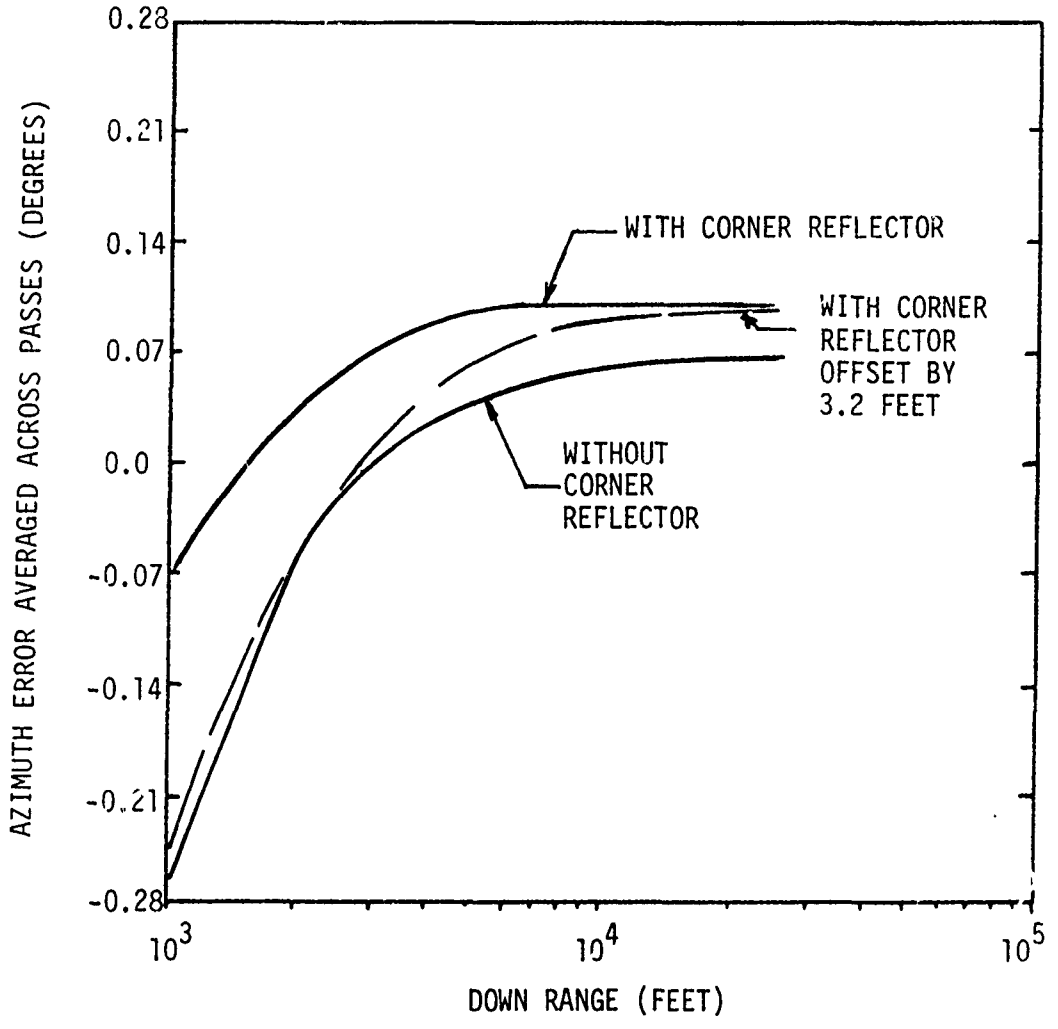

Figure 4.38. Average Azimuth Error With and Without the Corner Reflector

4.3.4 ELEVATION ERRORS AVERAGED ACROSS EQUIVALENT PASSES

These data are plotted in Figures 4.39 through 4.50. Some observations from these curves are noted below.

(1) There seems to be a constant -0.1^{o} error at long range in all the data. That is, the radar is indicating that the target is higher than it actually is.

(2) There appears to be a multipath lobe between 2000 and 3000 feet down range in many of the runs as indicated by the aircraft appearing to move downward in this region, as indicated by the error becoming more positive. The fence did not seem to be of any help.

(3) There are indications of elevation centroid wander on the aircraft when the corner reflector is not installed (e.g., Figure 4.46). With the corner reflector installed, the wander is markedly reduced (e.g., Figure 4.42).

Again, the general shape of the curves may be explained geometrically. If one assumes a constant angular offset of 0.1^{o} and a vertical offset between the ALTS reflector and the radar corner reflector (i.e., radar centroid) of six feet, then the dashed error curve of Figure 4.42 results. Similarly, with the same angular offset and a 1.5 foot difference between the ALTS and the radar centroid, then the dashed error curve of Figure 4.46 results. The excellent fit of these curves to the actual data lends credence to this hypothesis. Also, the sign of the error is in agreement with the postulated error source. That is, the radar centroid should appear to be higher than the laser centroid (since the laser reflector was mounted under the starboard wing of the test aircraft), and the error should be more negative with the radar corner reflector installed than with it removed; this occurs because the radar corner reflector (which will be the centroid) is at a higher elevation angle from the radar than the radar centroid of the aircraft when the corner reflector is removed. The constant 0.1^{o} offset error is unexplained at this time.

4.3.5 AZIMUTH RMS ERROR ACROSS EQUIVALENT PASSES

These data are presented in Figures 4.51 through 4.62. Several observations are noted below:

(1) If one compares Figures 4.53 and 4.54 to Figures 4.57 and 4.58, it does not appear that the corner reflector had much of an effect on the tracking performance. However, comparison of Figures 4.51 and 4.52 to 4.55 and 4.56 indicates exactly the opposite; that is, the corner reflector seems to enhance

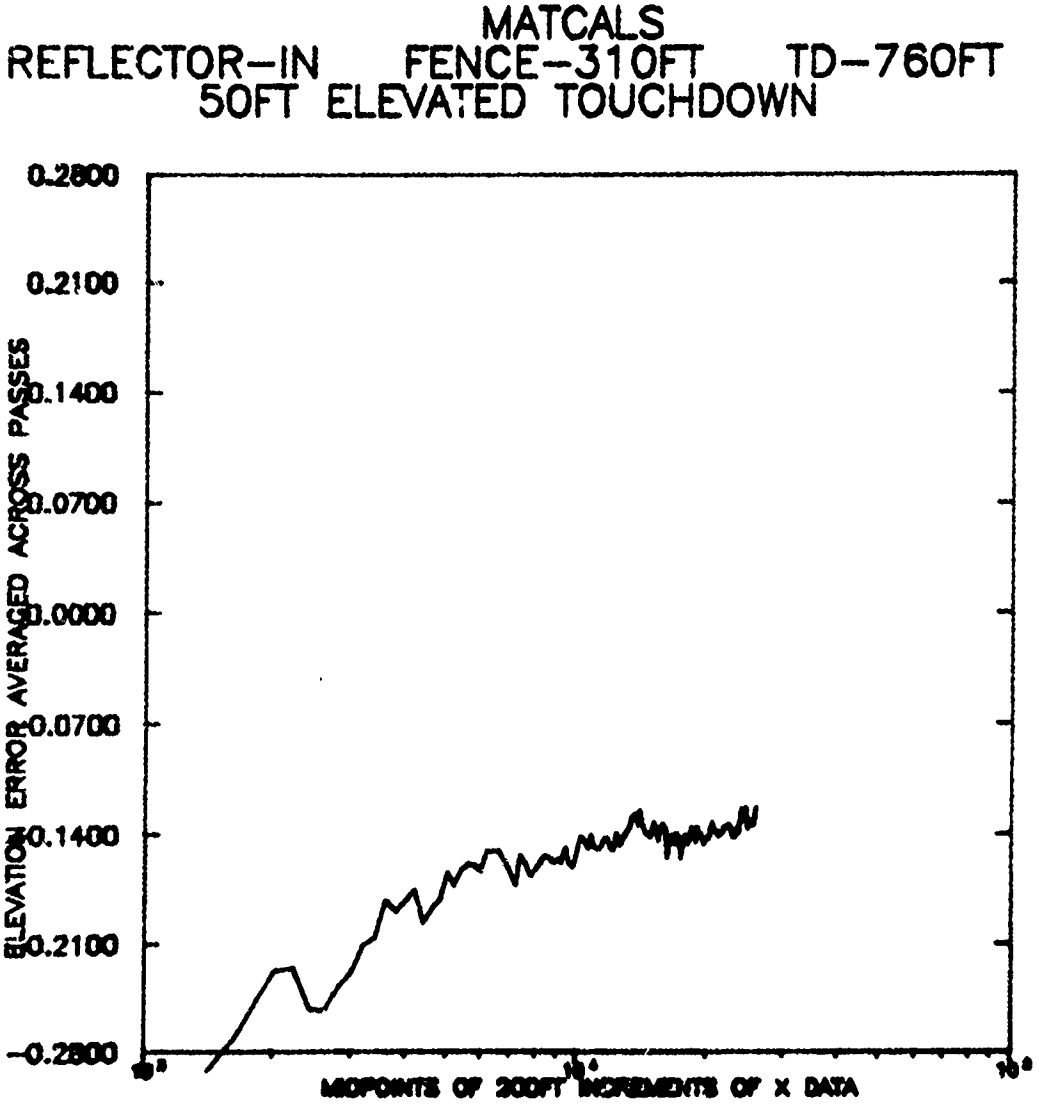

Figure 4.39. Elevation Error Averaged Across Passes, Configuration 1

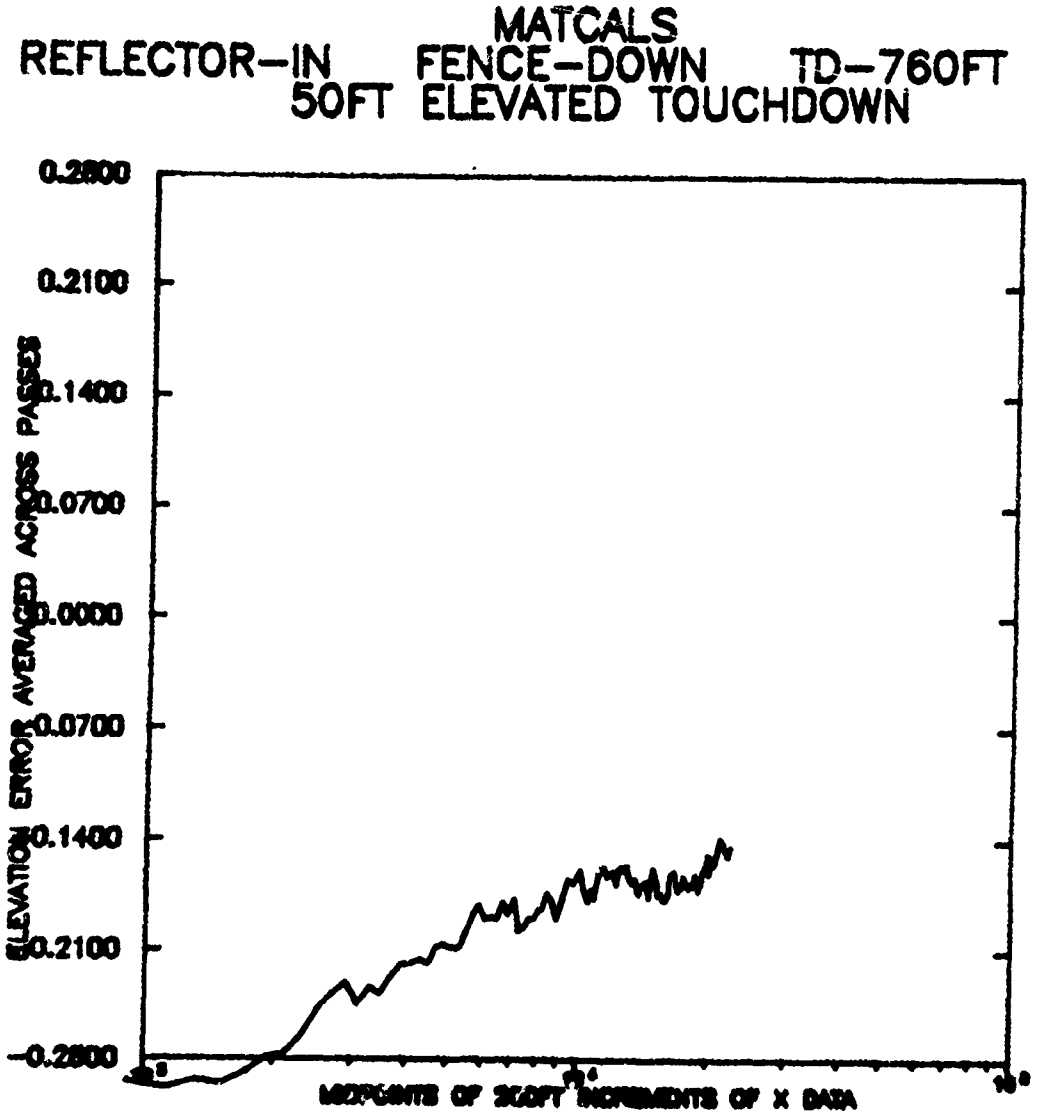

Figure 4.40. Elevation Error Averaged Across Passes, Configuration 2

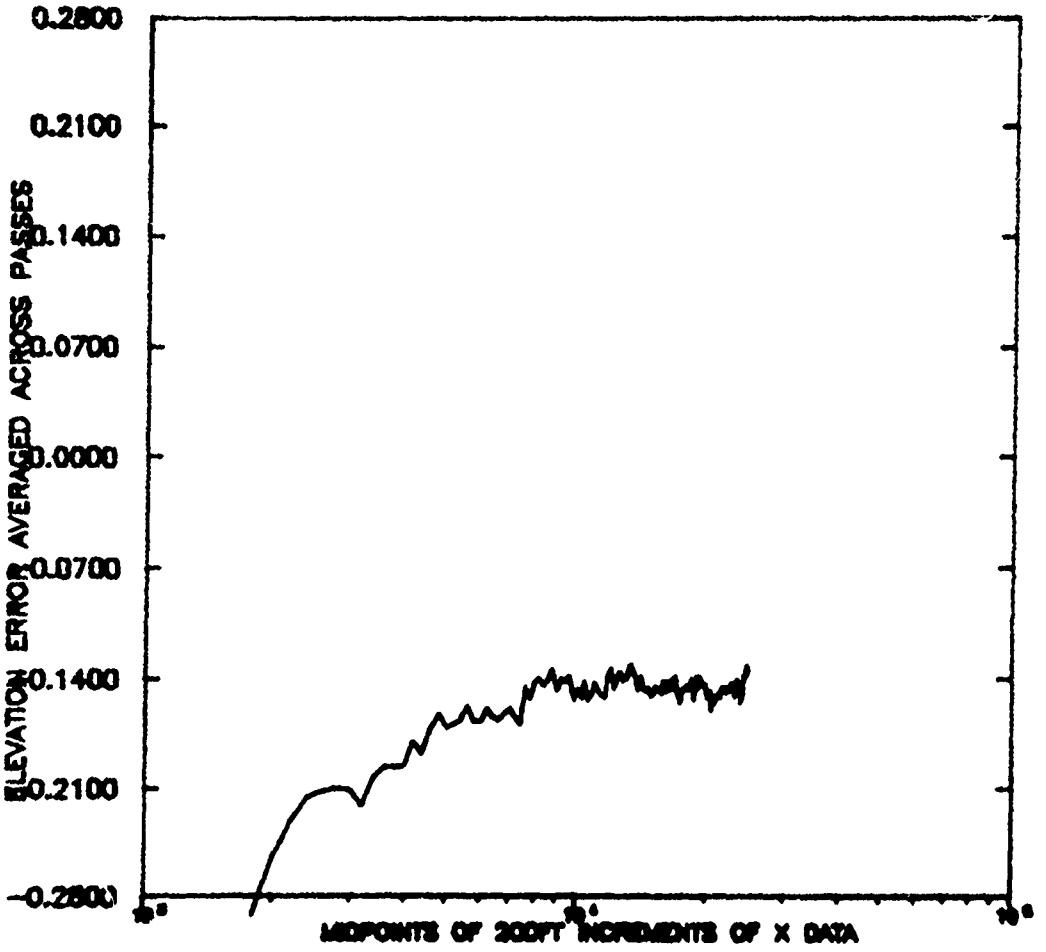

Figure 4.41. Elevation Error Averaged Across Passes, Configuration 3

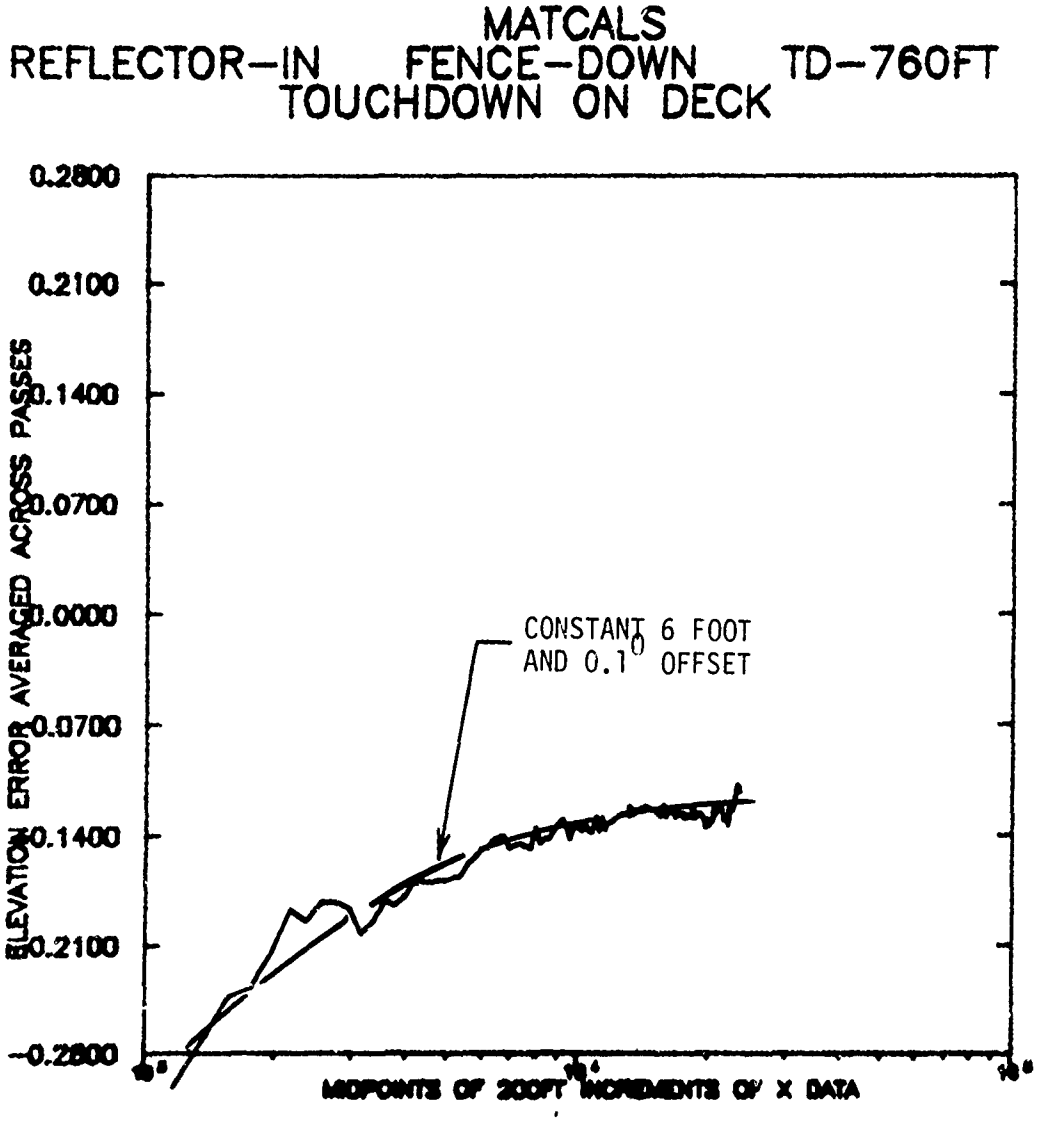

Figure 4.42. Elevation Error Averaged Across Passes, Configuration 4

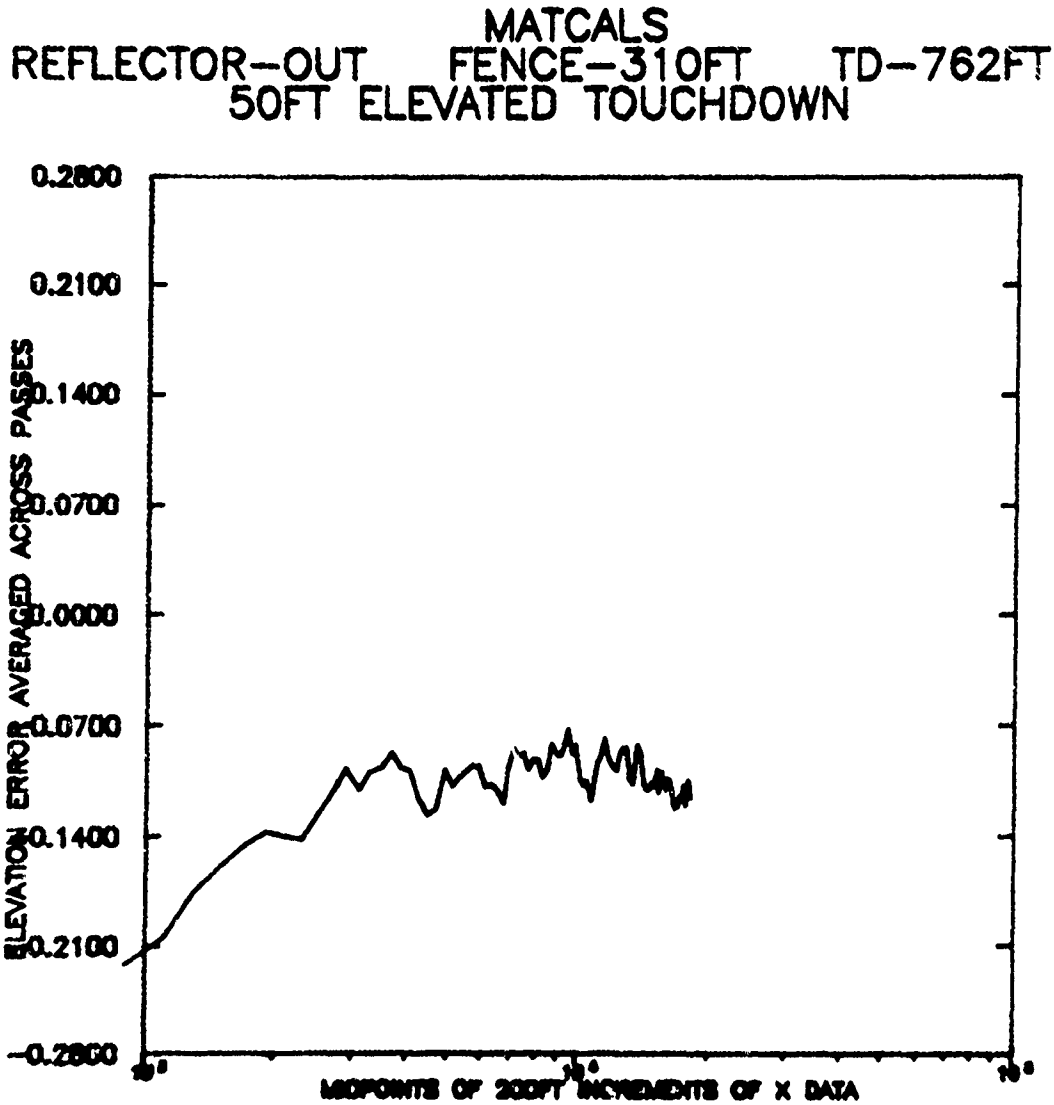

Figure 4.43. Elevation Error Averaged Across Passes, Configuration 5

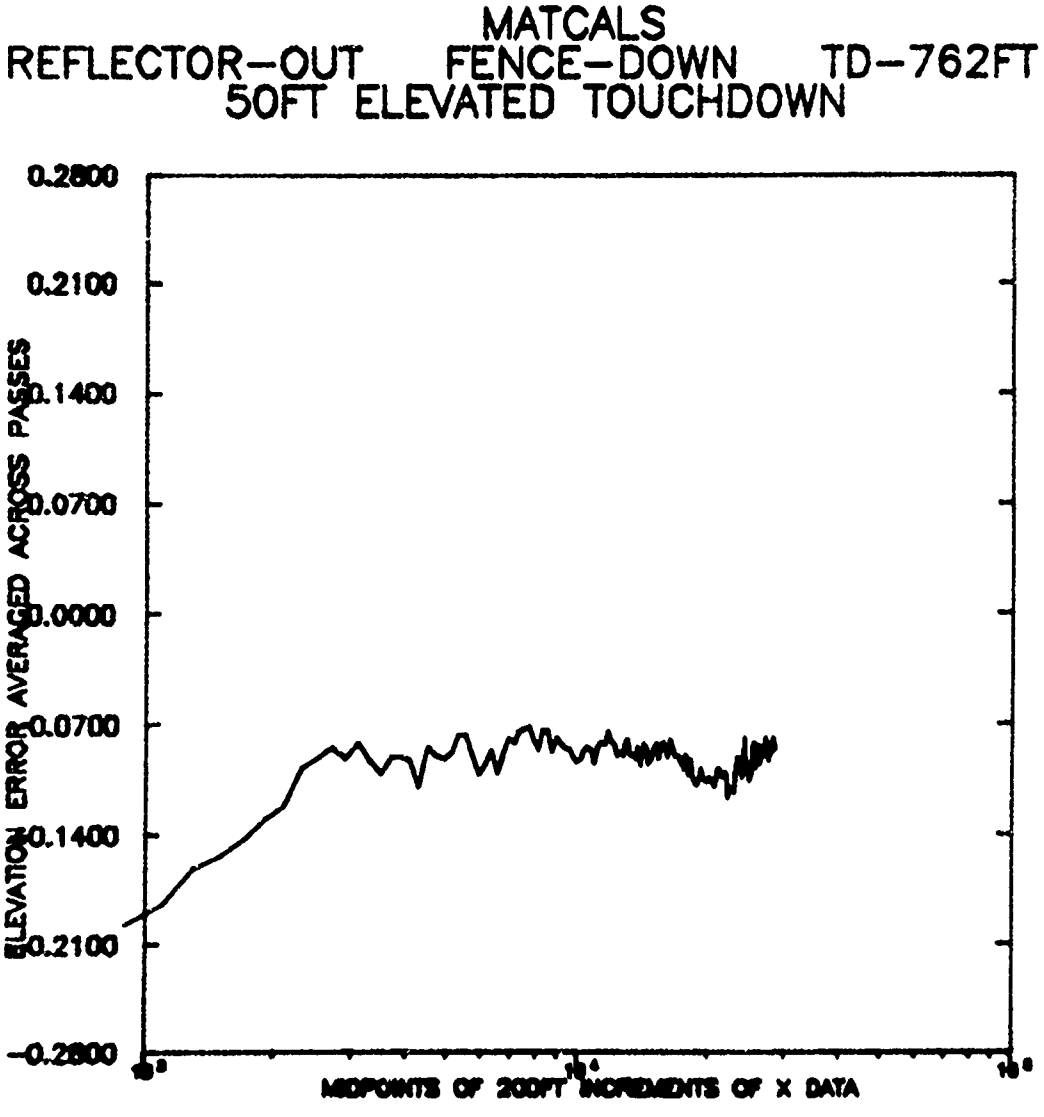

Figure 4.44. Elevation Error Averaged Across Passes, Configuration 6

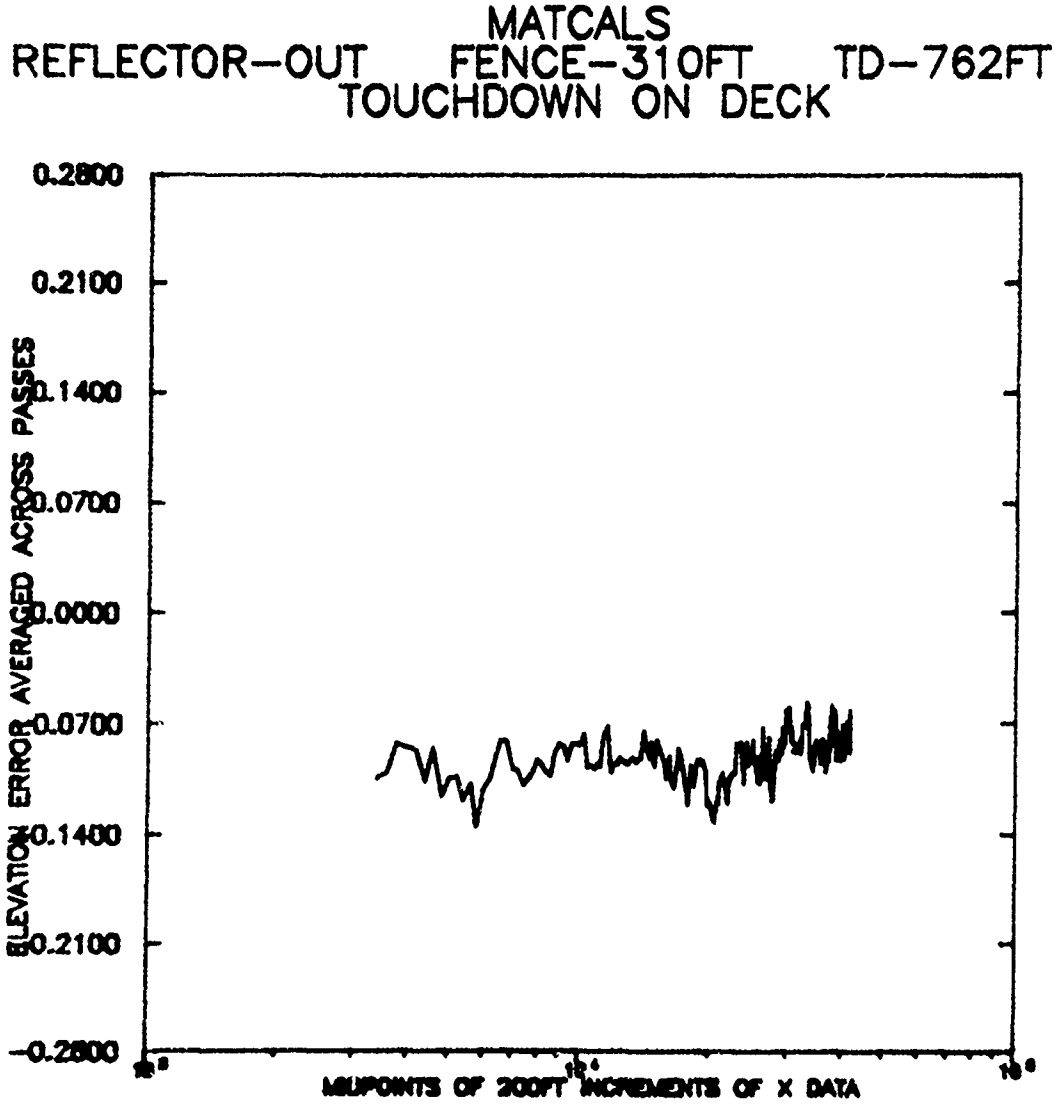

Figure 4.45. Elevation Error Averaged Across Passes, Configuration 7

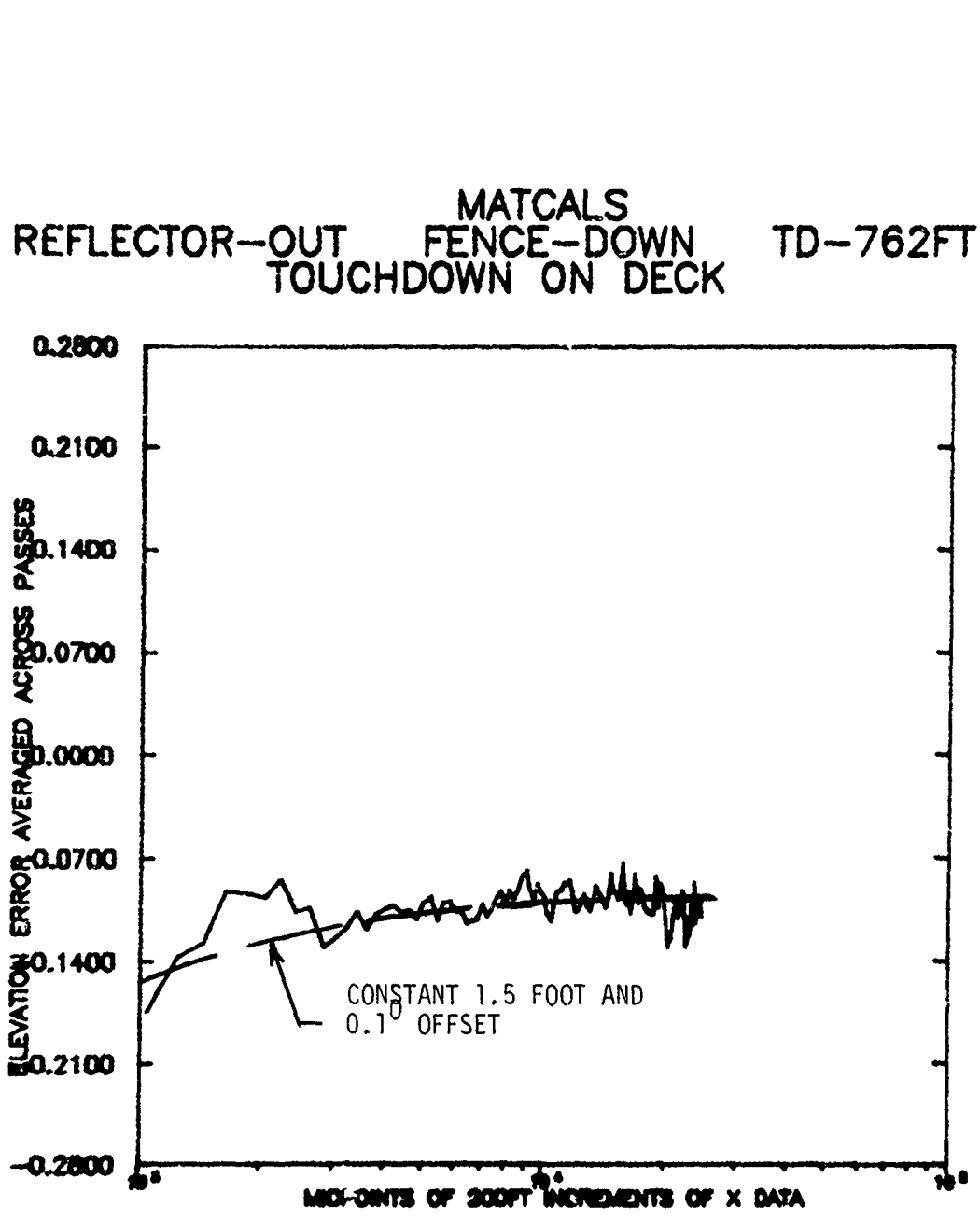

Figure 4.46. Elevation Error Averaged Across Passes, Configuration 8

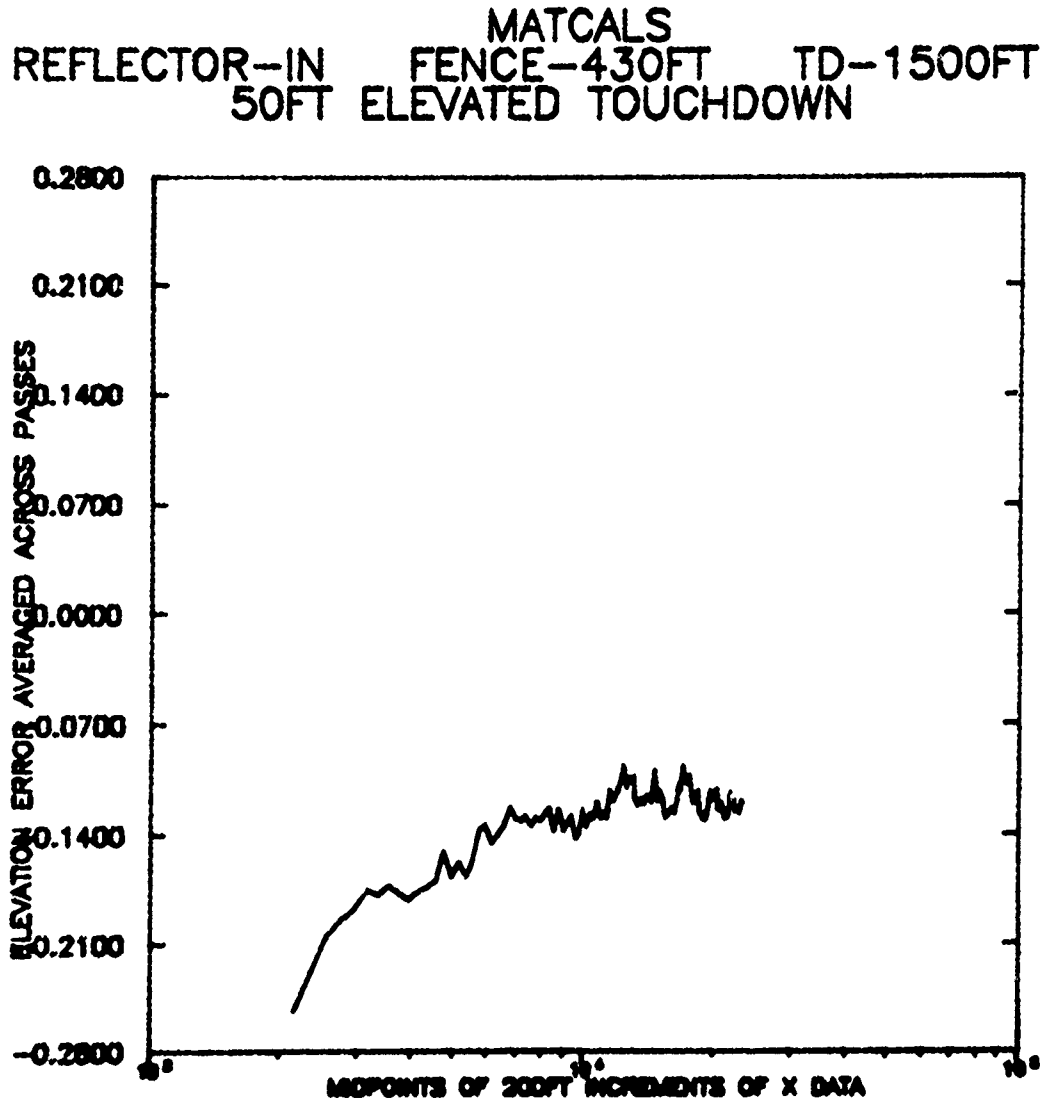

Figure 4.47. Elevation Error Averaged Across Passes, Configuration 9

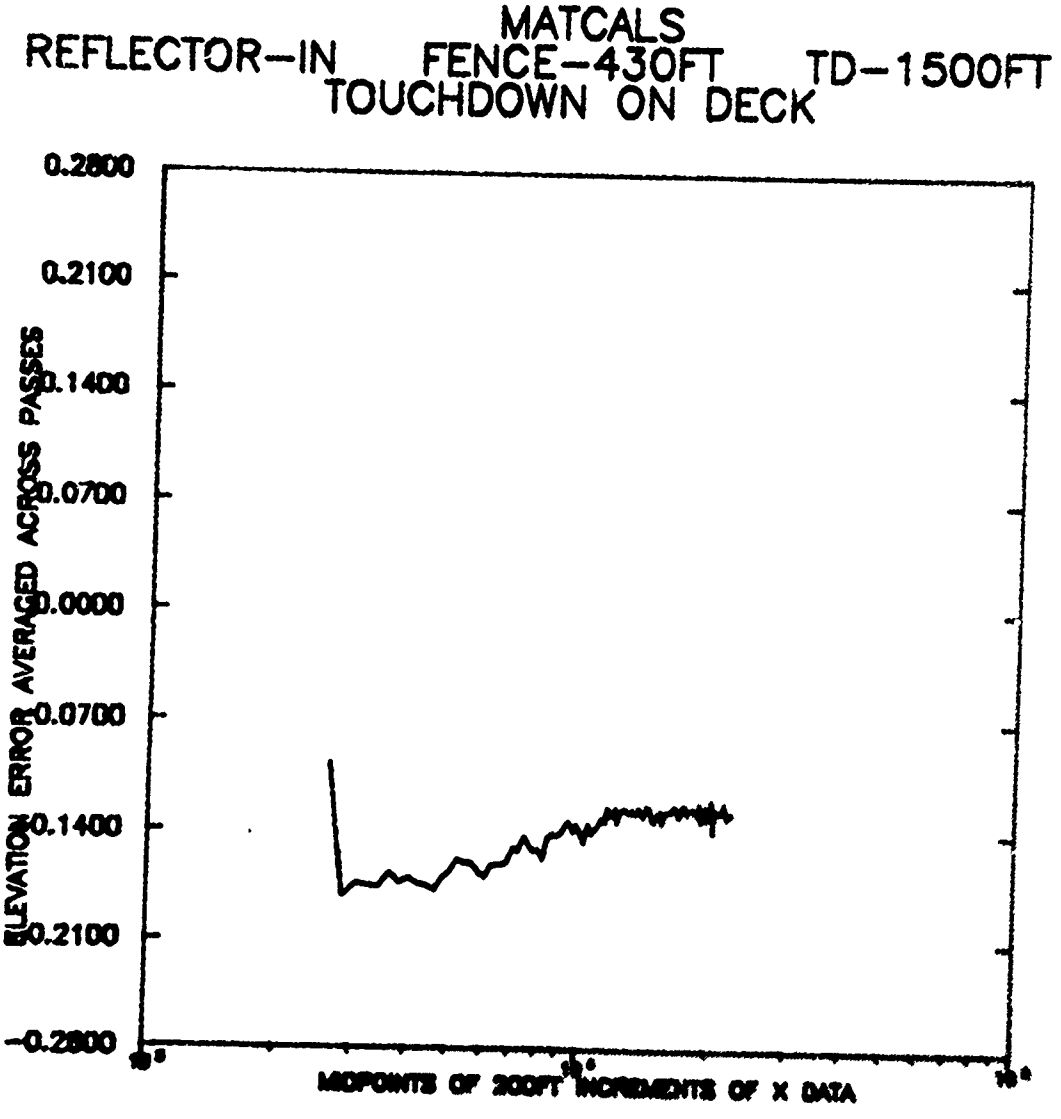

Figure 4.48. Elevation Error Averaged Across Passes, Configuration 10

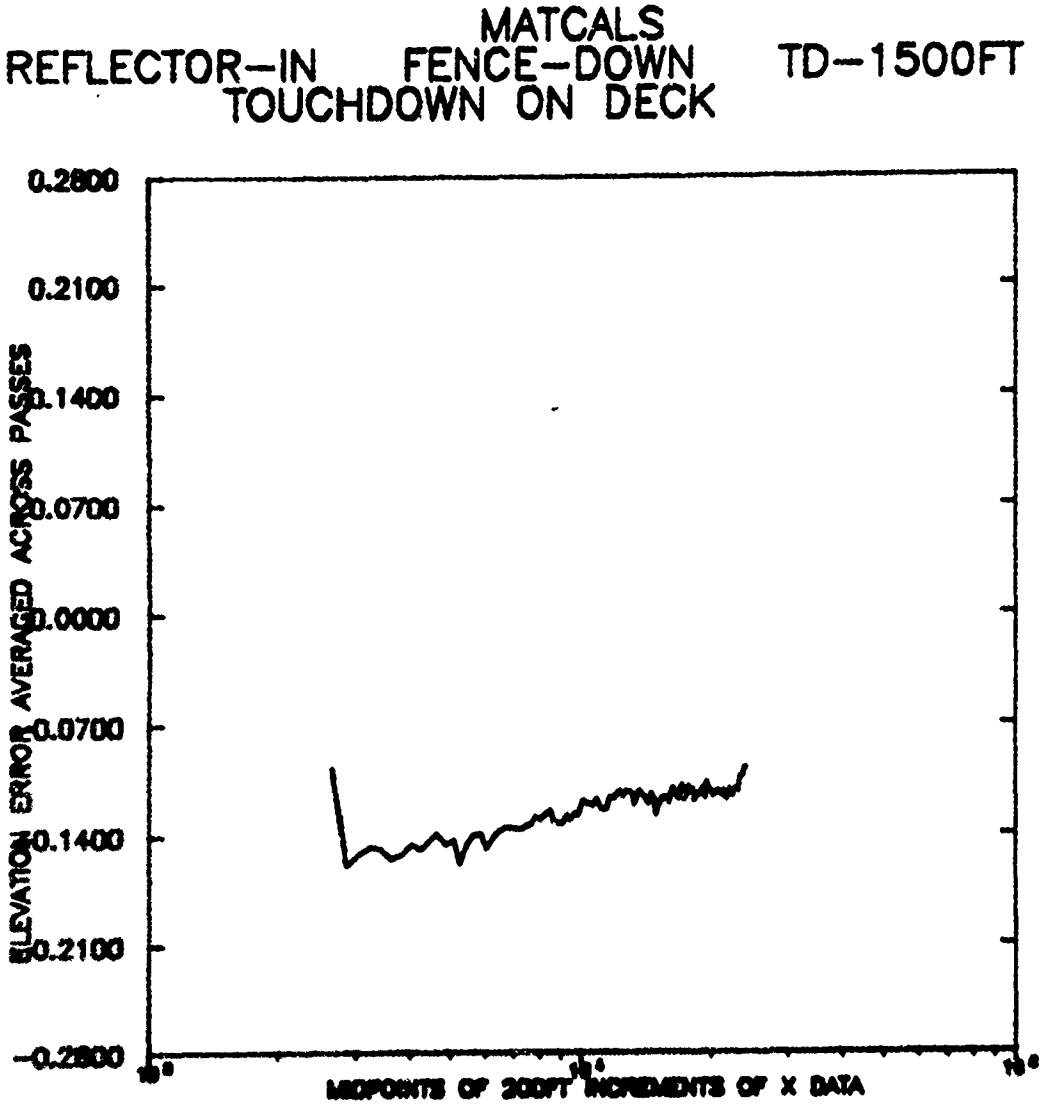

Figure 4.49. Elevation Error Averaged Across Passes, Configuration 11

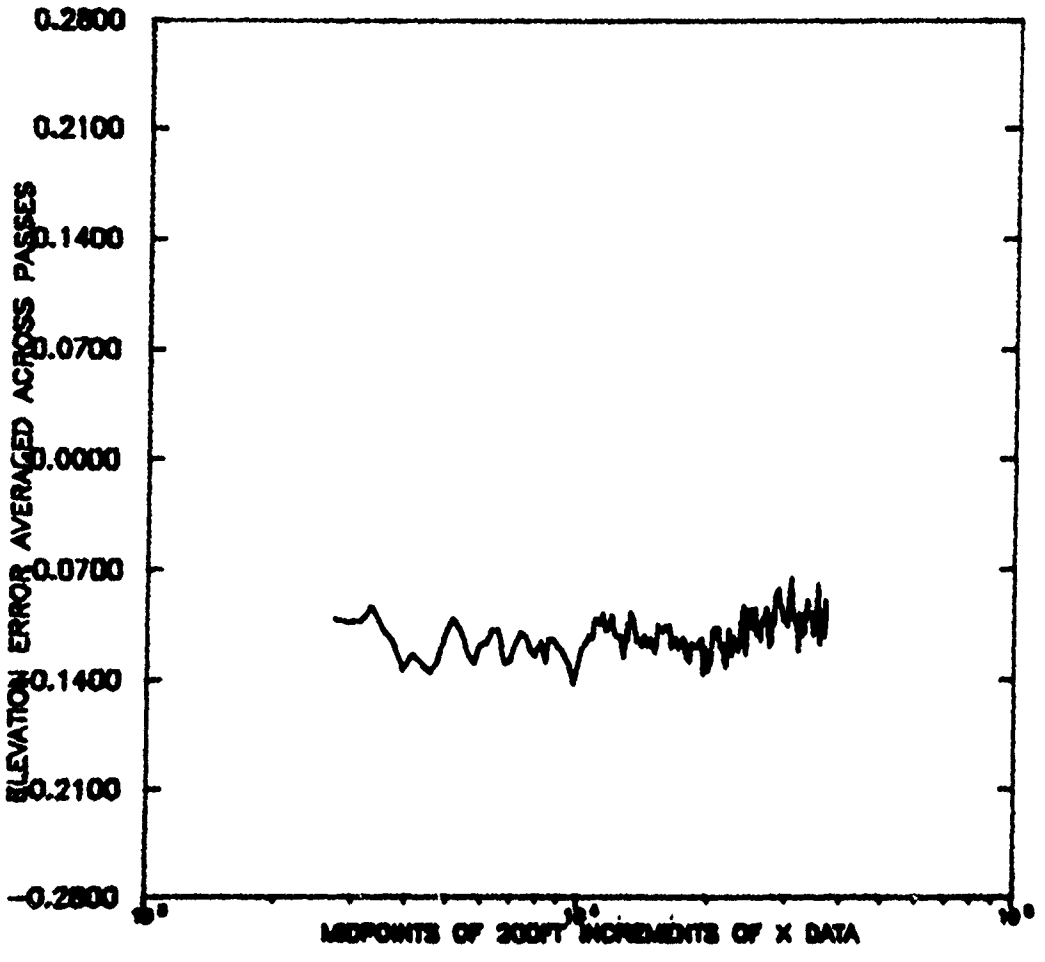

Figure 4.50. Elevation Error Averaged Across Passes, Configuration 12

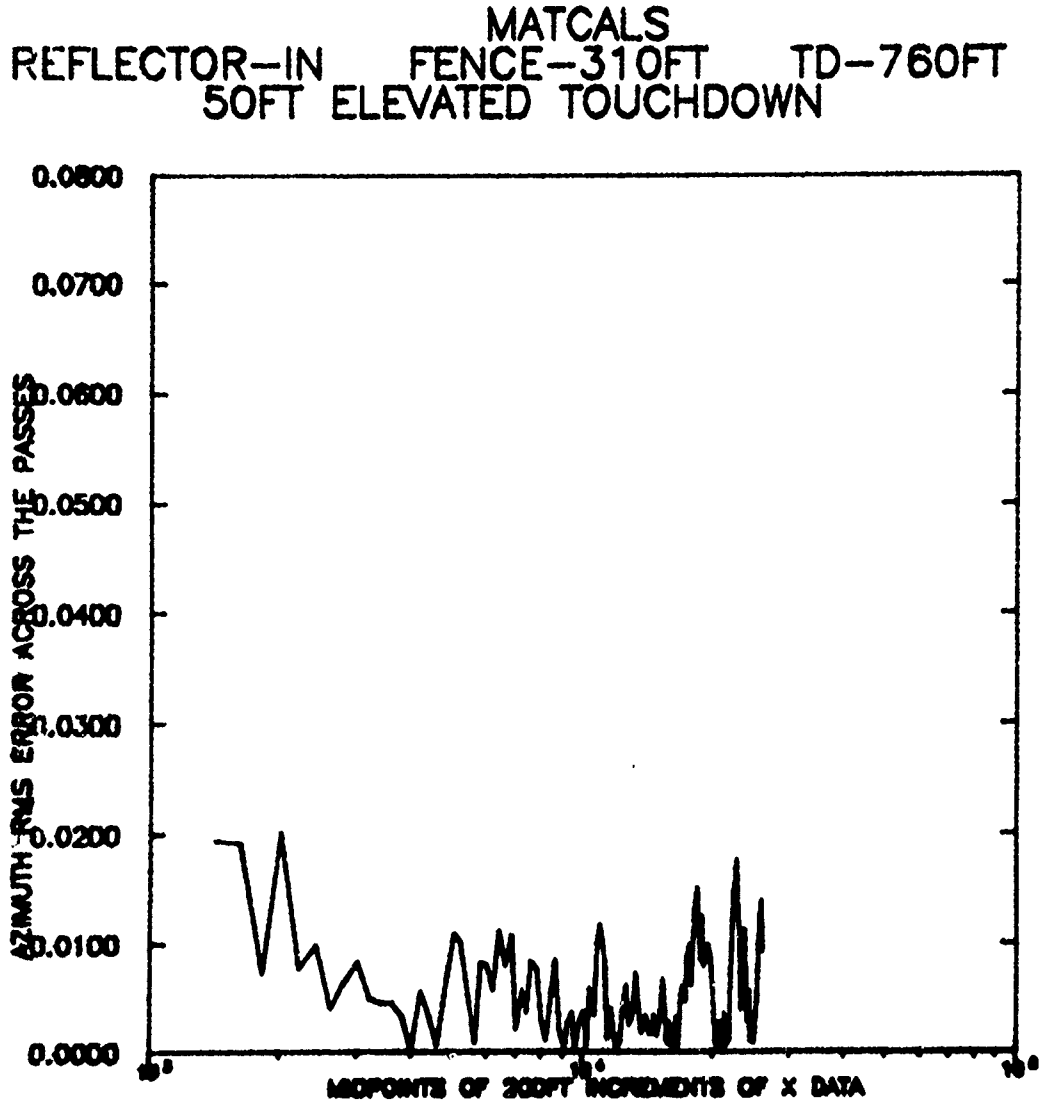

Figure 4.51. Azimuth RMS Error Across the Passes, Configuration 1

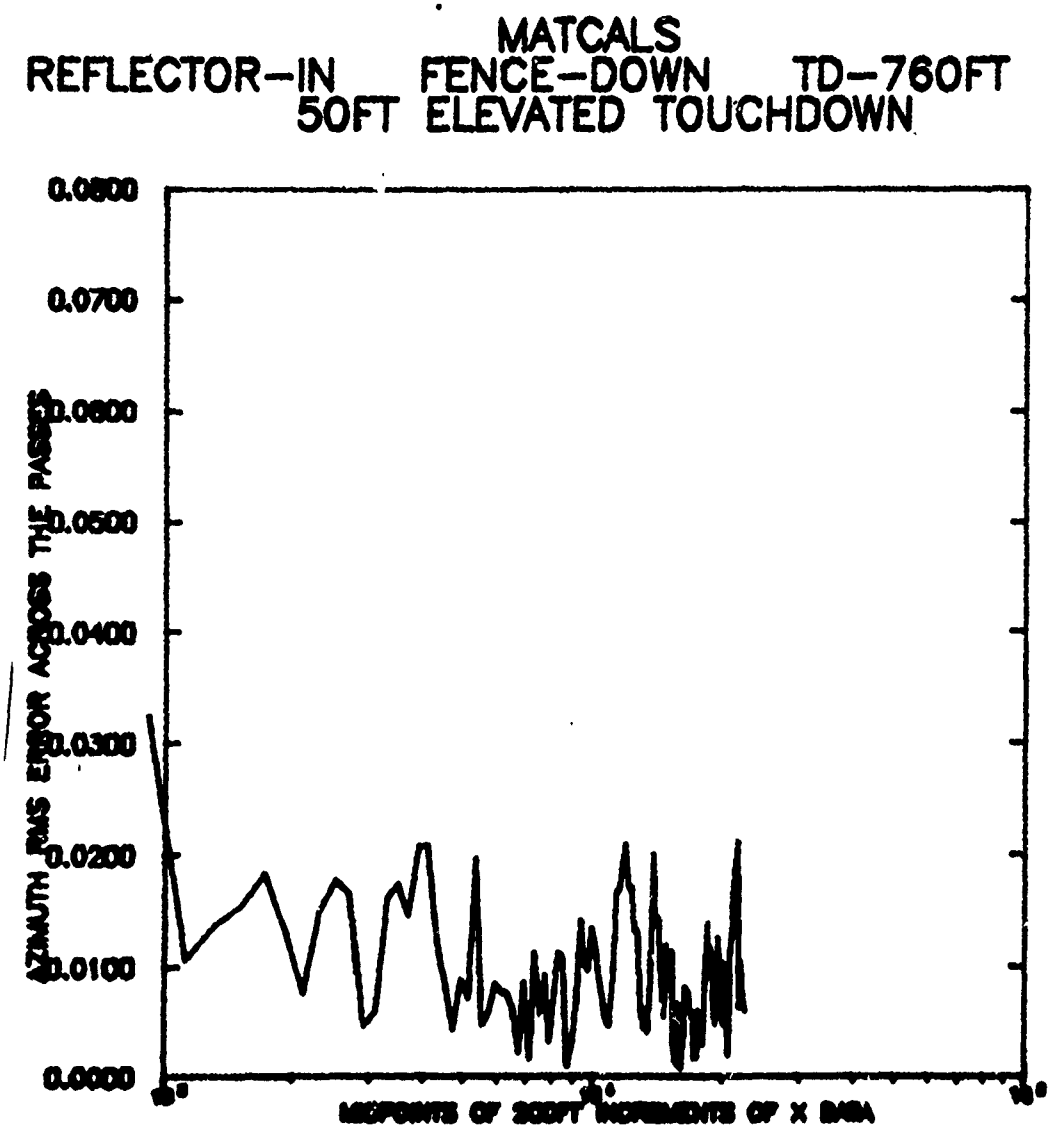

Figure 4.52. Azimuth RMS Error Across the Passes, Configuration 2

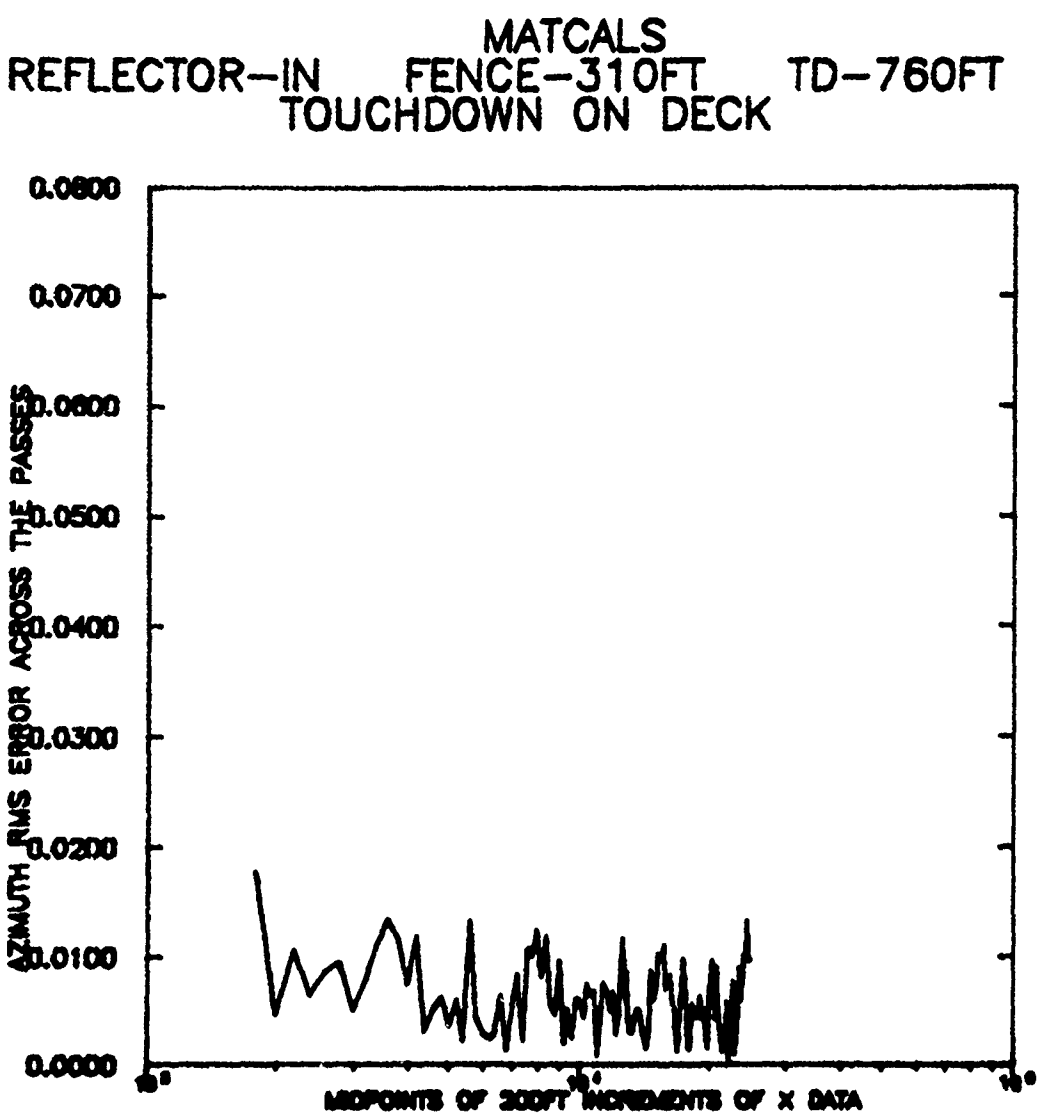

Figure 4.53. Azimuth RMS Error Across the Passes, Configuration 3

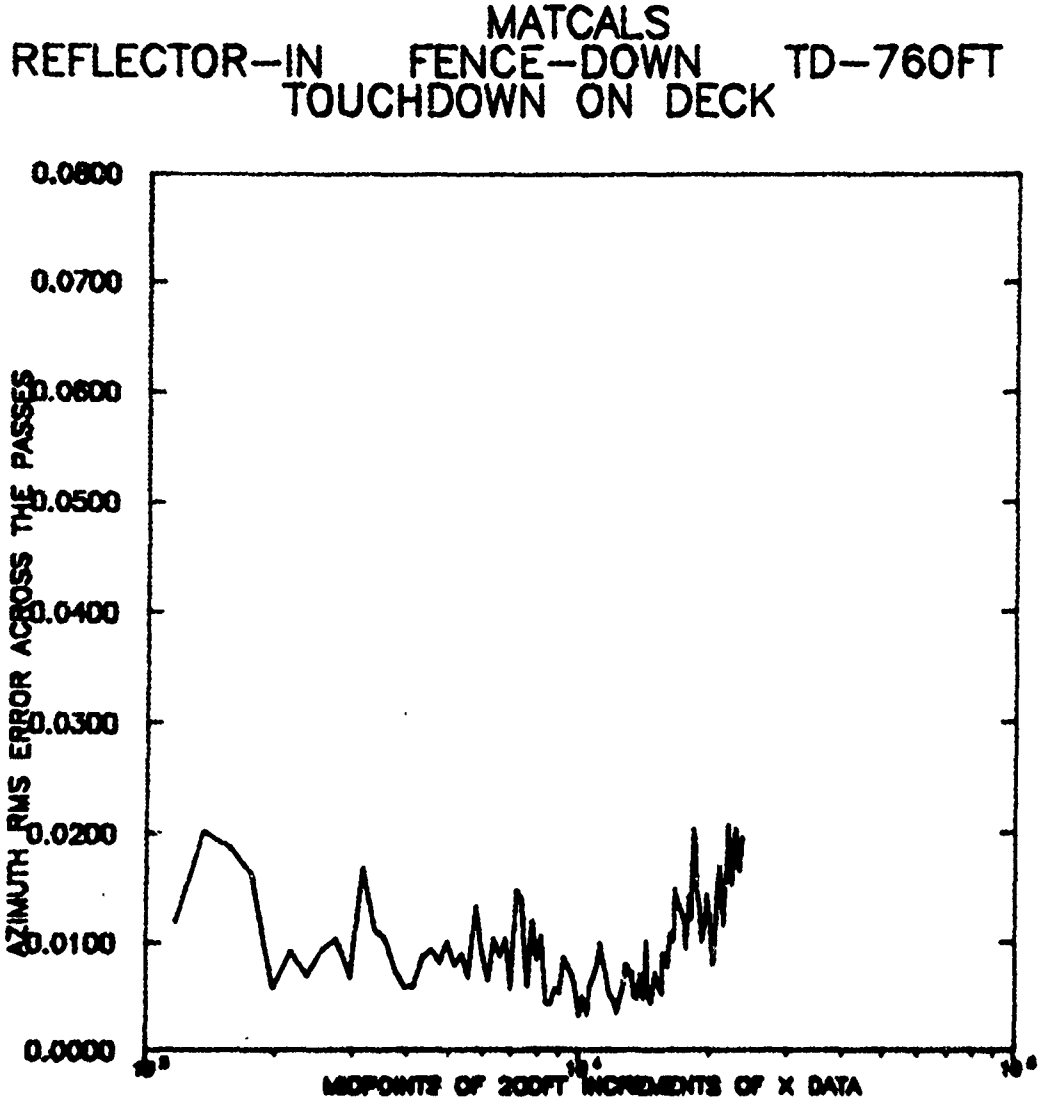

Figure 4.54. Azimuth RMS Error Across the Passes, Configuration 4

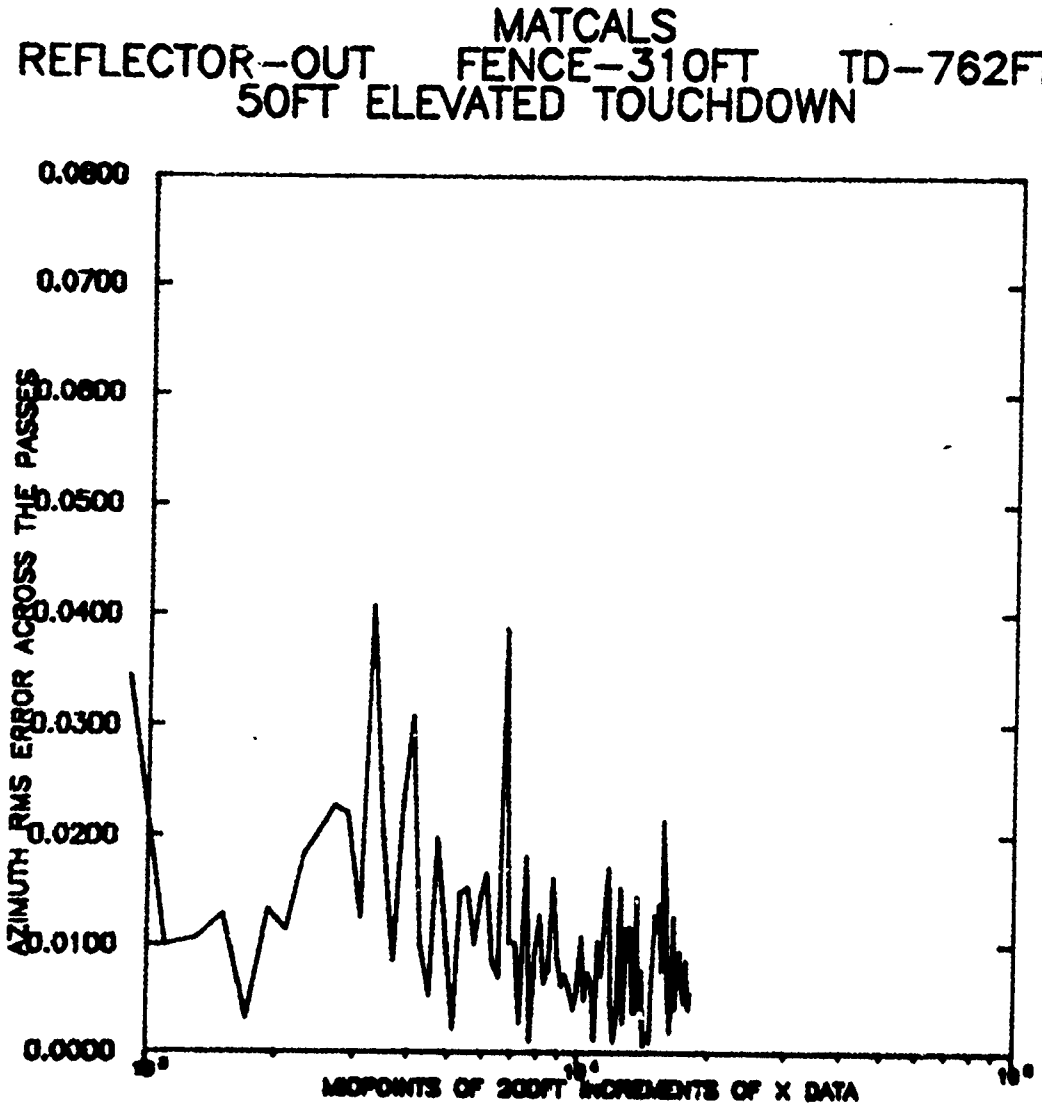

Figure 4.55. Azimuth RMS Error Across the Passes, Configuration 5

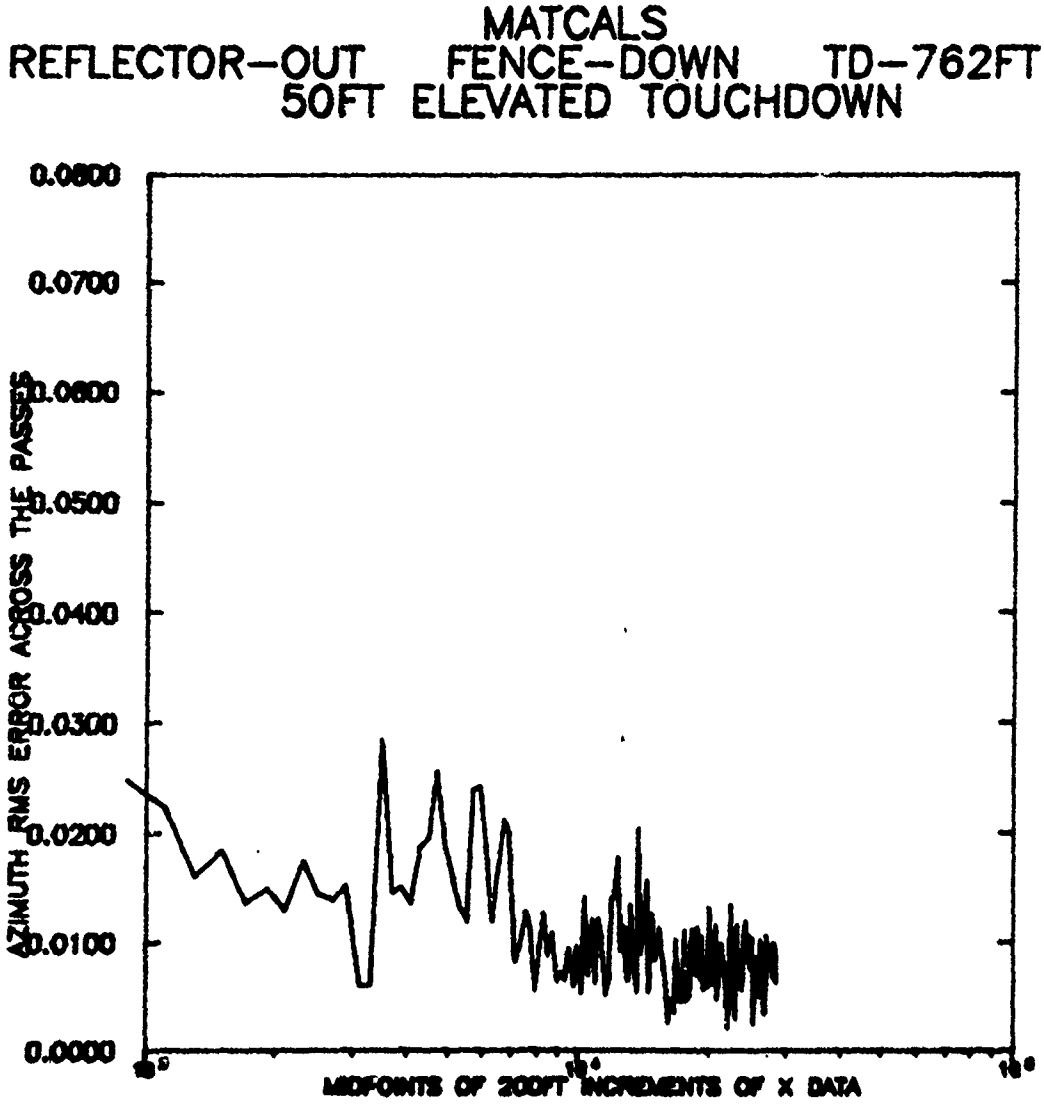

Figure 4.56. Azimuth RMS Error Across the Passes, Configuration 6

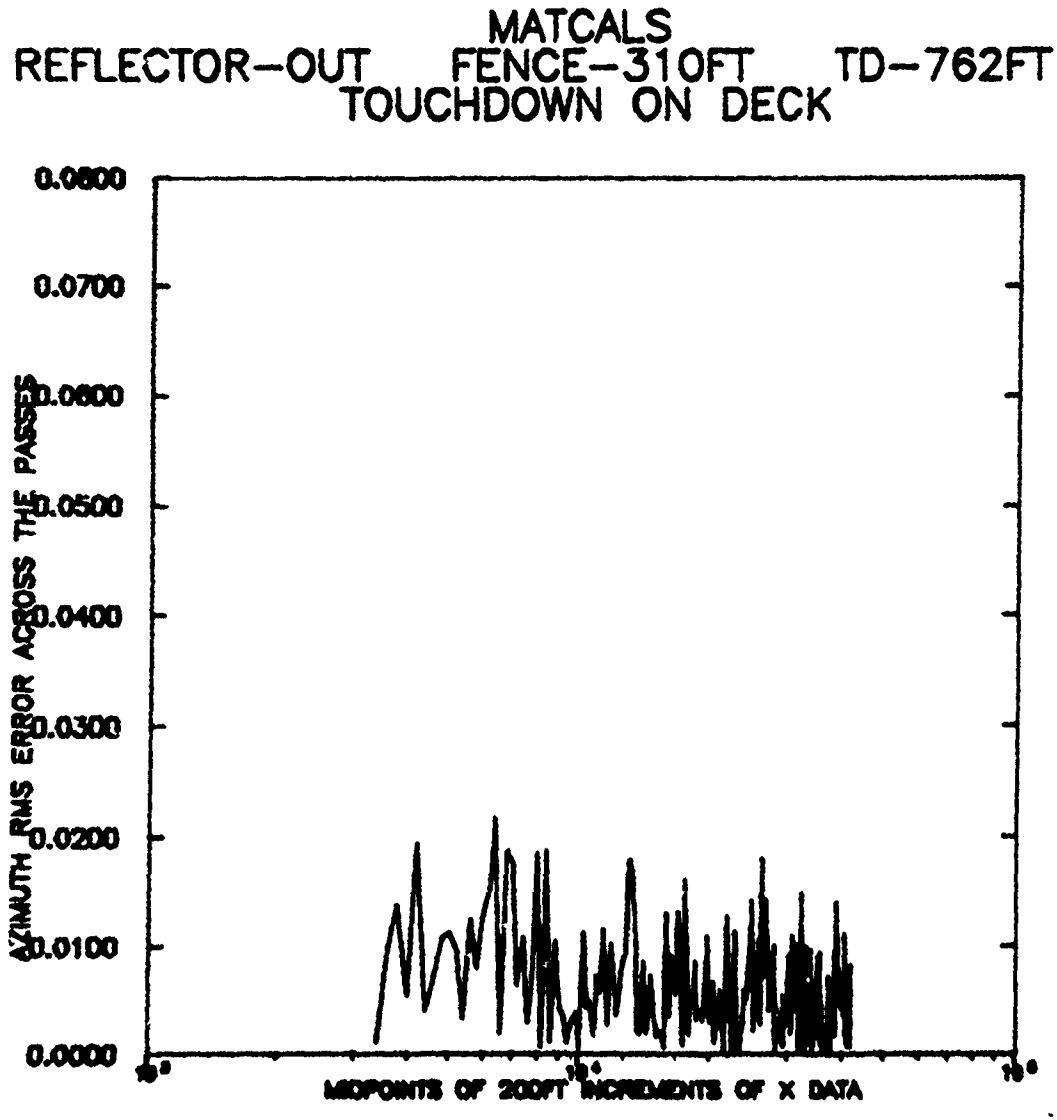

Figure 4.57. Azimuth RMS Error Across the Passes, Configuration 7

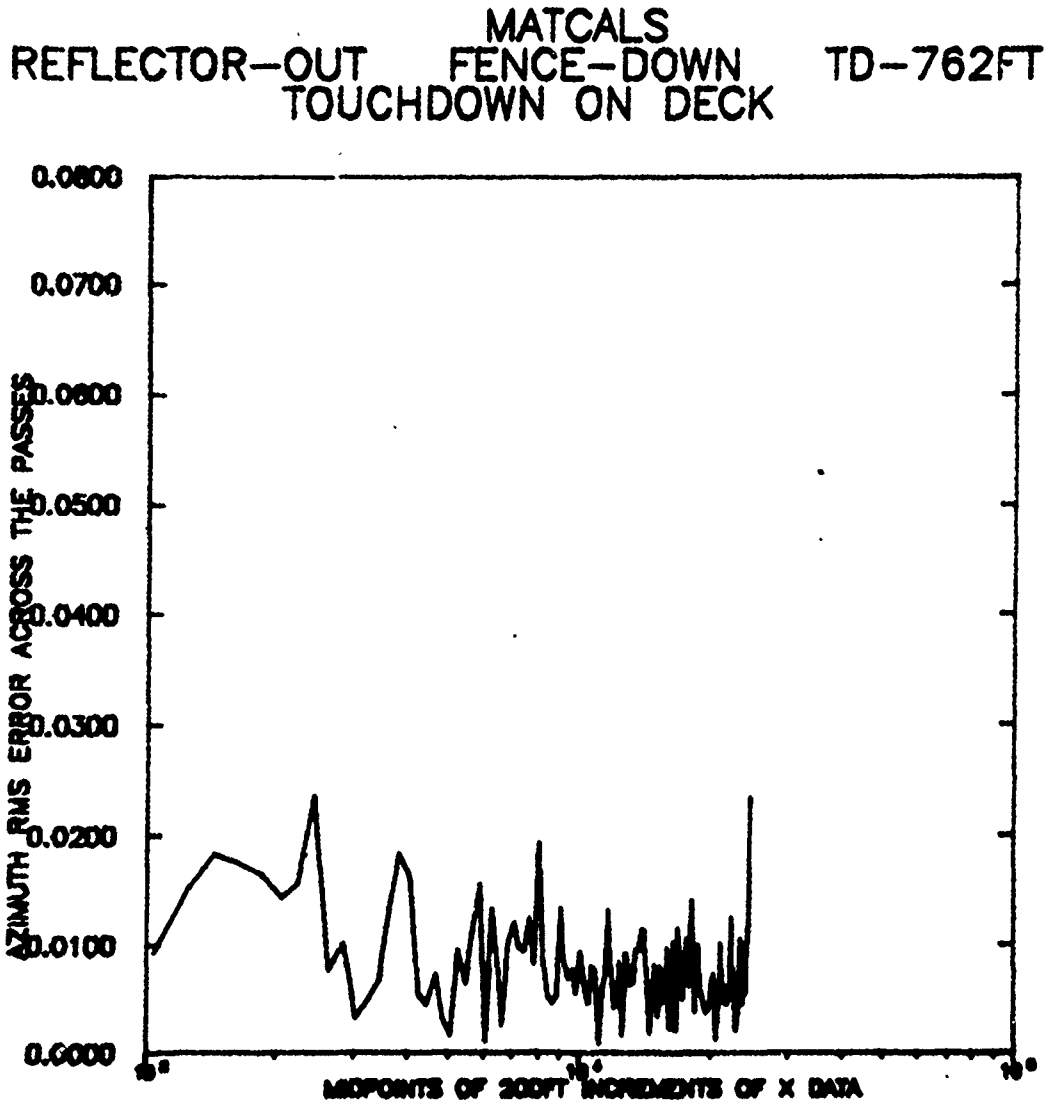

Figure 4.58. Azimuth RMS Error Across the Passes, Configuration 8

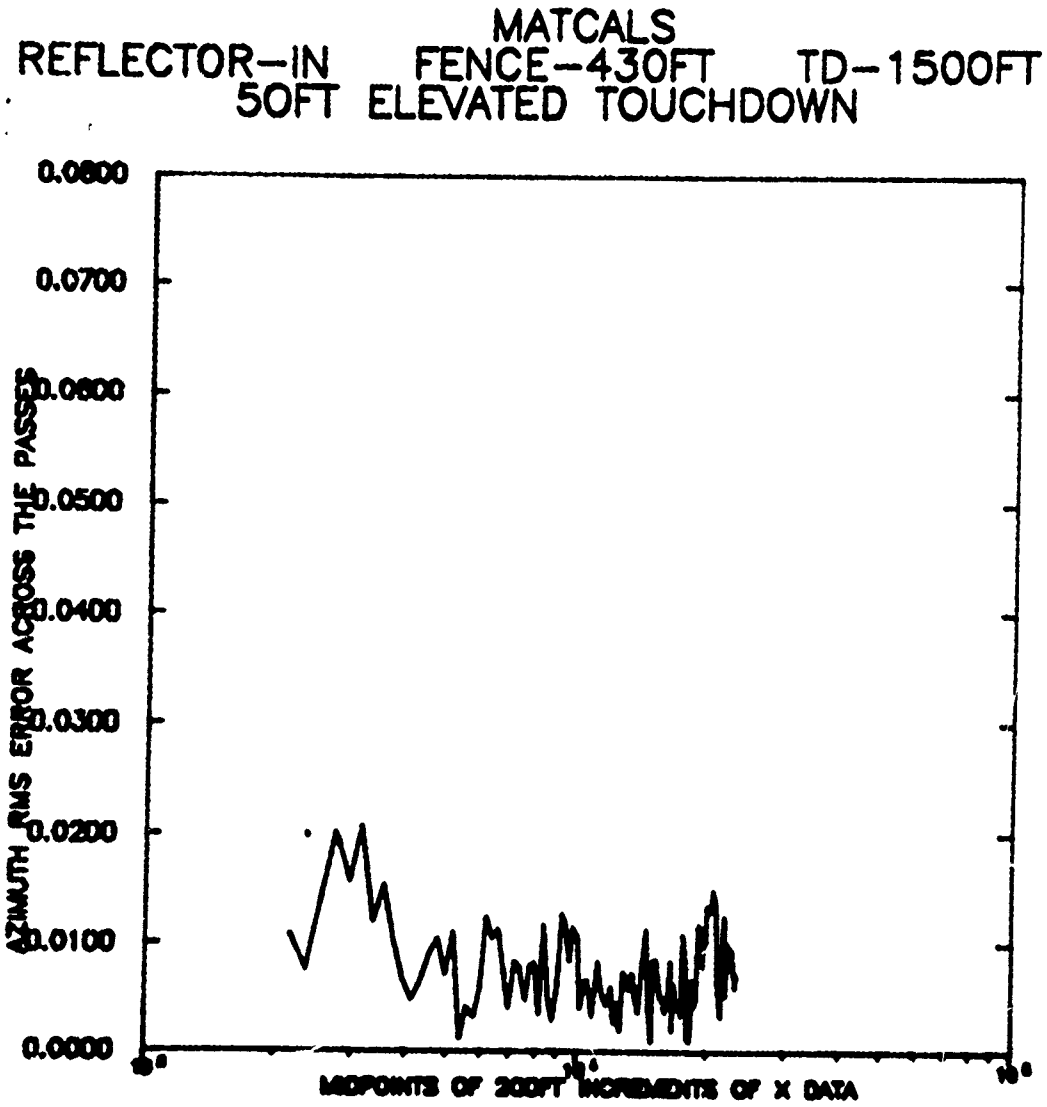

Figure 4.59. Azimuth RMS Error Across the Passes, Configuration 9

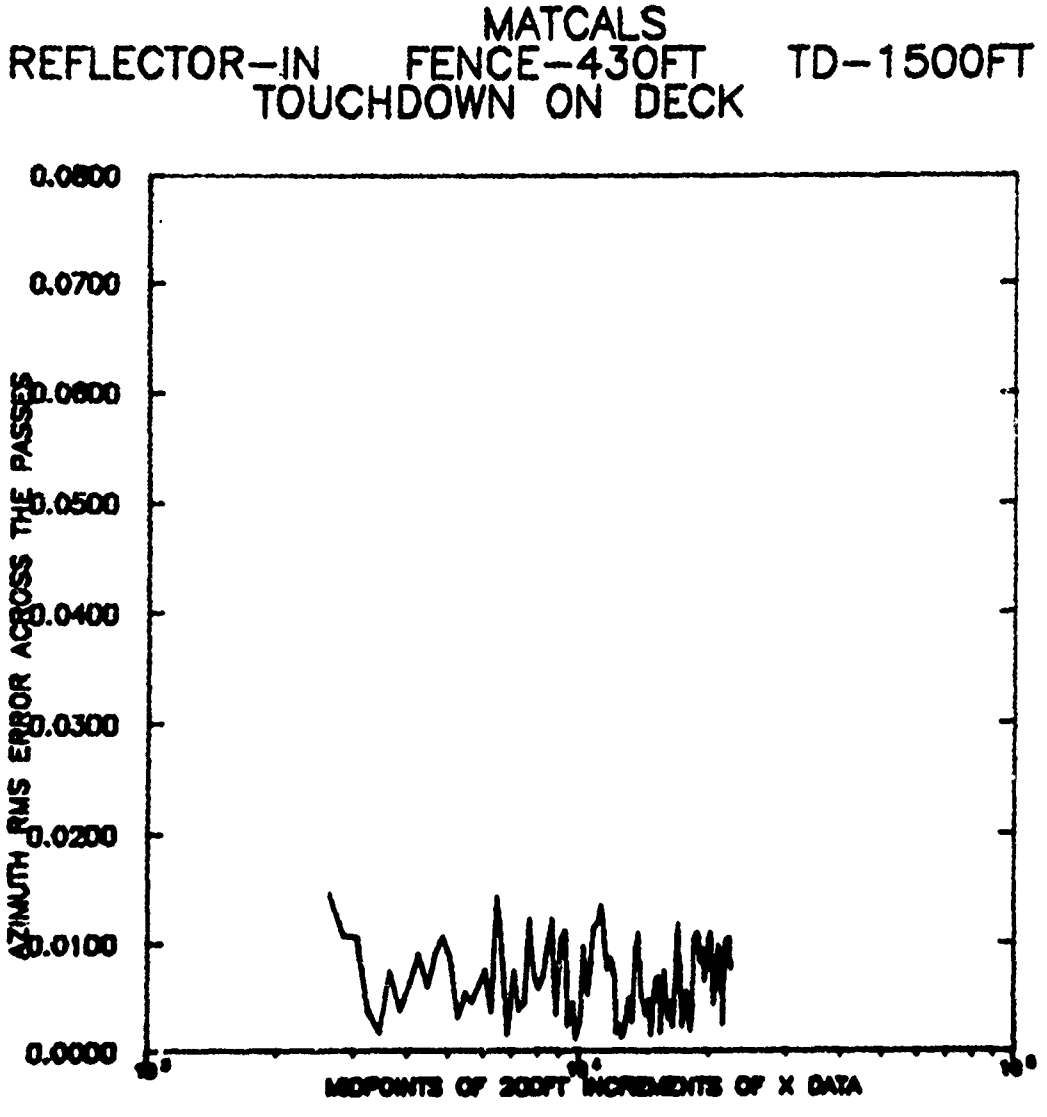

Figure 4.60. Azimuth RMS Error Across the Passes, Configuration 10

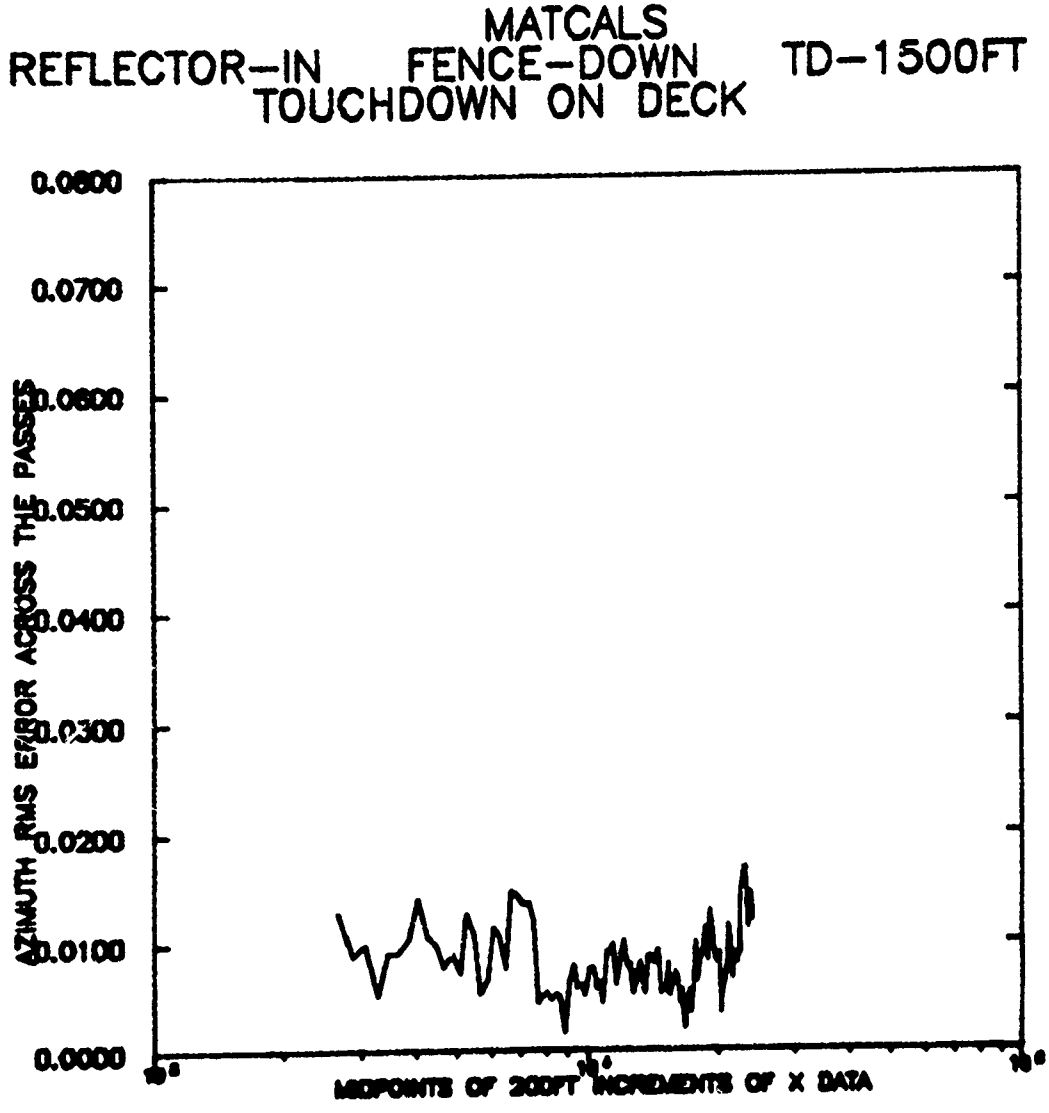

Figure 4.61. Azimuth RMS Error Across the Passes, Configuration 11

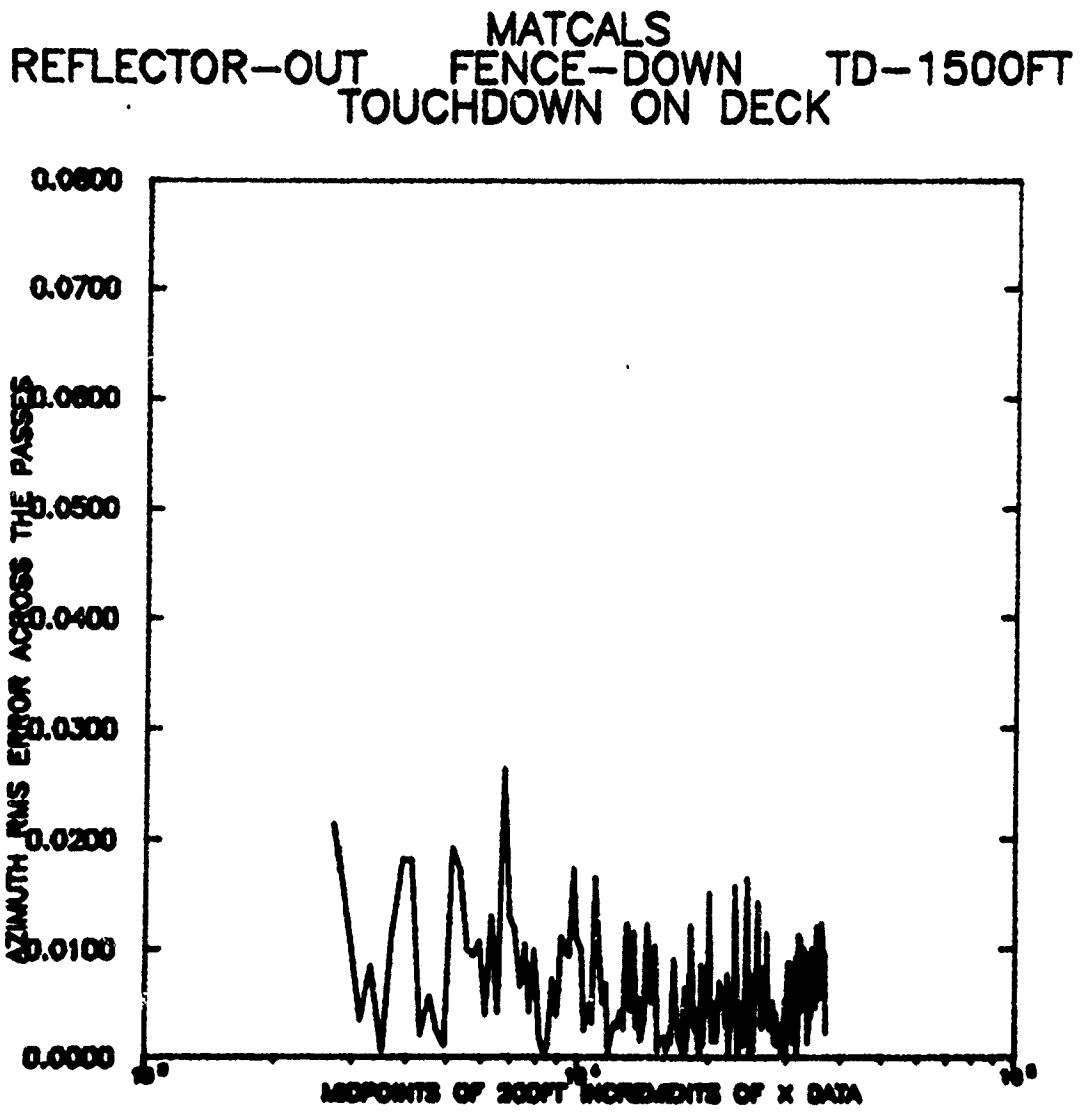

Figure 4.62. Azimuth RMS Error Across the Passes, Configuration 12

the tracking performance, especially at the 3000 to 5000 foot range. These results will be studied more closely in subsequent analyses.

(2) The fluctuation of the RMS error is determined mainly by the number of passes in each configuration. However, the corner reflector definitely reduced the amount of fluctuation of the RMS error versus range.

(3) The increasing error seen on Figure 4.54 starting at about 16,000 feet from the radar corresponds closely to the tipover point, where the aircraft transitions from a constant 800 foot altitude to the 3^{0} glideslope. The reason for the increased error is unknown.

(4) The multipath fence had no measurable effect.

Additional studies must be undertaken to interpret these data and to explain the inconsistencies.

4.3.6 ELEVATION RMS ERRORS ACROSS EQUIVALENT PASSES

Figures 4.63 through 4.74 present these data, and Figure 4.75 presents the theoretical multipath interference lobing structure for the MATCALS scenario. Some observations from these figures include:

(1) There definitely appears to be multipath interference present in the data. The incidence of peaks and valleys of the data being correlated with the theoretical predictions is just too great to ignore. Contrary to predictions, the multipath fence did not seem to have any effect on the measured errors. Another contradictory point is that there appears to be multipath interference on some of the 50 foot elevated touchdown passes where there should be no multipath interference at all, because under these conditions the main radar beam never intersects the ground. Hence, any multipath signal will be attenuated a minimum of 40 dB because of the antenna pattern and should not be detectable.

(2) Different tracking error plots seem to lead one toward different conclusions. For example, comparison of Figures 4.65 and 4.66 indicates that the multipath fence reduced the RMS errors significantly. On the other hand, comparing Figure 4.69 versus 4.70 indicates the fence was of no value. Similarly, the corner reflector seems to be responsible for lower errors when Figures 4.63 and 4.64 are compared to Figures 4.67 and 4.68. Conversely, comparing Figure

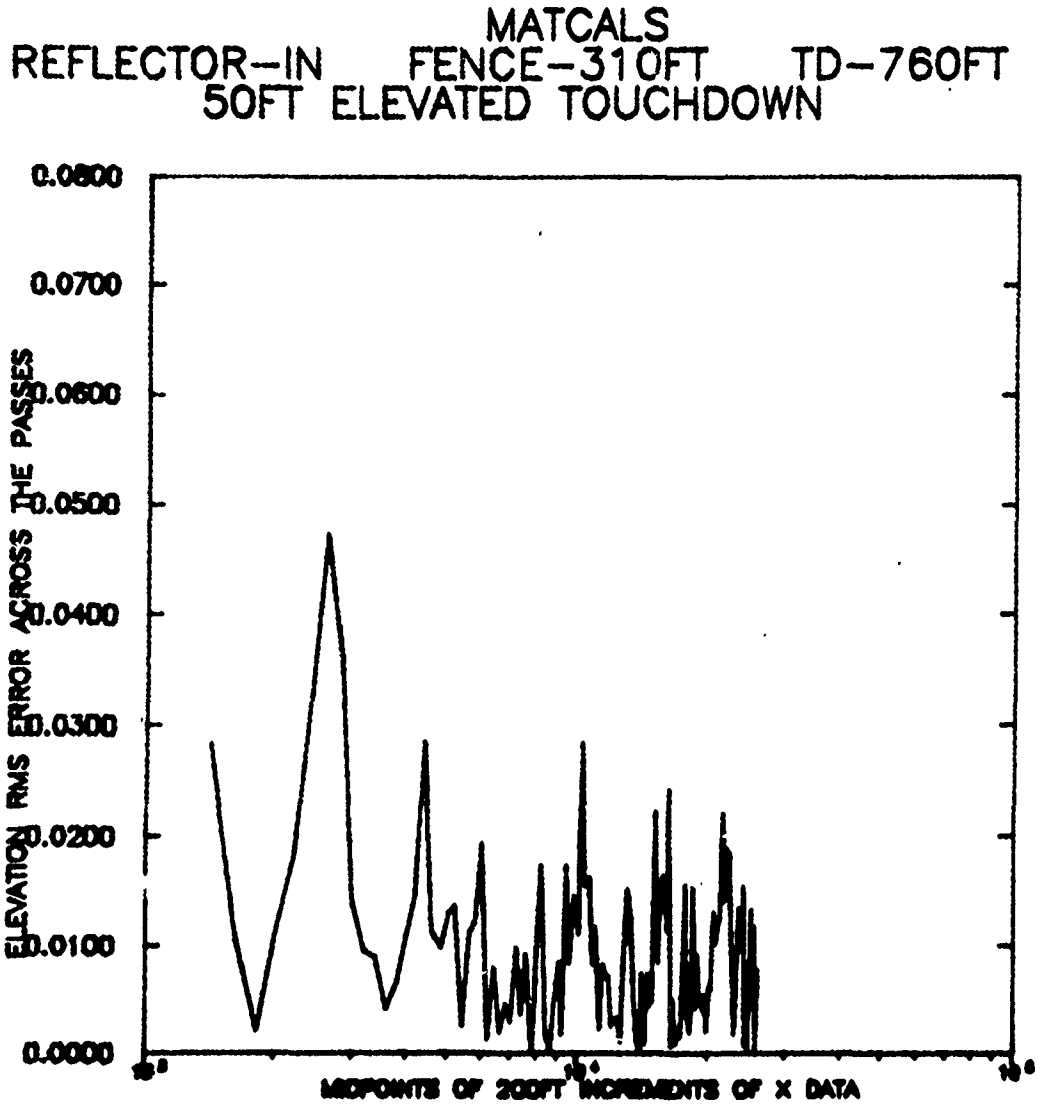

Figure 4.63. Elevation RMS Error Across the Passes, Configuration 1

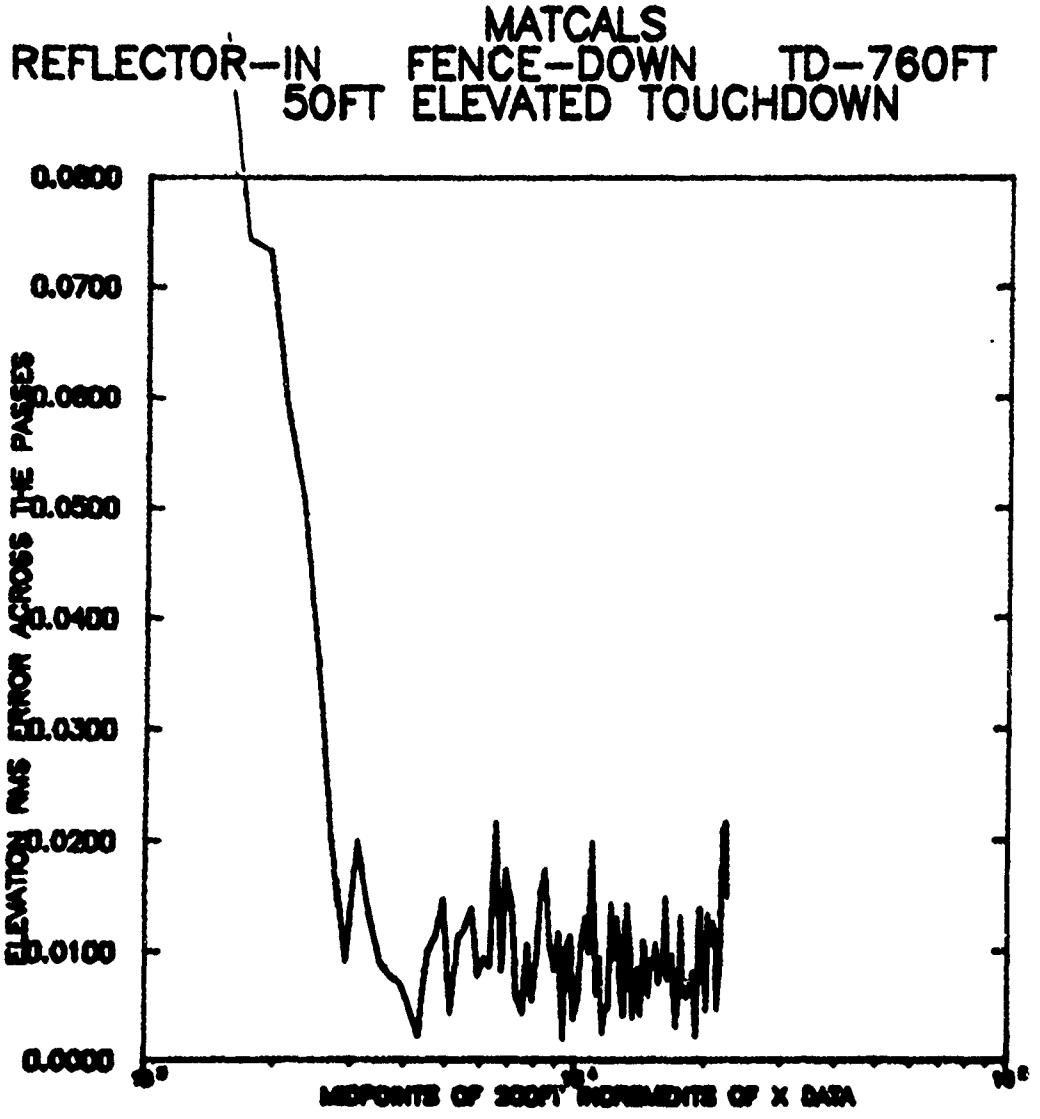

Figure 4.64. Elevation RMS Error Across the Passes, Configuration 2

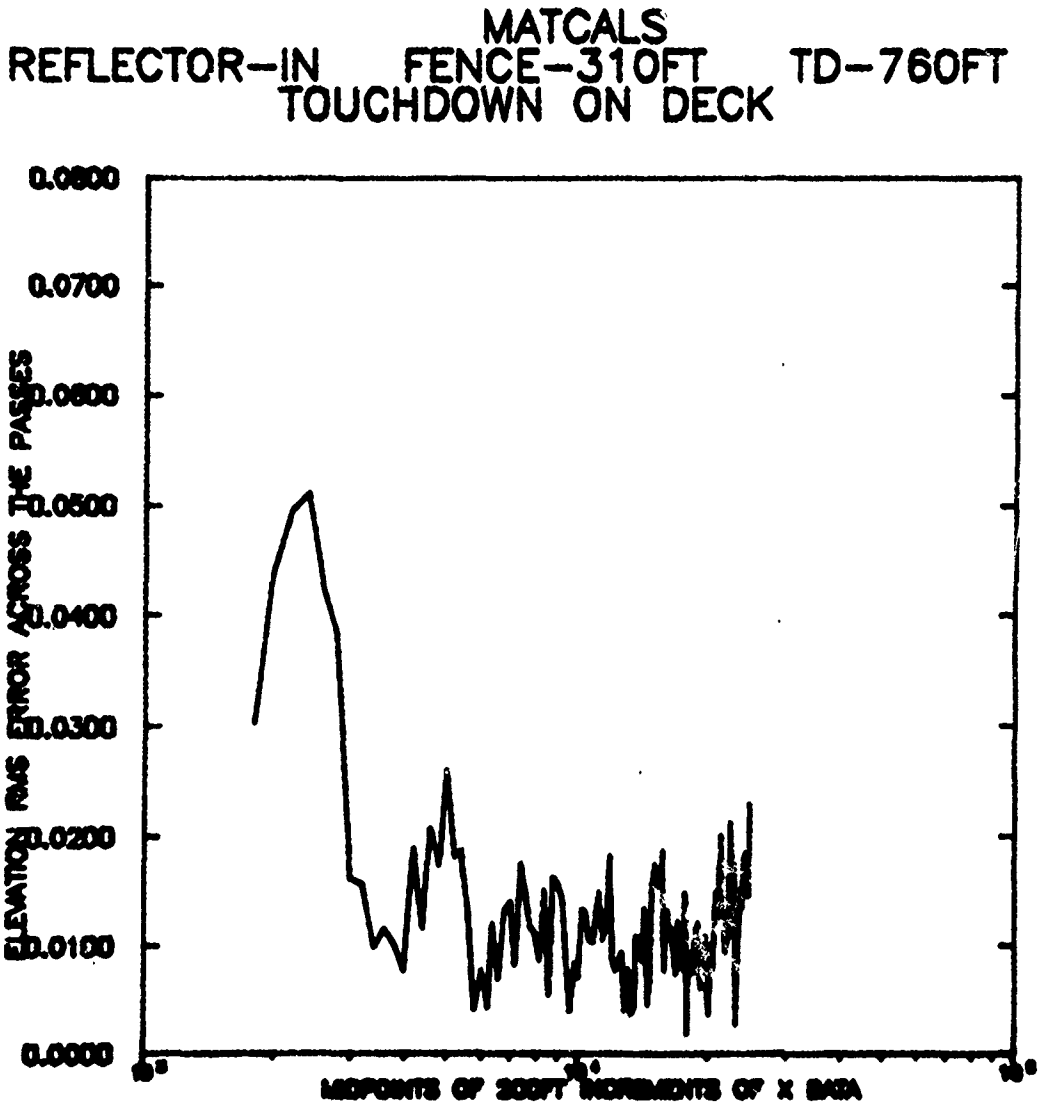

Figure 4.65. Elevation RMS Error Across the Passes, Configuration 3

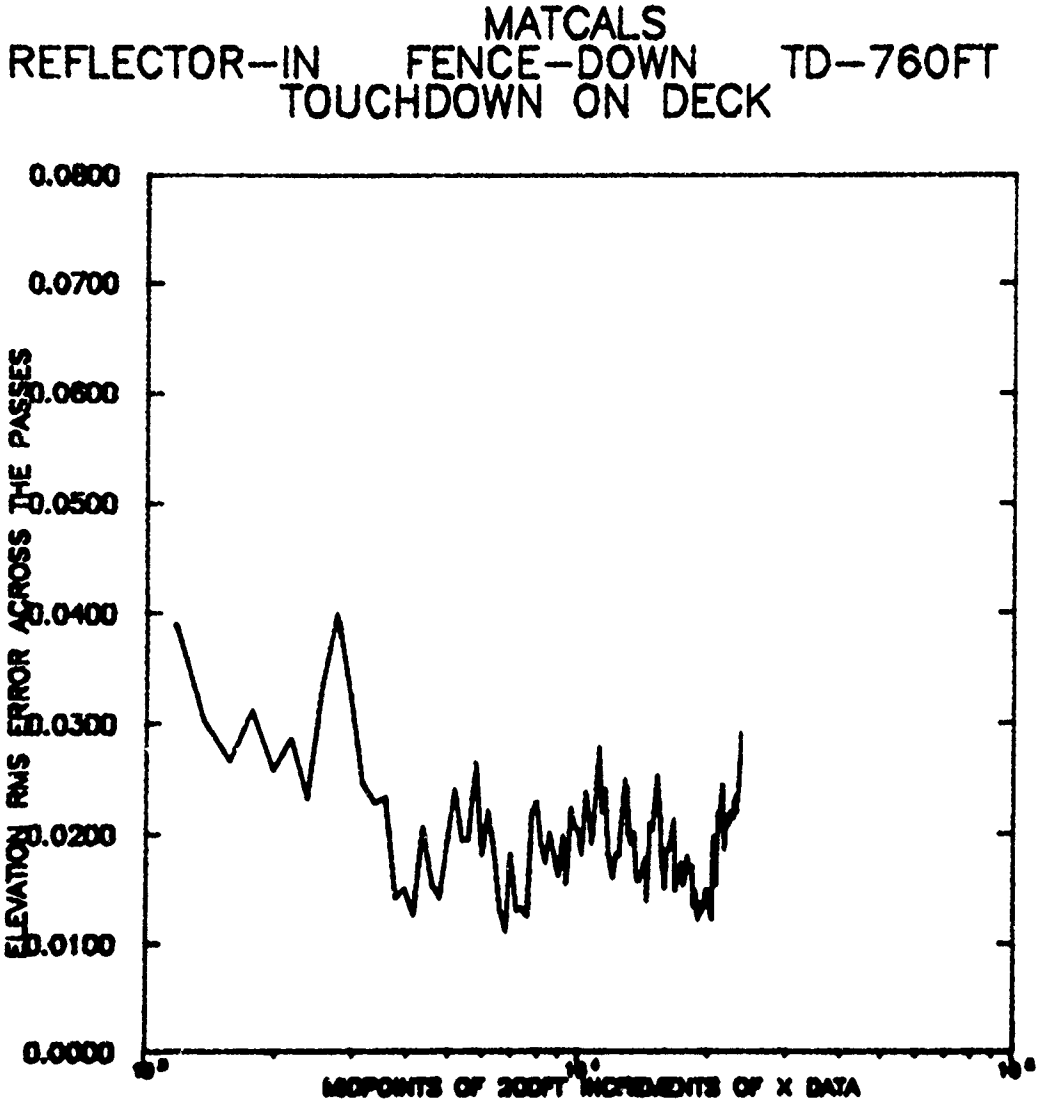

Figure 4.66. Elevation RMS Error Across the Passes, Configuration 4

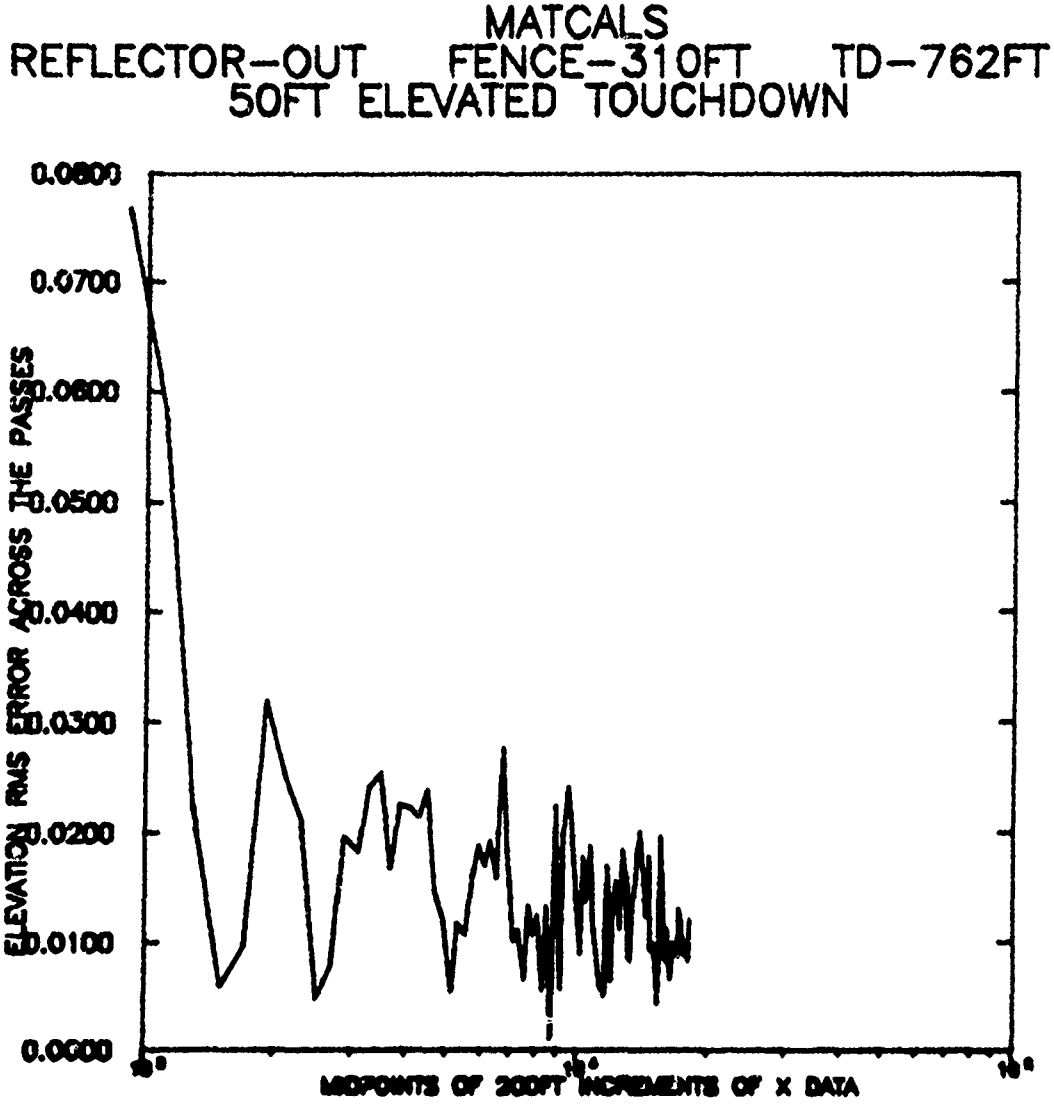

Figure 4.67. Elevation RMS Error Across the Passes, Configuration 5

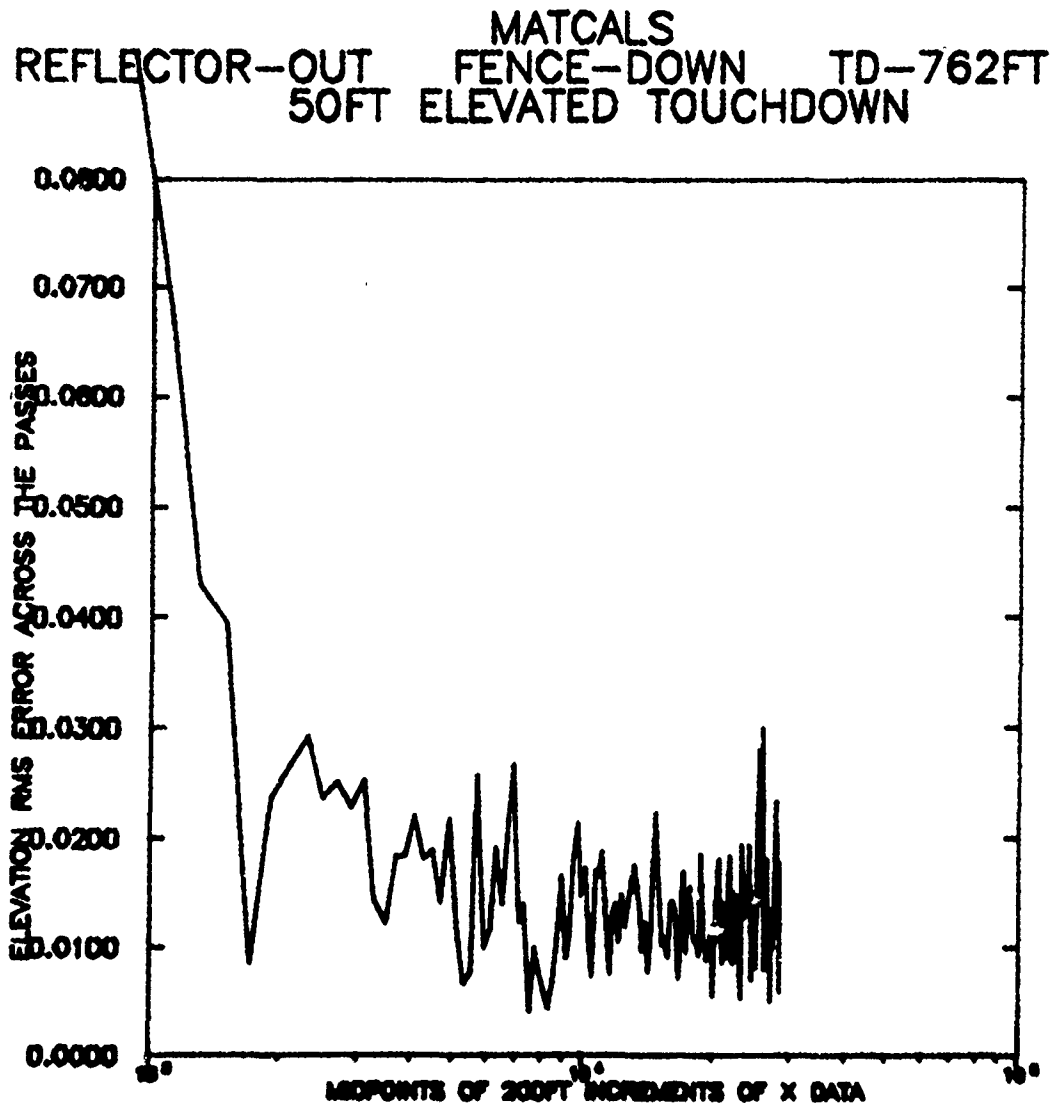

Figure 4.68. Elevation RMS Error Across the Passes, Configuration 6

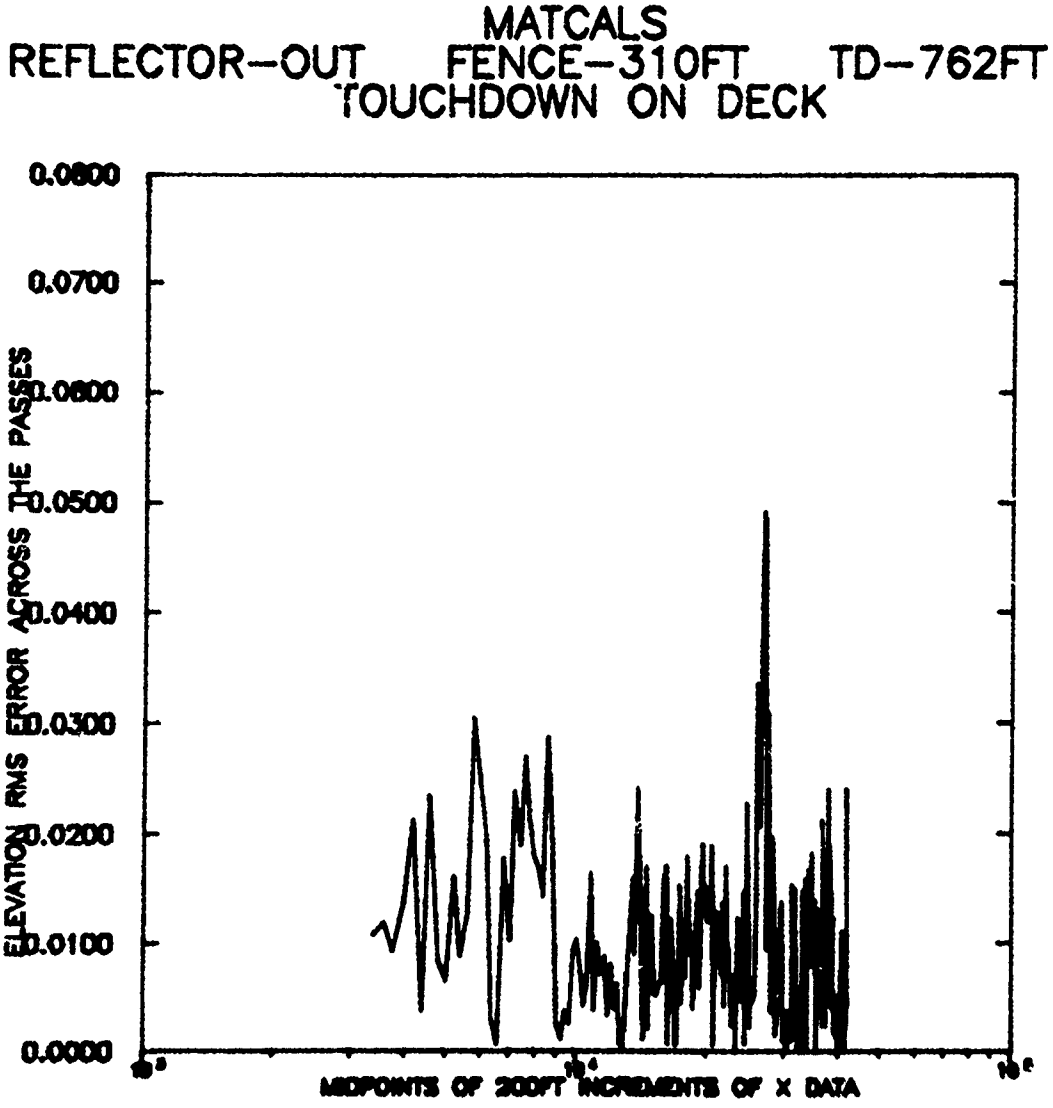

Figure 4.69. Elevation RMS Error Across the Passes, Configuration 7

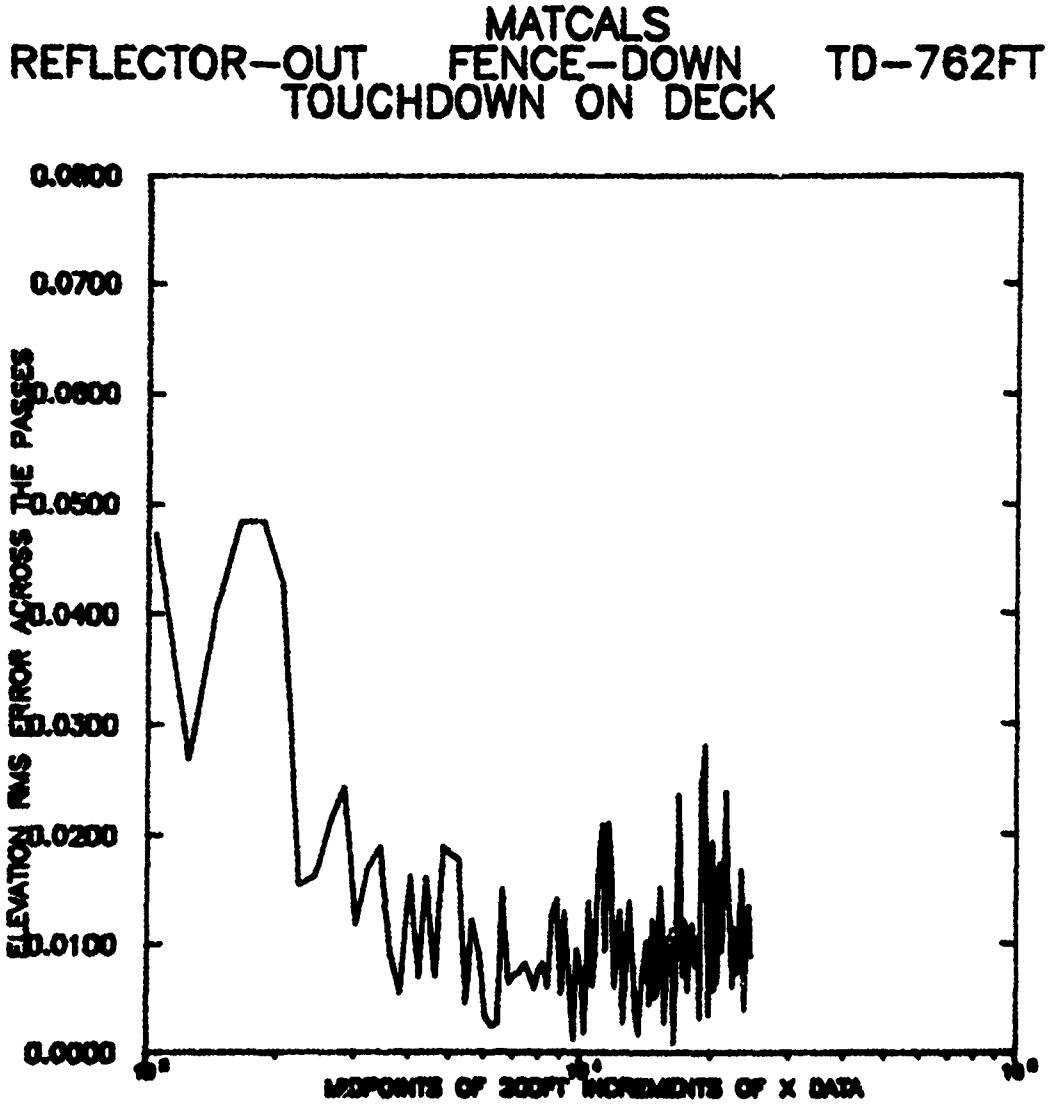

Figure 4.70. Elevation RMS Error Across the Passes, Configuration 8

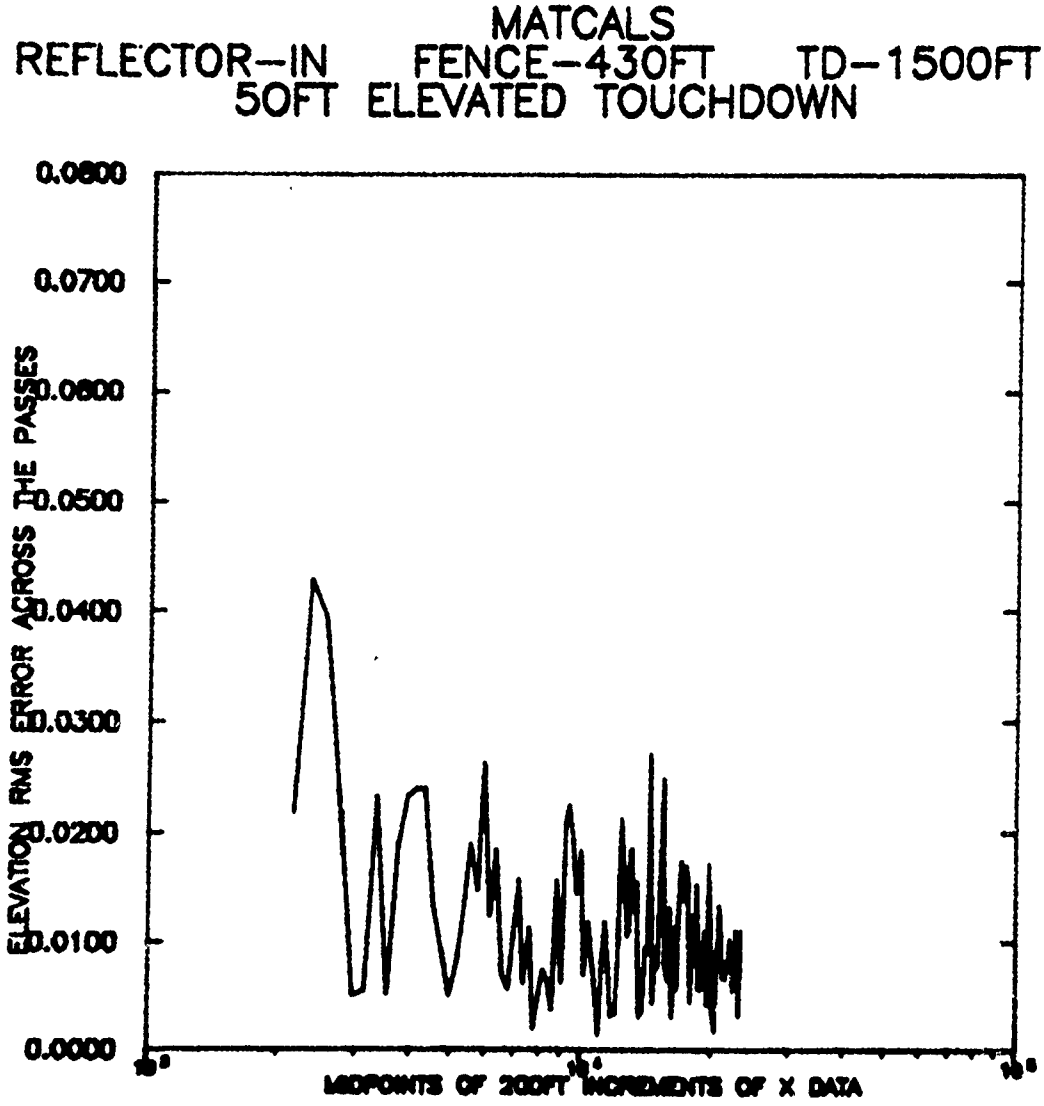

Figure 4.71. Elevation RMS Error Across the Passes, Configuration 9

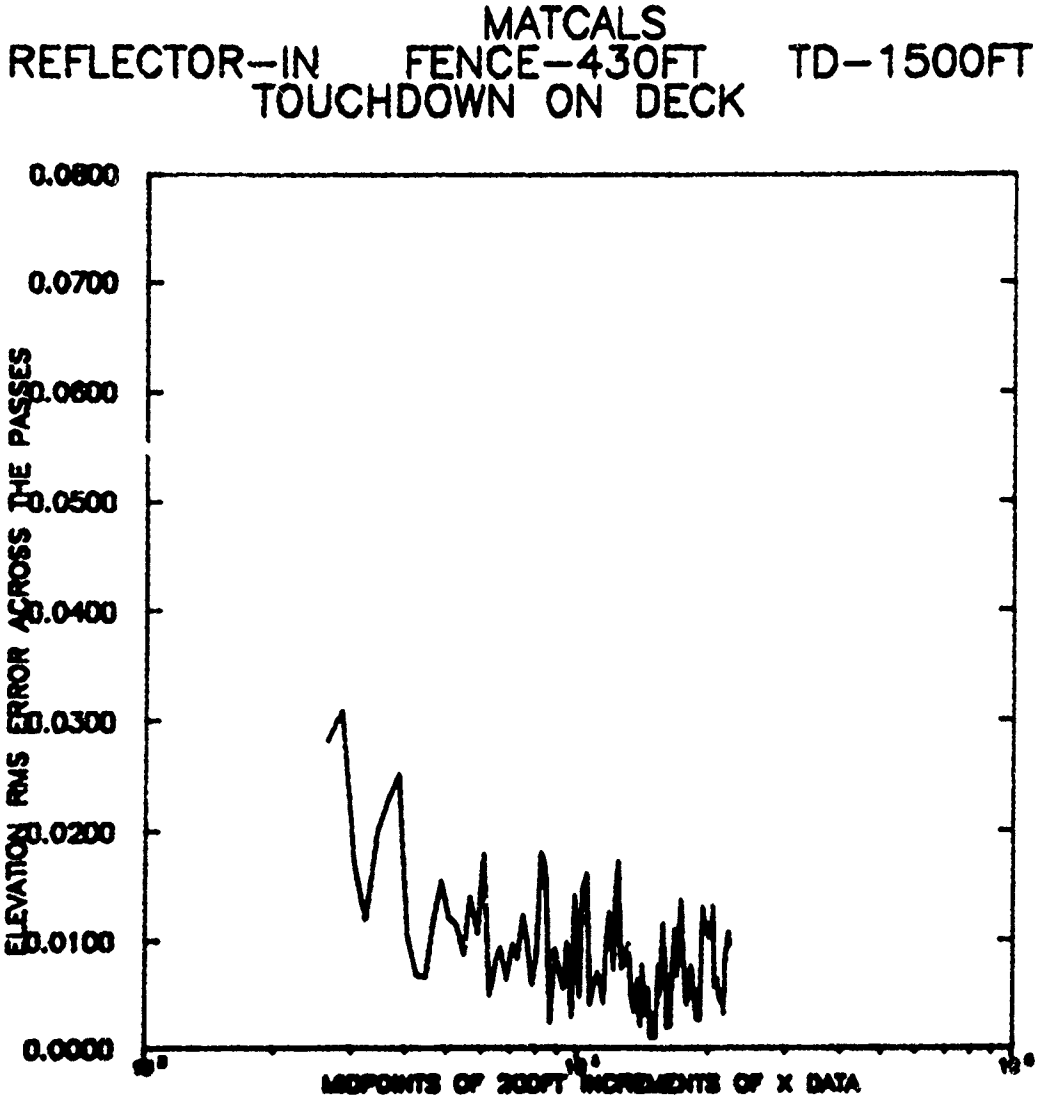

Figure 4.72. Elevation RMS Error Across the Passes, Configuration 10

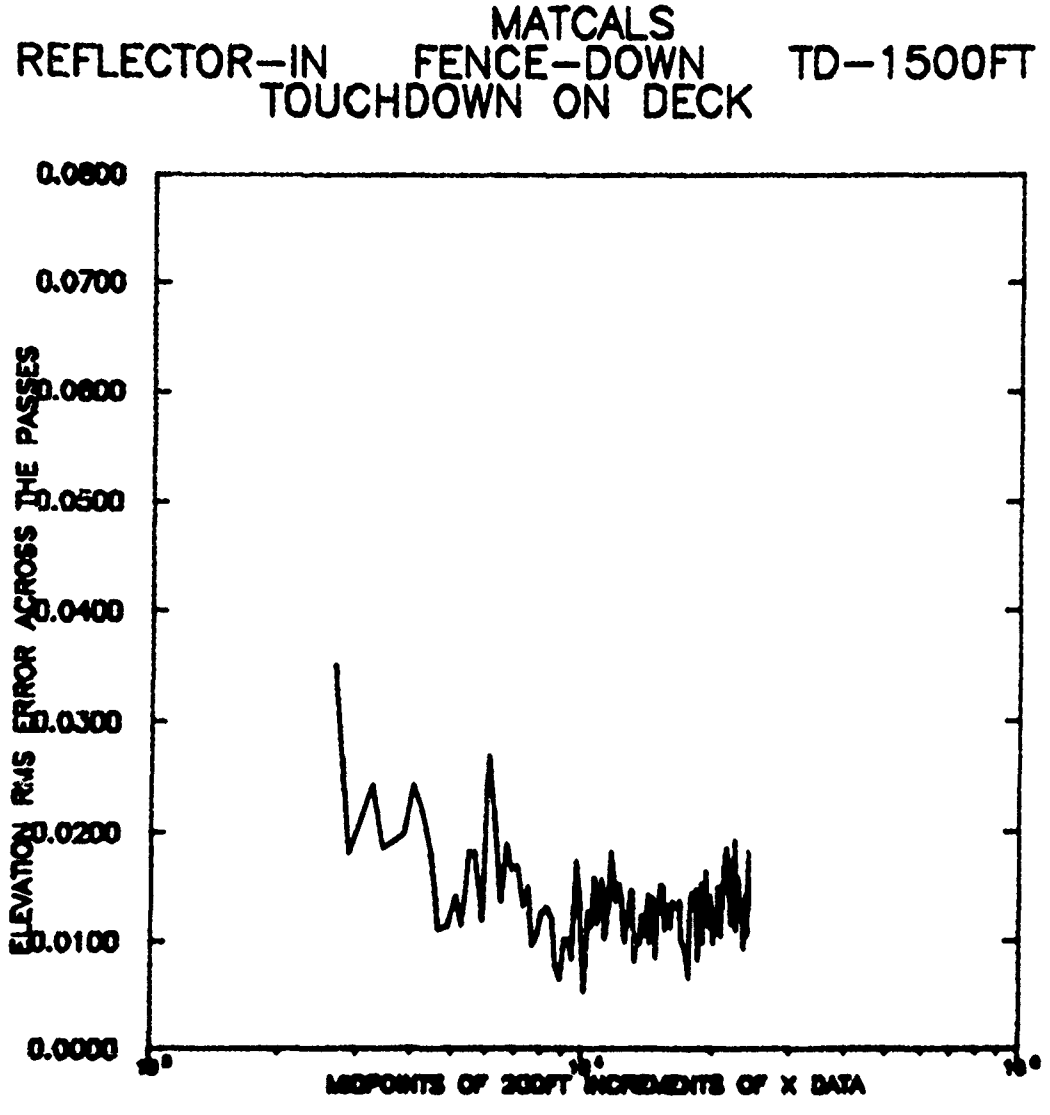

Figure 4.73. Elevation RMS Error Across the Passes, Configuration 11

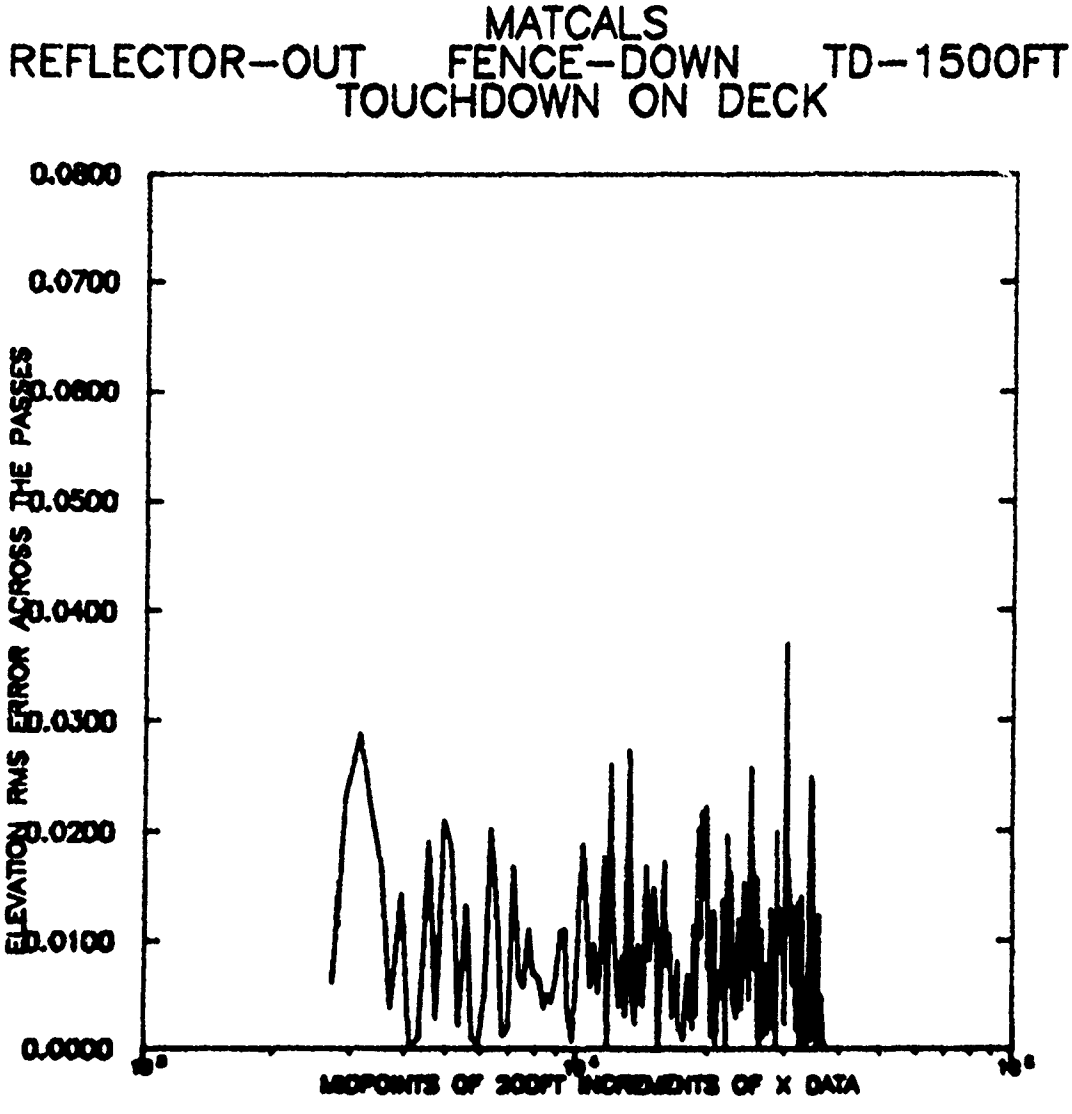

Figure 4.74. Elevation RMS Error Across the Passes, Configuration 12

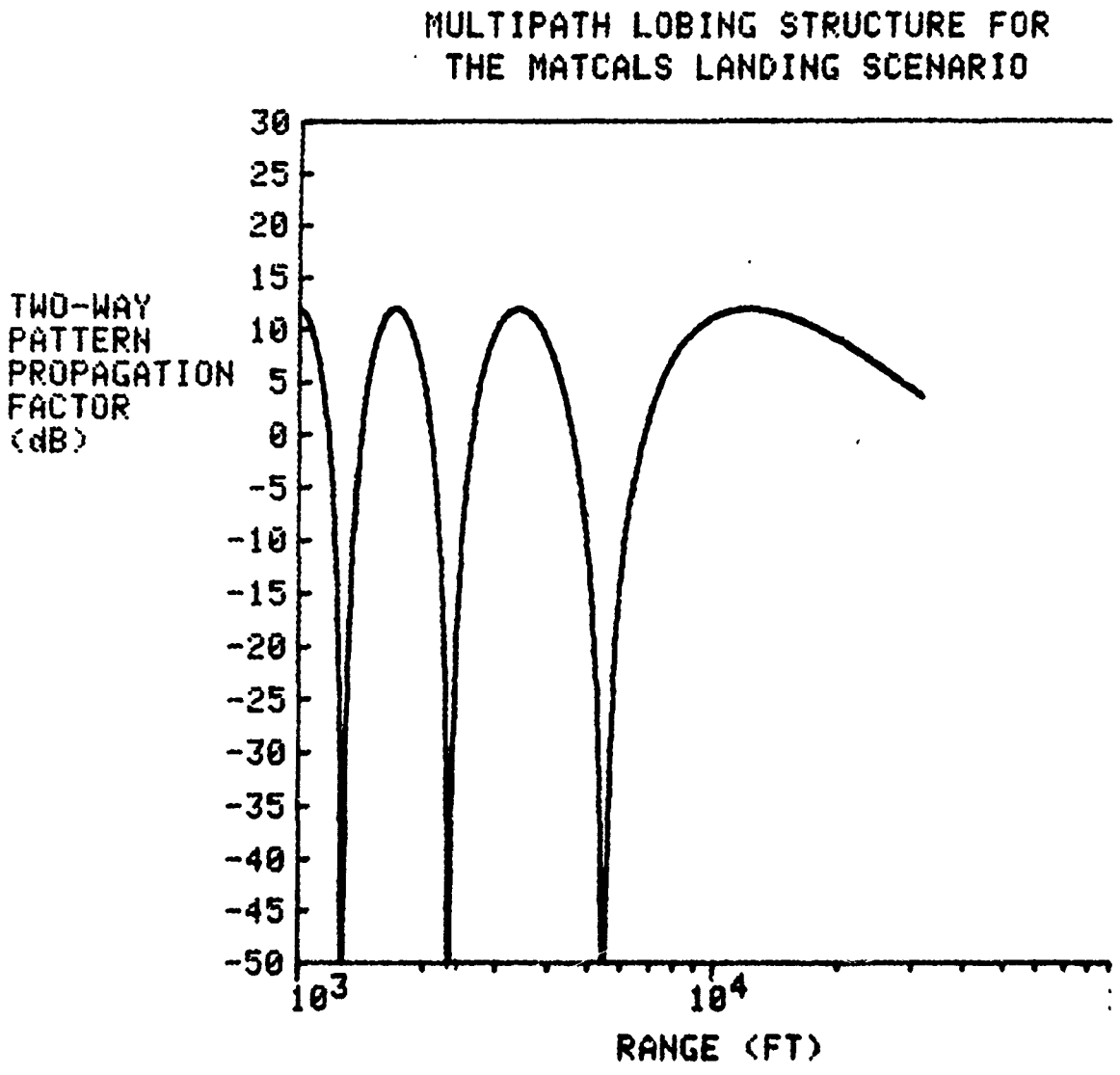

Figure 4.75. Theoretical Multipath Lobing Structure

4.65 to Figures 4.69 and 4.70 indicates no difference between when the corner reflector was installed and removed.

These inconclusive results may indicate poor experimental procedure, non-repeatable errors (i.e., changing conditions), or too small a data base. Certain of these possibilities may be eliminated. For example, by pooling certain parts of the data (e.g., runs with and without the multipath fence), a better statistical sample may be obtained. These types of analytical procedures will be employed in following analyses.

4.3.7 INTERPRETATION OF FLIGHT TEST DATA

Figures 4.76 and 4.77 present the best current estimate of the RMS tracking errors of the AN/TPN-22 PAR when tracking an aircraft making a standard landing approach. These curves were gleaned from the data presented earlier and are based on human interpretation only. The solid lines, in each case, represent the average RMS error versus range and the dotted lines are an estimate of the standard deviation of the data. The following preliminary conclusions may be drawn from these figures and the data presented previously.

(1) There appears to be multipath interference present in the elevation tracking error data. The multipath fence did not have any measurable effect on the elevation or azimuth errors. There seems to be contradictory data which require further analysis for a suitable explanation.

(2) The corner reflector reduced the RMS azimuth errors at short range by about 15% and had no effect at long ranges. Thus, the target induced errors of scintillation and glint appear to contribute only about 15% of the total azimuth error even at short range. Environmental errors should not be a major factor to the azimuth tracking performance. Hence, the radar instrumentation error is the primary source of azimuth tracking inaccuracies at all ranges.

(3) Within the experimental accuracy, the elevation RMS error displayed no sensitivity to the corner reflector being mounted in the aircraft. This is a very surprising result since it was predicted that frequency induced target scintillation would be the major source of elevation tracking error.[2] Georgia Tech hesitates to draw conclusions from these data without further analysis because the data are contradictory, contrary to theory, and the multipath fence did not seem to reduce multipath interference effects. Further study of the data should resolve these inconsistencies.

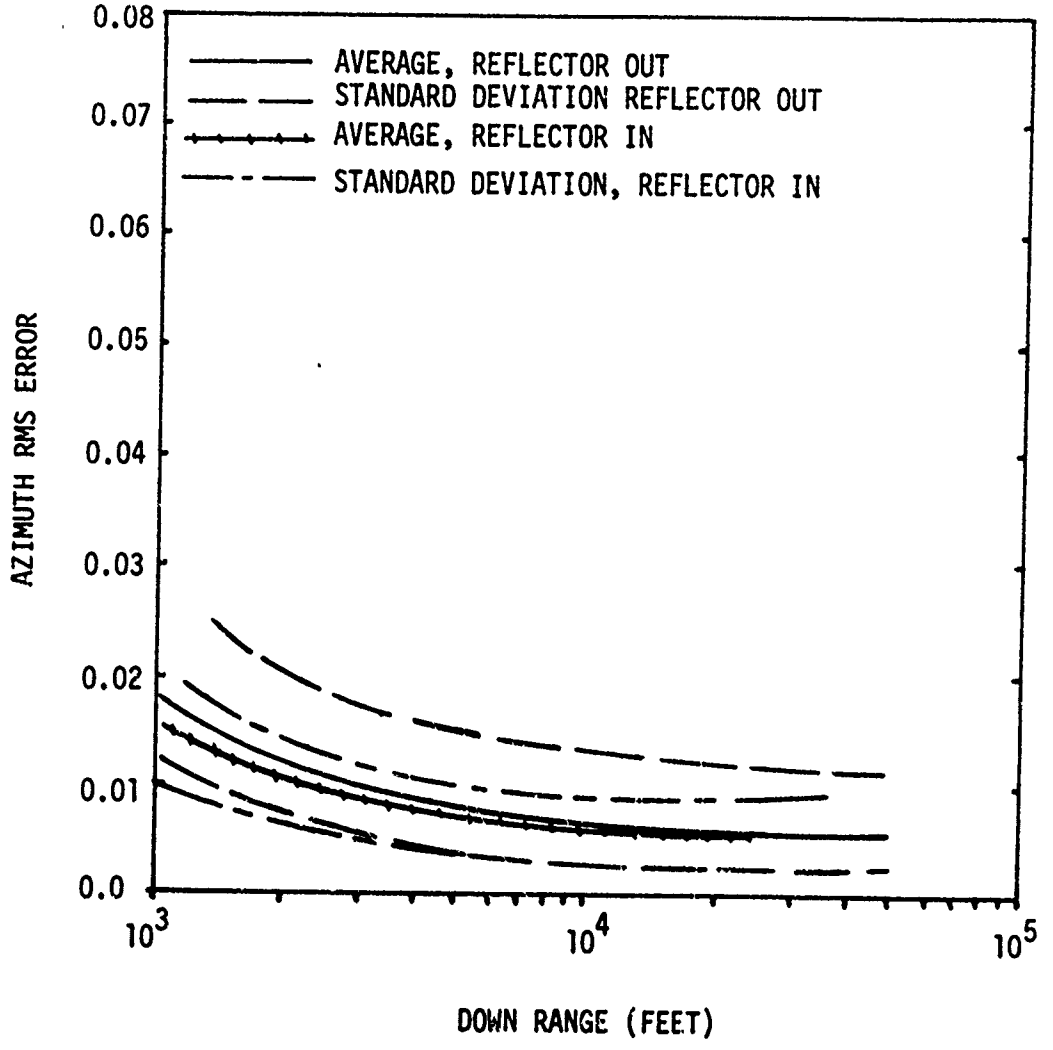

Figure 4.76. Azimuth RMS Error versus Range

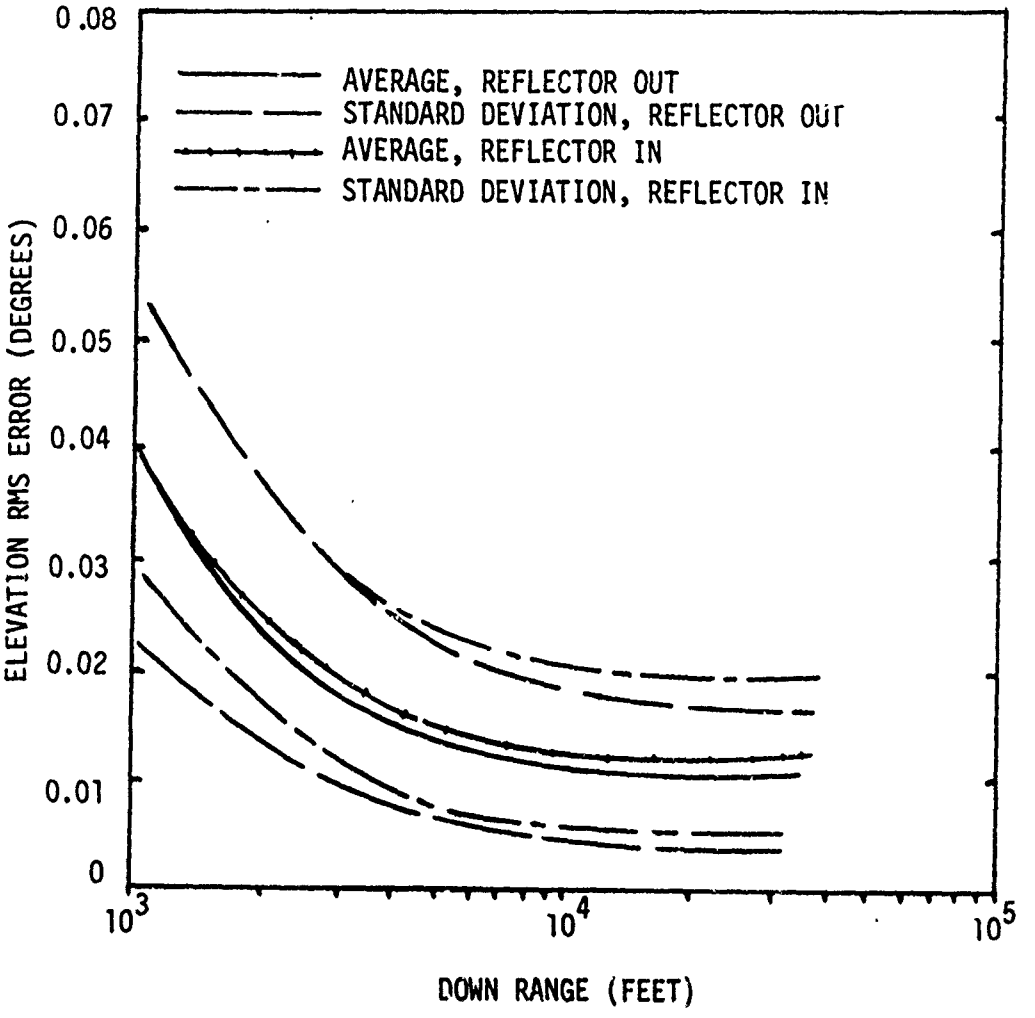

Figure 4.77. Elevation RMS Error versus Range

During subsequent analyses, the whole landing scenario should be studied to resolve the questions raised by these data. For example, there are several large structures offset laterally from the AN/TPN-22 radar at Patuxent NAS and the potential for azimuth multipath through a sidelobe from one of those structures should be evaluated. Also, the pointing angle of the corner reflector when it is installed in the F-4J test aircraft should be verified.

SECTION 5
ATC MISSION ANALYSIS

5.1 PURPOSE

The development of MATCALS by the Naval Electronic Systems Command will provide an automated terminal area air traffic control and ground derived landing control for all-weather operations. MATCALS comprises several elements which together provide for all the required functions and is organized into three subsystems: air traffic control subsystem, all-weather landing subsystem, and the control and central subsystem. The air traffic control subsystem consists of the airport surveillance radar (ASR) to provide range and bearing information, and the radar beacon component to provide range, bearing, and altitude information to transponder equipped aircraft and is the final subsystem to be developed.

In order to determine baseline performance specifications for this subsystem, a mission analysis was performed which addressed the overall Marine aviation mission, the organizational concept, operational scenarios, aircraft capabilities, and typical combat environments. The analysis was conducted with the intent of generating a revised set of parameters that describe the desired operational capabilities.

5.2 BACKGROUND

The Marine Corps, within the Department of the Navy, includes land combat and service forces with organic supporting aviation. The function of the Marines is to provide the combat arms necessary for the seizure or defense of advance naval bases and for the conduct of those land operations required for the successful accomplishment of a naval campaign. The primary mission of Marine Corps aviation is to participate as the supporting air component in the performance of the Marine Corps functions. The capability to conduct successful amphibious operations is dependent on the capability to provide effective tactical air operations support. To provide this capability, the Marine Corps requires a flexible, responsive, combat aviation element that can be specifically tailored to the tactical situation expected to be encountered.

The Marine aviation capabilities include not only those functional areas normally associated with combat such as air reconnaissance, anti-air warfare, assault support and offensive air support, but also the control of aircraft and missiles. The necessity to

provide direction, control, and coordination of the diverse elements of aviation has become increasingly important with the introduction of the highly sophisticated weapons systems of the last two decades.

5.2.1 ORGANIZATION AND MISSION

Marine Corps aviation, by law, consists of at least three Marine aircraft wings (MAW's). The specific composition of a MAW is not specified, but consists of various aviation groups that provide aircraft, support equipment, and personnel to perform the administration, operations, and training necessary for the conduct of the Marine Corps mission. The MAW's and the Marine aviation groups are task organized using squadrons, the only aviation units with published tables of organization, as the basic building blocks.

The MAW is the highest level tactical aviation command in the fleet Marine force and is a balanced combat force designed to support one Marine division in an amphibious operation. It is capable of providing all types of air support required in such an operation. A typical wing could be organized as shown in Figure 5.1. There are three types of Marine aviation groups: Marine Air Control Group (MACG), Marine Wing Support Group (MWSG), and Marine Aircraft Group (MAG), each of which is task organized. The number and type of subordinate MAG's may vary considerably among MAW's, but the MWSG and the MACG have relatively consistent structure among the wings due to the similar support requirements.

Because of the numerous possible environments where the Marine Corps could be engaged in military operations, a wide variety of both rotary wing and fixed wing aircraft are required in the inventory. There are 11 types of Marine aircraft squadrons which are the building blocks of the Marine Air Group. These include attack squadrons, electronic warfare squadrons, reconnaissance squadrons, and transport squadrons in the fixed wing class and also light, medium, heavy, and attack helicopter squadrons. Table 5.1 lists Marine aircraft currently in the inventory and an indication of the airspeed and altitude ranges.

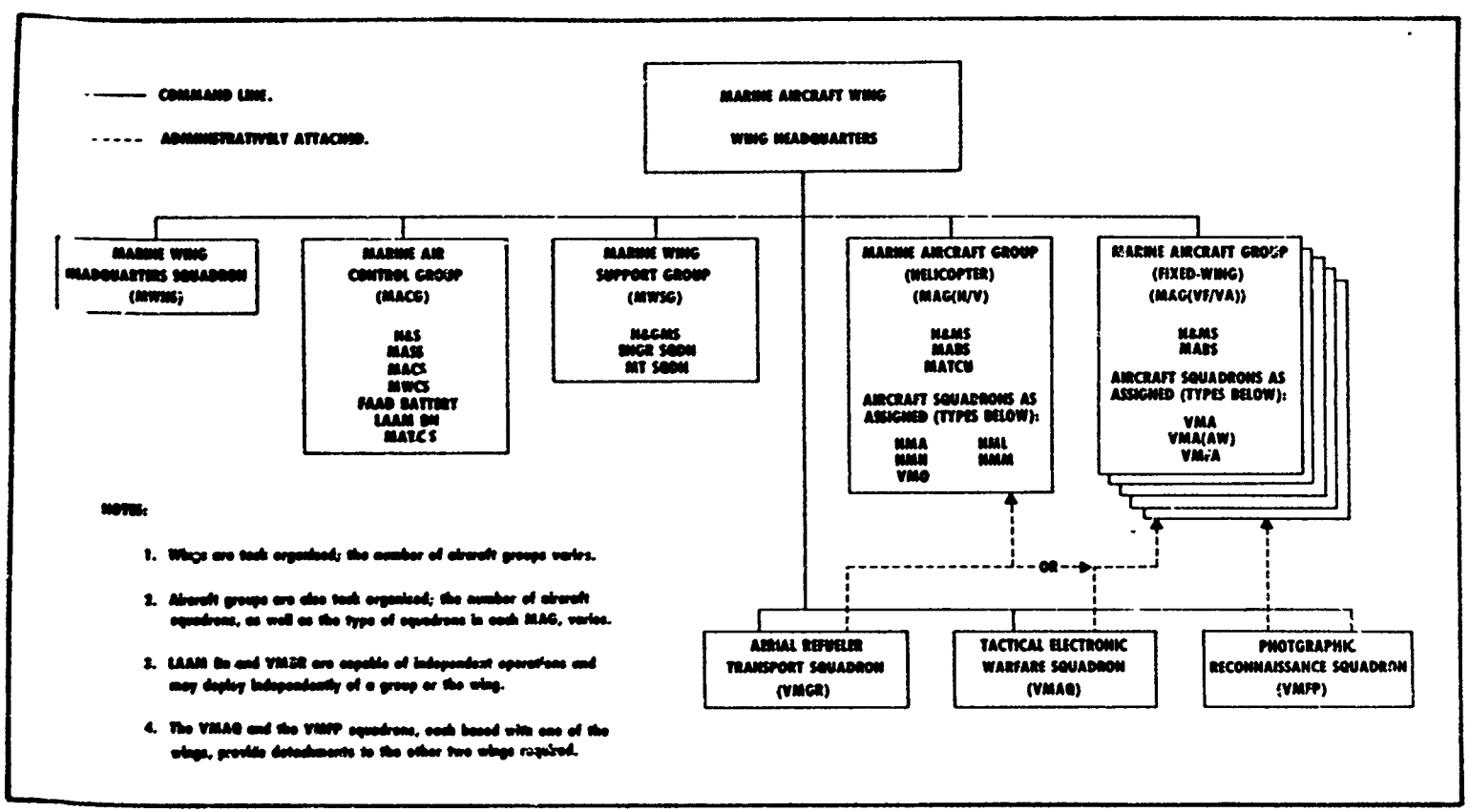

Figure 5.1. Marine Aircraft Wing

TABLE 5.1. MARINE AIRCRAFT

Aircraft	Type	Typical Airspeed (kts)	Ceiling (ft)
A4	FW	570	40,000
A6	FW	560	47,000
AV8	FW	640	50,000
C130	FW	335	33,000
OV10	FW	240	20,000
F4	FW	490	28,000
AH-1	RW	150	12,000
UH-1	RW	110	12,000
CH46	RW	140	15,000
CH53	RW	170	21,000

Each MAW, regardless of its composition of helicopter or fixed wing aircraft groups will have a MACG to provide, operate, and maintain the Marine air command and control system. Among other squadrons in the MACG are the Marine Air Support Squadron (MASS), the Marine Air Control Squadron (MACS), and the Marine Air Traffic Control Squadron (MATCS). These squadrons operate and maintain the air control facilities necessary for the effective air support of tactical operations.

The MACS has the primary mission of providing air surveillance and control of aircraft and missiles for the execution of anti-air warfare. Included in the mission are the tasks of installing and operating the equipment required for detection, identification and control, and also the task of providing enroute air traffic control of friendly aircraft. The MASS is equipped and organized to provide communication-electronics facilities for the control of aircraft while operating in direct support of the tactical operations.

The Marine Air Traffic Control Squadron, on the other hand, provides air traffic control service at the expeditionary airfields and remote landing sites under all weather conditions. The following tasks are among those necessary in the accomplishment of this mission.

(a) Install and operate the air traffic control and navigation system required at the expeditionary airfields and remote landing sites.

(b) Provide the air traffic control service within the designated area.

(c) Maintain the capability to deploy and operate as an integral unit.

(d) Maintain the capability to deploy independent air traffic control teams.

It is the MATCS that must provide, operate, and maintain the MATCALS in support of the Marine aviation wing.

5.2.2 MARINE AIR COMMAND AND CONTROL SYSTEMS

Because of the many different types of aircraft that support tactical operations, their considerable variation in ranges and speeds, the use of the airspace by a wide variety of missiles and artillery as well as aircraft, and the sophisticated threat systems likely to be encountered, a complex system of command and control over a large geographical area is required. The Marine Air Command and Control System (MACCS) provides centralized coordination and supervision at a high level with decentralized control authority. The control is exercised through airspace and air traffic control as well as through the employment of assets. Figure 5.2 is typical of a deployed MACCS showing the many control agencies and the communication links necessary for the control.

Not included in the figure are the air traffic control agencies providing terminal services at the expeditionary airfields and the remote landing sites. To provide these air traffic control services, the MATCS deploys detachments organized into approach control, ground controlled approach, and control tower sections. The MATCS detachments operate within the assigned control areas and procedures normally established by the airspace control authority in coordination with the indigenous national agencies. The approach control section is the controlling authority for all flights within the control area during instrument meteorological conditions (IMC). Control is shared with the control tower section during visual meteorological conditions (VMC). The airport surveillance radar, along with the beacon system, to be developed as a component of MATCALS, will be the primary equipment used by the approach control section to provide adequate separation among all IMC flights on approach to the airfield and for controlling departing and recovering aircraft.

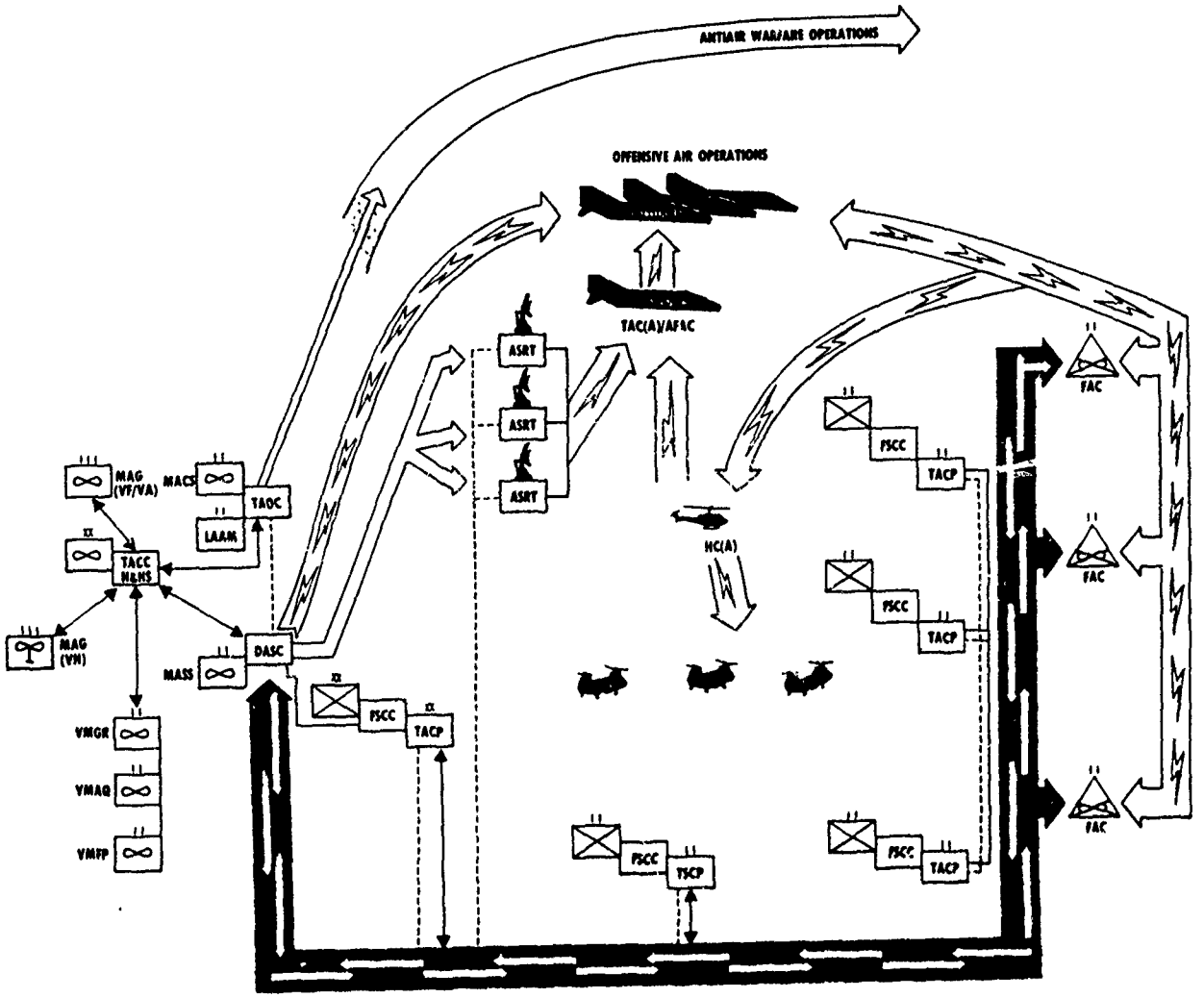

Figure 5.2. Marine Air Command and Control System

5.2.3 TACTICAL SCENARIOS

Because of the wide range of contingencies that a MATCS must be capable of supporting, a standard scenario for use in developing operational requirements for the MATCALS subsystems is not possible. Instead, a range of conditions must be examined and judgments must be made as to the effect of the conditions on the performance requirements.

Marine Corps aviation is normally an element of an amphibious task force. Because of the close integration of the air and ground operations, a Marine Air-Ground Task Force is normally formed with a separate headquarters to command the operation. The task force may be a Marine Amphibious Force (MAF) built around a division/wing organization, a Marine Amphibious Brigide (MAB) built around a regimental landing team and an aircraft group, or a Marine Amphibious Unit (MAU) built around a battalion landing team and a composite aircraft squadron. Although Marine aviation is normally deployed as a component of an amphibious task force, there are other special operations such as humanitarian missions, raids, and demonstrations of force in which an independent operation may be necessary.

Regardless of the type operation, the MATCS must be capable of providing the air traffic control service as required by the supported aviation unit. The MATCALS equipment, more specifically, the ASR and beacon systems, must therefore be suitable for a wide range of deployment missions.

The relocation of the aviation assets (i.e., deployment to the desired area of operations) is required to provide the commander the flexibility for optimum use of his forces. Advance base operations and carrier based operations are used to provide the aviation support. MATCS air traffic control service is not required for the carrier based operations, but is required for advance ground bases. The advance bases for fixed wing operations are best located at distances less than 300 nmi from the supported ground forces and may vary from major airfields with good facilities to expeditionary airfields, prefabricated, fully transportable airfields with minimum facilities. For helicopter operation, the advance base should normally be less than 50 nmi from the operational area and may also vary considerably in the degree of facilities available. A key variable in the decision of when and where to deploy the aviation assets is the degree to which air superiority has been obtained.

It is also likely that a MATCS equipped with MATCALS equipment would be required to operate at a major Marine airbase during peacetime performing air traffic

control functions with the same requirements as the Federal Aviation Administration (FAA). The MATCS could also be deployed to an area of operations anywhere in the world. It is staffed and equipped to provide ATC services at three geographically separated advance bases and several remote landing sites. The MATCALS subsystems must be suitable for operation in any of these scenarios.

5.3 ANALYSIS

For analytical purposes, two extreme situations may be postulated and operational performance characteristics of the ASR determined for each. Comparison of the parameters for each situation should result in a range of acceptable values for each parameter. Based on the discussions of the previous paragraphs, two realistic scenarios are: (1) approach control support at an advance base within 50 nmi of the assault area primarily supporting helicopter operations and (2) support at an advanced landing field approximately 300 nmi from the assault area supporting fixed wing operations and some helicopter logistics flights.

Figure 5.3 depicts the significantly different operational environments that exist at the two locations. Assuming that the opposing forces possess a sophisticated threat capability, the forward area MATCS approach control section operating an ASR would be providing primarily terminal control for helicopters and possibly some fixed wing observation aircraft. There could be a significant volume of "transit" traffic, probably at low altitudes, proceeding to and from the mission area. The rearwardmost base would provide the terminal area control for a wide range of aircraft on a wide range of administrative, logistic, combat support, and combat missions.

The MATCS operating an approach control facility within 50 nmi of the forward edge of the battle area (FEBA) could have considerable restrictions that would influence air traffic control operations. Primary among these restrictions is the degree of the enemy air defense threat. Figure 5.4 depicts the surface-to-air missile threat that will likely restrict Marine air operations to relatively low altitudes, except for extremely short periods of time or for special operations. It shows that the survivable flight regimes are directly dependent on the distance from the threat. Combat flights that orginate from bases further to the rear will likely utilize flight tactics similar to that shown in Figure 5.5. Coordination and control of aircraft transitioning through the forward approach control area at low altitude for penetration of the enemy air defenses will be required. In addition, restricted areas within the control zone are likely to exist

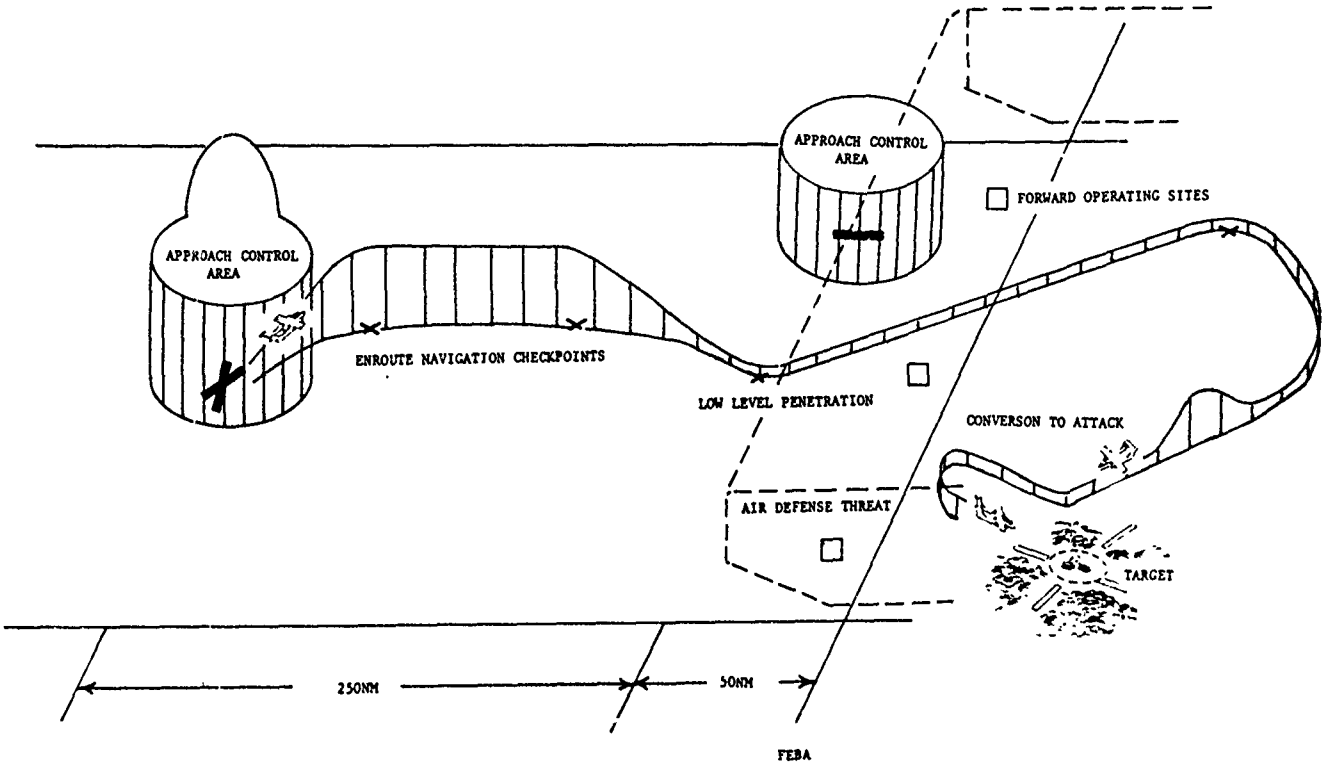

Figure 5.3. Approach Control Environments

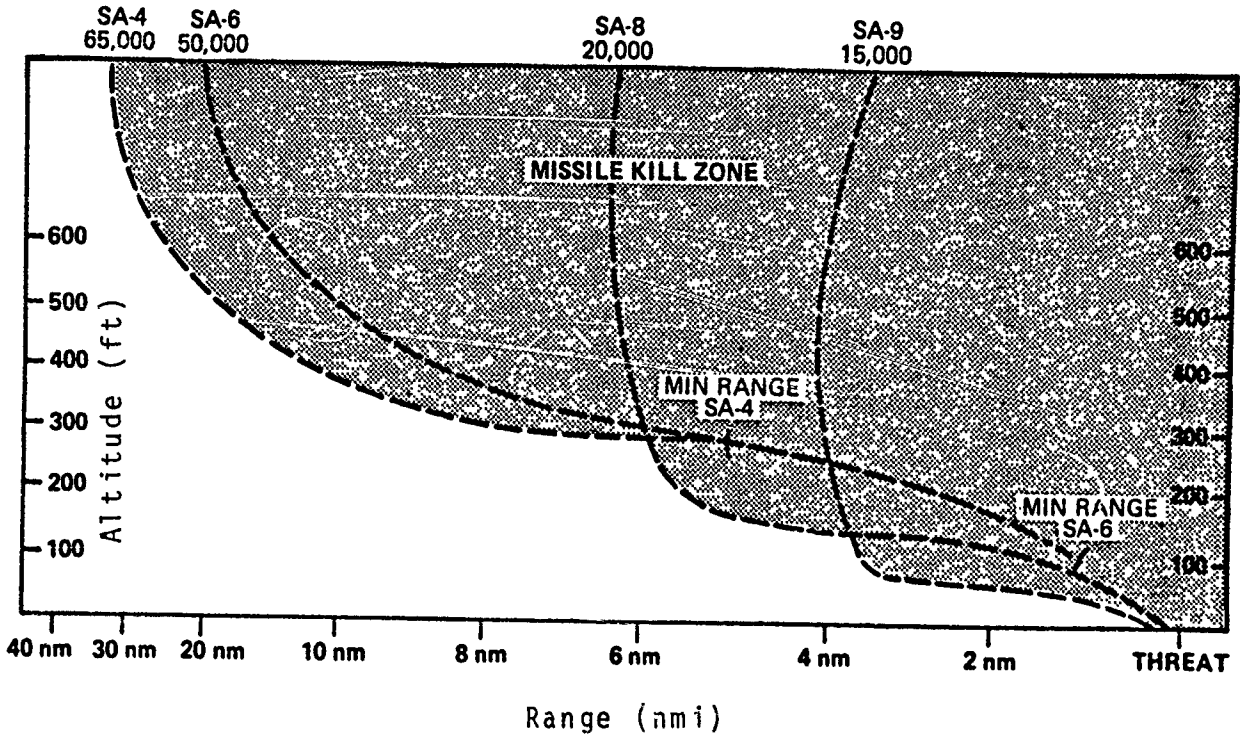

Figure 5.4. Surface-to-Air Missile Threat

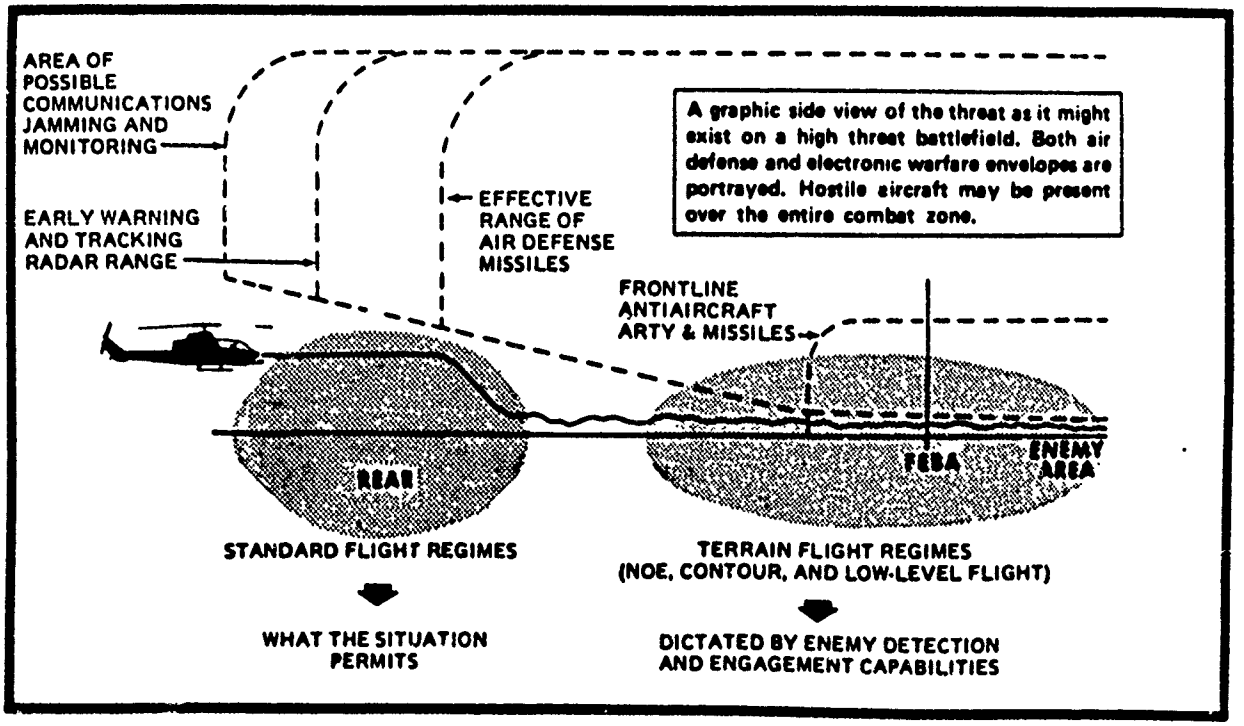

Figure 5.5. Flight Regimes

due to enemy anti-aircraft guns and supporting friendly artillery fire. These restrictions could range in altitude from the surface up to several thousand feet.

The desired operational cabapilities of an ASR required for this scenario can be subjectively concluded to be the following:

Maximum Detection Range	-	20 - 25 nmi
Coverage-Azimuth	-	360^{o}
Altitude	-	near surface to 10,000 feet
Target Size	-	small RCS helicopters and aircraft
Target Velocity	-	50 kts - 300 kts

Additionally, the air traffic controller needs the capability to rapidly plot, display, and update the location and type of restricted areas.

The operation of the radar system within 50 nautical miles of the enemy forces presents the opportunity for the enemy force to use airborne electronic countermeasures to reduce the effectiveness of the MATCALS system. Similarly, intercept and location of the ASR signals are likely.

The MATCS providing air traffic control service at a more rearward base, located beyond the air defense threat, could operate in a manner similar to a peacetime environment. Flights including close air support, anti-aircraft, reconnaissance, and other combat support missions would be operating on a 24 hour basis in all weather conditions. The approach control area would be assigned by the airspace control authority and could vary considerably in size and shape. The control area is unlikely to be affected by enemy action if air superiority is maintained. Altitude coverage should allow for normal operation of the aircraft. As a terminal area facility, approaching aircraft will be descending from enroute altitudes under approach control direction in preparation for an approach to the airfield. As such, flight directly overhead is seldom required. Departing aircraft are climbing to enroute altitude under the direction of the approach control agency (departure control) at a previously agreed upon altitude. Flight over the airfield is seldom required on departure. Aircraft that are transiting the area may be required to overfly the airfield and will typically maintain the assigned enroute altitude unless a conflict exists; in which case, a new altitude would be assigned. The normal IMC enroute altitude would vary considerably from a few thousand feet for helicopters up to 40,000 feet or greater for high performance fixed wing aircraft depending on the type aircraft.

Radar altitude coverage up to 40,000 feet is adequate for all these situations. It would be desirable to provide coverage directly overhead, but this is not physically possible with a single antenna system. The optimum antenna design would provide for continuous coverage from the radar horizon to 40,000 feet at the maximum range while maximizing altitude coverage at minimum range. A cosecant squared antenna pattern meets this objective.

The desired operational capabilities required for this scenario can also be subjectively concluded to be the following:

Maximum Detection Range	-	60 nmi
Coverage-Azimuth	-	360^{o}
Altitude at Max. Range	-	radar LOS to 40,000 feet
Target Size	-	variable from small to large radar cross section aircraft
Target Velocity	-	50 kts - 600 kts

It is likely that, as an assault progresses and the ground forces move forward, the type of required air traffic control support will change. A forward operating site with only VMC helicopter traffic could evolve into a major support base with a full range of capabilities requiring significant air traffic control services. This was typified by several airfields in Vietnam.

The MATCS mission is to provide air traffic control service at expeditionary airfields and remote landing sites under all weather conditions. To provide safe and efficient approach control service, the airport surveillance radar must be capable of detecting and tracking the supported aircraft at the maximum required range with minimum degraduation due to the weather conditions. Two conflicting requirements result from this desired capability. The controllers need to "see through" the weather to detect and track the aircraft and they desire to "see" the weather to vector the aircraft around the severe storms.

In general, the only weather condition that significantly degrades radar performance at the frequencies of interest is rain. Although spatial rain data have been collected by many investigators, a universal description of rain for use in radar design is not available. The season of year and the geographical location as well as the area size and length of observation time significantly affect the data collected. In general, rain

cells typically cover only 50 to 80 percent of an ASR's surveillance area. Rain cells may vary in size from 2 to 4 nmi in diameter with rain rate varying from 3 to 20 mm/hr. Higher rain rates of 50-80 mm/hr may occur but only for short periods of time (i.e., under one minute). Separation of cells is typically 5-8 nmi. Rain cells in central Europe are usually somewhat smaller than those in central USA and are closer together.

For MATCALS radar performance analysis, two rain conditions may be assumed to represent worse case, yet certainly possible, conditions that may be encountered in areas throughout the world. These conditions are as follows: a steady 4 mm/hr rain over 100% of the radar line of sight, or two rain cells with a 5 nmi diameter separated by 8 nmi containing 25 mm/hr rain within the radar line of sight. These conditions could be expected to occur only a small percentage of the time (less than 1/2%).

The aircraft that are likely to be controlled by the MATCS vary considerably in size and shape. A significant variation in the radar cross section (RCS) of the different aircraft therefore exists. Although documented RCS data on each aircraft are not available, experience has shown that minimum RCS will exist with the nose-on view of smaller aircraft and helicopters and it will be on the order of one square meter. Considerable work is ongoing within the services to reduce the RCS of future aircraft through design goals and of existing aircraft through cost effective modifications. It is too early to predict the impact of this work so an RCS of one square meter is a reasonable one to use for ASR design calculations at this time.

The primary purpose of the ASR component of the MATCALS is to provide the air traffic control with sufficient position data (2 dimensions) to allow safe and efficient control of aircraft. Target resolution and target location accuracy are key system parameters that affect how well that control can be accomplished. Target resolution relates to the system capability to distinguish between targets in a multiple target environment. Air traffic control procedures require different separation minima for different conditions, but the minimum is never less than three miles. When aircraft are being controlled as a flight (i.e., formation flying), there is no requirement to resolve the separate aircraft. One could conclude that the resolution required is less than three miles. Spatial resolution consists of two elements: range resolution, a function of the pulse width, and azimuth resolution, a function of the beamwidth. If the desired beamwidth is calculated using a safety factor of 100% (resolution of 1.5 nmi), multiple targets separated by 3 nmi will always be resolved at 3 nmi regardless of the orientation. For example, a beamwidth of 2.2^{0} will provide the 1.5 nmi resolution at 39

nmi. Most often, however, targets will be resolved in range at separation distances much smaller than the 3 nmi.

The desired range resolution, based on controller judgement, is one that allows resolution of two aircraft about 150 meters apart as they join up for formation flight or as they break up the flight. The air traffic controller must transition from controlling a flight of aircraft to controlling multiple aircrafts. A pulsewidth of 1 μ sec. provides that range resolution.

The desired antenna scan rate is one that provides information to the operator fast enough to prevent conflicts from arising between scans, but slow enough to ensure solid detections on each scan. Marine air traffic controllers who have controlled aircraft with variable scan rates have the opinion that 15 revolutions per minute is the desired scan rate. This rate is consistent with scan rates of other ASR's that typically vary from 7 to 15 rpm.

The operational requirement for range and azimuth accuracy is not particularly severe. The primary concern of the ASR operator is that of aircraft separation, rather than accurate location of each aircraft. It is more important to know that two aircraft are separated by five miles than to know that an aircraft is over a particular location with some given accuracy. It is occasionally desirable to provide position information to an aircraft for on-board navigation system checks. Radar position checks would be satisfactory for air traffic control navigation systems (such as TACAN), but would not be satisfactory for precise all weather navigation systems with accuracies on the order of 10 meters. A spatial accuracy of about 100 meters at 10 nmi would be sufficient for an ASR radar. This translates into a 0.3^{o} azimuth accuracy and a 100 meter range accuracy.

The desired operational characteristics, suitable for a wide range of operational scenarios, based on the above analyses are summarized in Table 5.2.

TABLE 5.2. DESIRED OPERATIONAL PERFORMANCE CHARACTERISTICS

Maximum Range	60 nm
Target RCS	1 m^2
Target Velocity	50 - 600 kts
Range Resolution	150 m
Range Accuracy	100 m
Azimuth Resolution	2.2^o
Azimuth Accuracy	0.3^o
Half Power Azimuth Beamwidth	2.2^o
Elevation Beam Shape	csc^2
Maximum Altitude Coverage	40,000 ft
Azimuth Coverage	360^o
Scan Rate	15 rpm

In addition to the performance characteristics of the ASR, the logistics aspects are extremely important in the development of a radar system intended for tactical use, and a balance between these considerations and the performance considerations must be made. Included in these considerations are: maintenance and test equipment, supply support, transportation and handling, and operator and maintenance personnel training.

Interviews with operational Marine Air Traffic Control Squadron personnel revealed that these considerations are perceived to be significantly more important than minor variations in the performance characteristics. Their rational is that the present radar systems operational performance (detection range, etc.) is adequate. The ability to deploy in a timely manner, repair a failure in a timely and efficient manner, obtain a replacement component, train a maintenance person in the allotted school program time will, in the final analysis, determine the operational readiness of the radar unit. The following points were made by active Marine Corps personnel.

(1) The MATCS, the user of MATCALS, is an integral part of the fighting force and as such is supported by the same logistic system as their sister units. Compatability with radars being developed for other Marine Air Control Group functions such as the TAOC will be extremely beneficial in training, maintenance, and supply support.

(2) Design of the radar for maintainability and transportability should be equally as important as design for performance characteristics. The requirement to deploy rapidly is considered to be a real requirement. The design must also anticipate that the number of Marine personnel available to prepare the system for movement and bring the system up to an operational status after relocation will always be minimal. The antenna system design should be such that two persons can configure the system for transit easily and excessive strength should not be required. The radar should be housed in a standard Marine Corps shelter and should be transportable by USMC helicopter and transport aircraft without damage to the antenna system.

(3) The system should be designed for routine servicing without interruption of the operation and sufficient built in test equipment (BITE) should be incorporated to ensure that a system fault can be identified rapidly. The shelter lay-out should be such that routine maintenance and fault correction can be accomplished easily. The design should be such that on-site Marine Corps personnel can troubleshoot and correct system faults without higher echelon support.

The following specific comments concerning maintainability were made by MATCS personnel:

(1) Provide a dual channel system.

(2) Provide simple switching so that maintenance personnel can safely work on one channel while the other is operational.

(3) Provide non-pressurized waveguides.

(4) Provide other than water cooled system.

(5) Provide a rugged, adjustable antenna that is easily erectable and not easily damaged.

(6) Provide easily repairable components (cards) or ensure that an adequate supply of replacement parts are available at the unit.

Trade-offs between the operational performance parameters, cost, and integrated logistic support should be made by the government during the requirement definition process and should be continued by the contractor during the design phase. Emphasis in the ASR replacement portion of the MATCALS program should be on the integrated logistics support.

APPENDIX

SUMMARY OF GEORGIA TECH PROJECT A-3151

ITT Electro-Optical Products Division subcontracted to Georgia Tech EES under Contract 38434 for the evaluation of the multiplexing and remoting requirements of eight Air Force radars and instrument landing systems. The prime contract (Air Force Contract F30602-81-C-0189) was with the Rome Air Development Center, Hanscom AFB, New York. The overall purpose of the prime contract was to design a cost effective set of multiplexers for use in fiber optic remoting of 24 Air Force radars and communication systems. Included in the study performed by Georgia Tech EES was the evaluation of current remoting configurations for eight specified systems along with a proposed generic radar multiplexing configuration (GRMC) which met the remoting requirements of the designated systems.

The eight Air Force systems studied included six radar systems and two instrument landing systems (ILS). The ILS requires only low bandwidth telephone cable remoting. The radar systems include two air surveillance radars (ASR), the AN/GPN-12, and the AN/GPN-20; two precision approach radars (PAR), the AN/FPN-62, and the AN/GPN-22 (actually a high precision approach radar (HI-PAR)); and two aircraft landing systems, the AN/TPN-19 and the AN/GPN-24. The landing systems include both an ASR and a PAR. The remoting of these radars consists of point-to-point signal transfer between the radar transmitter site and the operations shelter. The remoting requirements analyzed include the number, type, and bandwidths of the signals as well as the current means of remoting and the link distances. The types of signals remoted can be categorized as video, azimuth, narrow bandwidth analog, computer, control (on/off), voice, beacon, and antenna synchro data. The number of each of these signal types required for each radar is listed in Table A.1, and signal types are described more fully in Table A.2. The video signals, each of which is less than 6 MHz, and the antenna azimuth data are sent only from the radars to the OPS. Other information is transferred both to and from the OPS.

The amount of electronic multiplexing of the various signals before transmission varies substantially among the different radar systems. The AN/GPN-12 and the AN/GPN-20 radars employ very little electronic multiplexing. The electronic multiplexing of the signals in the AN/TPN-19, AN/GPN-22, AN/GPN-24, and AN/FPN-62 includes multi-level time-division multiplexing (TDM) and frequency-division

TABLE A.1. SUMMARY OF AIR FORCE RADAR AND INSTRUMENT LANDING SYSTEMS INVESTIGATED.

System	Manufacturer	Description	Total Number of Remoted Signals (Including Both Paths)							Current Electronic Multiplexing
			Video	Azimuth (acp, ARP)	Analog (low Bandwidth)	Computer Data	ON/OFF	Voice	Other	
AN/GPN-12	Texas Instruments	Air surveillance radar (ASR, same as FAA ASR-7	3	2	-	-	52	10	Synchro (2)	None
AN/TPN-19:	Raytheon	Tactical landing system comprised of								
AN/TPN-24		ASR	3	2	12	-	84	12	fsk (1)	Multilevel incl tdm and fdm
AN/TPN-25		Precision approach radar (pac)	1	-	12	2	56	12		Multilevel incl tdm and fdm
AN/GPN/20:	Texas Instruments	ASR	3	2	-	-	128	2	fsk (1) power	ON/OFF control signals converted to 21-bit serial code
AN/GPN-22	Raytheon	High precision approach radar (HI-PAR)	1	-	12	2	56	2		Multilevel incl tdm and fdm
AN/GPN-24:		Air traffic control and landing system comprised of ASR (discussed above) and one of the following: HI-PAR (discussed above) par (discussed below)								
AN/GPN-20										
AN/GPN-22										
AN/FPN-62										
AN/FPN-62	Raytheon	par	1	-	12	-	56	2	-	Multilevel incl tdm and fdm

TABLE A.2. DESCRIPTION OF SIGNAL TYPES

VIDEO DATA:

These signals, including radar video, moving target indication (MTI) video, log video, and beacon video, have bandwidths of up to 6 MHz. Triggers associated with these signals are usually combined in the video. Beacon video consists of the beacon synchronized trigger (BST), mode pairs (MP), and the defruited video. Beacon video, in general, requires more bandwidth (5 MHz) than most radar videos because the integrity of the leading and trailing edges of the pulses must be maintained to a high degree. Linearity and signal-to-noise (S/N) ratio requirements are typically 1-2% and 30-40 dB, respectively.

AZIMUTH (ACP, ARP) DATA:

Azimuth change pulses (ACP) are generated at a rate of 4096 per antenna rotation. Azimuth reference pulses (ARP) are generated at a rate of one per antenna rotation. The rise and fall times of these pulses is 1.0 microsecond. The bandwidth of the lines carrying these signals varies, but is approximately 20 kHz. Pulse shaping circuitry at the receiving station reshapes the pulses.

ANALOG (NARROW BANDWIDTH) DATA:

For the radar systems, these are narrow bandwidth analog (or DC) signals which are sampled at 20 Hz and converted to digital data, then serially multiplexed. For the ILS systems, these are control tones with bandwidths less than 3 kHz.

COMPUTER DATA:

These are 32-bit data words that are transferred between the OPS and the radar shelters. These words are converted to serial data and transferred at 128 kHz.

ON/OFF CONTROL DATA:

These include control/status/readback data of very narrow bandwidth (10 Hz or less each). All the radar systems, except the AN/GPN-12, multiplex these into serial data with a bandwidth of less than 2 kHz.

TABLE A.2. DESCRIPTION OF SIGNAL TYPES
(Continued)

VOICE DATA:

Intercom lines between the shelters have bandwidths of between 3 and 10 kHz.

FSK DATA:

Beacon 3-tone FSK data are transferred in the AN/GPN-20 and AN/TPN-24 radars. This signal is used to transfer the 88 bits/target report data. The three tones are usually at 12 kHz (sync signal), 24 kHz (logical 0), and 48 kHz (logical 1), with a total transfer rate of 24 kHz. A bandwidth of 100 kHz is sufficient to transmit this signal.

OTHER DATA:

Antenna synchro data (110 V) are transferred for the AN/GPN-12. Power is transferred over No. 2/0 CU conductor cable for the AN/GPN-20.

Multiplexing (FDM). As an example, the resulting FDM composite baseband of the AN/TPN-24 is shown in Figure A.1. The number and bandwidths of all signals at the output of the electronic multiplexing for each radar system is listed in Table A.3. The maximum bandwidth of the multiplexed signals is less than 10 MHz. This limit is primarily due to the increasing attenuation of the coaxial cable with frequencies above 10 MHz. For example, the cable most often used in radar remoting, RG-216/U coaxial cable, has a loss of 0.5 dB per 100 feet at 5 MHz; however, at 20 MHz the attenuation doubles. Fiber optic cables are not limited by this bandwidth constraint.

TABLE A.3. REQUIRED RADAR/OPERATIONS SHELTER REMOTED SIGNAL PATHS

RADAR SYSTEM	NUMBER OF CHANNELS	APPROXIMATE MAXIMUM BANDWIDTH (EACH)
AN/GPN-12	3	5 MHZ
	2	20 kHz
	10	3 kHz
	52	10 Hz
		Antenna synchro (110V lines, total of 10 pairs no. 19 needed)
AN/TPN-19		
AN/TPN-24	3	10 MHz
AN/TPN-25	2	10 MHz
AN/GPN-20	3	5 MHz
	1	100 kHz
	2	20 kHz
	2	3 kHz
	2	300 Hz
AN/GPN-22	2	10 MHz
AN/GPN-24		
AN/GPN-20	see above	
AN/GPN-22	see above	
AN/FPN-62	see above	

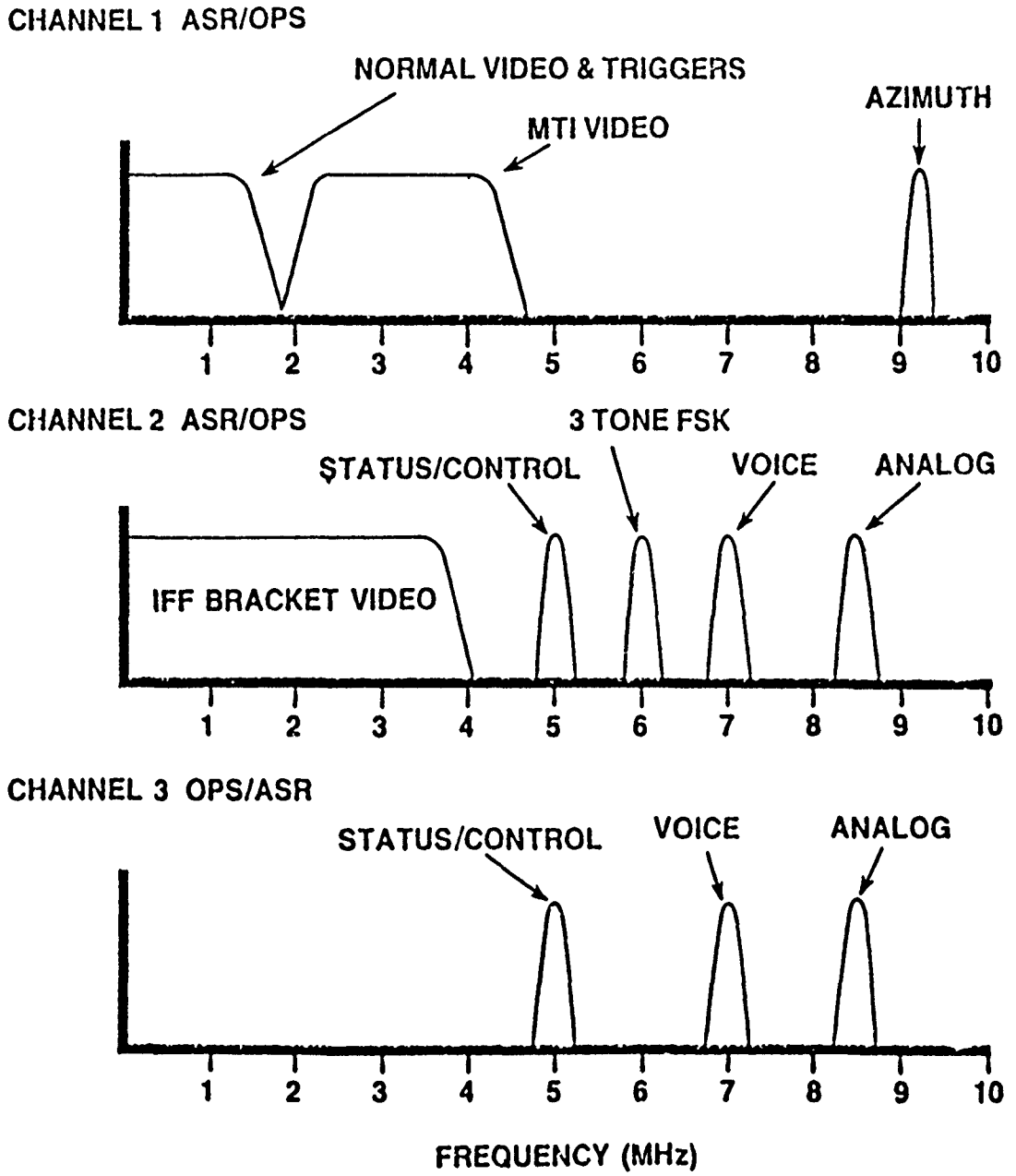

Figure A.1. AN/TPN-24 Baseband Frequency Allocation.

REFERENCES

1. R. N. Trebits, E. S. Sjoberg, et al., "Marine Air Traffic Control and Landing System (MATCALS) Investigation," Interim Technical Report on Project A-2550, Contract No. N00039-80-C-0082, Georgia Institute of Technology, Engineering Experiment Station, June, 1981.

2. R. N. Trebits, E. S. Sjoberg et al.," Marine Air Traffic Control and Landing System (MATCALS) Investigation," Final Technical Report on Project A-2550, Contract No. N00039-80-C-0082. Georgia Institute of Technology, Engineering Experiment Station, February, 1982.

3. M. I. Skolnik, Introduction to Radar Systems, McGraw Hill, 1979.

4. M. I. Skolnik, editor, Radar Handbook, McGraw Hill, 1970.

5. F. E. Nathanson, Radar Design Principles, McGraw Hill, 1969.

6. M. W. Long, Radar Reflectivity of Land and Sea, D. C. Heath Co., 1975.

7. E. J. Barlow, "Doppler Radar," Proceedings of the IRE, April 1949.

8. F. R. Williamson, et al., "MX Horizontal Shelter, MX Security System Radar Trade Studies (U)," Final Technical Report on Projects A-2733 and A-2870, Georgia Institute of Technology, Engineering Experiment Station, January, 1981 (CLASSIFIED).

9. N. C. Currie, F. B. Dyer, R. D. Hayes, "Analysis of Radar Rain Return at Frequencies of 9.375, 35, 70, and 95 GHz," Technical Report 2 on Project A-1485, Georgia Institute of Technology, Engineering Experiment Station, February 1975.

10. Louis Battan, Radar Observation of the Atmosphere, University of Chicago, 1973.

11. D. K. Barton, Radar System Analysis Artech House, 1976.

12. D. P. Meyer, H. A. Mayer, Radar Target Detection Academic Press, 1973.

13. AILTECH 75 Precision Noise Figure Indicator Instruction Manual, AIL Division of Cutler Hammer.

14. W. W. Mumford, E. H. Scheibe, Noise Performance Factors in Communication Systems, Horizon House, 1968.

15. T. S. Laverghetta, Microwave Measurement and Techniques, Artech House, 1976.

16. G. Evans, C W. McLeigh, RF Radimeter Handbook, Artech House, 1977.

17. H. F. Wolf, editor, Handbook of Fiber Optics, Garland Publishing Inc., 1979.

REFERENCES
(continued)

18. E. O. Rausch, M. A. Corbin, R. B. Efurd, and B. E. Huitt, "Fiber Optic Storage/Delay Filter," Final Technical Report on Project A-2956-004, Contract No. D67821, Boeing Aerospace Company, Georgia Institute of Technology, Engineering Experiment Station, January 1982.

19. R. B. Efurd, E. O. Rausch, M. A. Corbin, and B. E. Huitt, "A Fiber Optic Beam Controller for Phased Array Radars," Final Technical Report on Project A-2832, RADC-TR-82-173, Georgia Institute of Technology, Engineering Experiment Station, June 1982.

20. G. R. Grimes, S. J. Monaco, D. R. Stevens, and B. Washburn, "Fiber Optic Slip Rings for Rotating Test Fixture Data Acquisition," Proceedings of the 23rd International Instrumentation Symposium, Las Vegas, NV, May 1-5, 1977, pp. 11-19.

21. C. W. Kleekamp and B. D. Metcalf, "Fiber Optics for Tactical Radar and Radio Remoting," NTC Conf. Rec. Natl. Telecommun. Conf., Washington, DC, November 27-29 1979, pp. 42.5.1-42.5.4.

22. W. Goodwin and M. Beyer, "Radar Remoting," Conf. Proc. of Military Electronics Defence Expo '78, Weisbaden, Germany, October 3-5, 1978, pp. 237-260.

23. M. A. Corbin and R. B. Efurd, "Fiber Optic Remoting Multiplexer Study," Final Technical Report on Project A-3151, Subcontract No. 38434, ITT Electro-Optical Products Division, Georgia Institute of Technology, Engineering Experiment Station, October 1982.

24. P. Sierak and B. Demarinis, "Ground-based Tactical Fiber Optic Communications System Program," Military Electronics/Countermeasures vol. 8, number 5, May, 1982. pp 25-82.